



UNIVERSITY *of the* WESTERN CAPE

Antifungal and cytotoxic potential of green synthesized silver nanoparticles

MSc by thesis in Restorative Dentistry: Dr Widadh Klein

Student Number: 2924325

Supervisor: Dr Razia Z Adam (PhD), Faculty of Dentistry, Department of Conservative Dentistry, UWC.

Co-Supervisor: Professor Ahmed Mohammed (PhD), Department of Chemistry, CPUT.

KEYWORDS

Silver nanoparticles

Berzelia lanuginosa

Helichrysum cymosum

Searsia crenata

Nanotechnology

Green synthesis

Candida albicans

Denture stomatitis

Oral candidiasis

Cytotoxicity

Biofilm



ABSTRACT

The rate at which the population is ageing is much faster than in the past. An increase in age results in an increase in oral diseases. One of the most common types of oral diseases in the elderly are fungal infections caused by *Candida albicans*. It has been noted that drug resistance to fungal pathogens is developing into a serious threat to public health and healthcare systems worldwide. This has consequently led to the need to develop effective and innocuous treatment modalities. The purpose of this study was to explore the antimicrobial and cytotoxic potential of silver nanoparticles (AgNPs) synthesised from *Berzelia lanuginosa*, *Helichrysum cymosum*, and *Searsia crenata*.

To explore the antimicrobial and cytotoxic potential of AgNPs synthesised from South African plant species, namely: *Berzelia lanuginosa*, *Helichrysum cymosum*, and *Searsia crenata*.

Silver nitrate was used as the inorganic metal oxide precursor and extracts of *Berzelia lanuginosa*, *Helichrysum cymosum*, and *Searsia crenata* were the organic constituents for reducing and capping the AgNPs. The synthesized AgNPs were characterised by standard characterisation methods such as, ultraviolet-visible spectroscopy (UV-Vis), Fourier-transform infrared spectroscopy (FTIR), high-resolution transmission electron microscopy (HRTEM) with energy-dispersive X-ray spectroscopy (EDX), selected area electron diffraction (SAED) and dynamic light scattering (DLS). The antifungal potential of the AgNPs was assessed using the modified Kirby-Bauer (disc diffusion) and 2, 3-Bis-(2-Methoxy-4-Nitro-5-Sulphophenyl)-2H-Tetrazolium-5-Carboxanilide (XTT) staining assays against *C. albicans*. Cytotoxicity testing of both AgNP and plant extract was done at concentrations of 1 wt%, 3 wt%, 5 wt%, 10 wt% and 25 wt% using human Oral Fibroblast cell line (Buccal Mucosa Fibroblasts).

The UV-Vis results for *Berzelia lanuginosa*, *Helichrysum cymosum*, and *Searsia crenata* revealed AgNPs with a peak at 430 ± 1.5 nm, 440 ± 1.5 nm and 428 ± 1.5 nm respectively whilst HRTEM revealed that *Helichrysum cymosum* revealed various shapes and sizes. The shapes predominantly seen were triangular, hexagonal, spherical, and pentagonal shapes. *Berzelia lanuginosa* and *Searsia crenata* revealed spherical shapes of different

sizes. The AgNPs size for *Berzelia lanuginosa*, *Helichrysum cymosum*, and *Searsia crenata* were 16-20nm, 31-60nm and 57-72nm respectively. *Candida* growth inhibition zones for *Berzelia lanuginosa*, *Helichrysum cymosum*, and *Searsia crenata* ranging between 18mm, 18.67mm and 18.33mm were recorded in response to AgNPs exposure. The XTT testing revealed that at four hours, *Helichrysum cymosum* showed consistently higher growth than *Berzelia lanuginosa* and *Searsia crenata* (OD at 562-630nm). *Berzelia lanuginosa* lowered the fungal growth the most across the observed time. Minimum inhibitory concentration (MIC₅₀) for all three AgNPs was determined below 6.25%. The plant extracts seemed to have a lower effect in 4-24 hours when compared to their respective AgNPs with OD readings consistently above 0.5 for the plant extract.

The AgNPs exhibited promising antifungal activity that was size- and concentration-dependent. Further investigation could confirm its application in therapeutic dentistry.



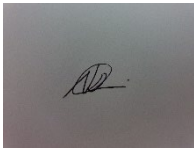
DECLARATION

I hereby affirm that the Research Project “Antifungal and cytotoxic potential of green synthesized silver nanoparticles” submitted to the Department of Conservative Dentistry, Faculty of Dentistry, University of the Western Cape (UWC), is an authentic document of an original and bona fide research project investigated by me (Doctor Widadh Klein) under the supervision of Doctor Razia Adam (Department of Conservative Dentistry, UWC) and Professor Ahmed Mohammed (Department of Chemistry, CPU).

Date: 22/02/2022

Place: Elfindale

Signature(s):

A small, dark rectangular box containing a handwritten signature in black ink.

DEDICATION

This thesis is first and foremost dedicated to the Almighty whom without none of this would be possible. To my dearest husband, Abdul Muez Abderoof, who has been a constant source of encouragement and support during the challenges of completing my masters and in life. I am forever thankful for having you in my life. My thesis is also dedicated to my beloved parents, Kieyaam and Shereen Klein, who have always supported me and whose good examples have taught me to work hard for the things that I aspire to achieve. Finally, to my son Yahya Abderoof, to inspire you to achieve everything you set your mind to.



ACKNOWLEDGMENTS

- First and foremost, praises and thanks to the Almighty, only with his blessing and mercy was I able to complete my research work successfully.
- I would also like to express my deepest and sincerest gratitude to my supervisor, Dr R.Z Adam, for giving me the opportunity to do research and providing invaluable guidance throughout this research project. Your vision, motivation and sincerity have truly inspired me. It was a great honour and privilege to study and work under your guidance.
- To my co-supervisor Professor A. Mohamed, I am pleased to express my gratitude to you, for your insights on the research subject and the insightful observations and suggestions you have made.
- To the members of the Chemistry department, CPUT, I sincerely appreciate the support and collaboration that ensured a pleasant and successful experience.
- To Mr Ernest Maboza, Head of the Oral and Dental Research Institute (ORDI), UWC, as well as Yolanda I would like to say thank you for the support given during the microbiology phase of the study.
- To Mrs Annette Olivier, ODRI, thank you for your unwavering support during the cytotoxicity phase of my work.
- To my beloved family, thank you for your unwavering support and encouragement.
- Finally, my thanks go to everyone who has supported me in completing my research work directly or indirectly.

Presented by: Dr Widadh Klein, Student no: 2924325

CONTENTS

KEYWORDS	1
ABSTRACT	2
DECLARATION	4
DEDICATION	5
ACKNOWLEDGMENTS	6
LIST OF FIGURES	12
LIST OF TABLES	15
ABBREVIATIONS	16
SYMBOLS	17
CHAPTER 1	18
INTRODUCTION	18
1.1 Introduction to the study	18
CHAPTER 2	21
LITERATURE REVIEW	21
2.1 Introduction	21
2.2 Nanoparticles (NPs)	21
2.2.1 Classification of NPs	23
2.2.1.1 <i>Organic NPs</i>	23
2.2.1.2 <i>Inorganic NPs</i>	24
2.2.1.3 <i>Carbon-based NPs</i>	24
2.2.2 Synthesis of NPs	25
2.2.2.1 <i>Bottom-up method</i>	25
2.2.2.2 <i>Top-down method</i>	25
2.2.3 General and biomedical applications of NPs.....	25
2.2.3.1 <i>Types of NPs</i>	26
2.2.3.2 <i>Drug delivery through the use of nanorobots</i>	27
2.2.3.3 <i>Anti-cancer treatment</i>	27
2.2.3.4 <i>Tissue engineering</i>	27

2.2.3.5 Antibacterial agents.....	27
2.3 NP Dental Applications.....	28
2.3.1 Applications of nanotechnology in diagnosis and treatment.....	28
2.3.2 Nanoshells	29
2.3.3 Bionanosurface technology and dental implants/nanocoatings.....	29
2.3.4 Nanoanaesthesia	30
2.3.5 Dental materials.....	30
2.3.5.1 Prosthodontics	30
2.3.5.2 Nanocomposites artificial teeth	31
2.3.5.3 Endodontics.....	31
2.3.5.4 Nanocomposite.....	32
2.3.5.5 Tooth whitening agents.....	33
2.3.5.6 Nanosolutions	33
2.3.5.7 Impression materials.....	33
2.3.5.8 Dentine hypersensitivity treatments.....	33
2.3.5.9 Orthodontic treatment.....	34
2.3.5.10 Nanotechnology for preventing dental caries.....	34
2.4 Biocompatibility of Nanoparticles	35
2.5 Toxicity of NPs in Dental Materials	35
2.5.1 Dental environment	35
2.5.1.1 Inhalation/dust.....	36
2.5.1.2 Ingestion of NPs.....	36
2.5.1.3 Titanium NPs from dental implants	36
2.5.1.4 Toxicity of AgNPs in dental materials	37
2.5.1.5 Cytotoxicity.....	37
2.6 Silver Nanoparticles (AgNPs).....	38
2.6.1 Synthesis of AgNPs	39
2.6.2 Synthesis of AgNPs using physical and chemical methods	39
2.6.3 Biological approach for the synthesis of AgNPs.....	40
2.6.4 NP characteristics and effects on cytotoxicity and antibacterial properties	41
2.6.5 Biomedical applications of AgNPs.....	42

2.6.5.1 Wound dressings	43
2.6.5.2 Cardiovascular implants.....	43
2.6.5.3 Drug delivery systems	43
2.6.5.4 Catheters	44
2.6.5.5 Bone cement	44
2.6.5.6 Bio-diagnosis	44
2.6.5.7 Other medical applications.....	45
2.6.6 Dental applications of AgNPs	45
2.6.6.1 Dental composites.....	45
2.6.6.2 Dental adhesives	45
2.6.6.3 Root canal materials	46
2.6.6.4 Surgical implants	46
2.6.6.5 Dental unit waterline	47
2.6.6.6 Maxillofacial prosthesis.....	47
2.6.6.7 Tissue conditioners	48
2.6.6.8 Acrylic resin	50
2.6.7 Biosynthesis of AgNPs using natural plant extract	52
2.6.8 Advantages of biologically synthesised NPs over conventionally synthesised NPs	55
2.6.8.1 <i>Candida albicans</i>	56
2.6.8.2 Oral candidiasis.....	58
2.6.8.3 Pseudomembranous candidiasis.....	59
2.6.8.4 Erythematous candidiasis	59
2.6.8.5 Chronic hyperplastic candidiasis	60
2.6.8.6 Angular cheilitis.....	60
2.6.8.7 Linear gingival erythema.....	61
2.7 Conclusion.....	61
CHAPTER 3.....	62
RESEARCH DESIGN AND METHODOLOGY	62
3.1 Introduction	62

3.2 Aim.....	62
3.3 Objectives.....	62
3.4 Null Hypothesis.....	63
3.5 Study Design	63
3.6 Materials and Instruments	63
3.7 Plant Collection.....	64
3.7.1 Plant identification.....	64
3.7.2 Preparation of plant extracts	65
3.8 Biosynthesis of AgNPs	65
3.9 Characterisation of AgNPs.....	65
3.9.1 UV-Vis spectroscopy.....	65
3.9.2 Dynamic light scattering (DLS) analysis.....	66
3.9.3 High Resolution Transmission Electron Microscopy (HRTEM) and Energy Dispersive X-ray Spectroscopy (EDX) analysis	66
3.9.4 Stability testing of synthesised AgNPs.....	67
3.9.5 Fourier-transform infrared spectroscopy analysis	67
3.10 Testing Antimicrobial Activity of AgNPs	67
3.10.1 Acquisition of yeast culture.....	68
3.10.2 Testing the effect of the NPs on <i>Candida</i>	68
3.10.2.1 Kirby-Bauer test.....	68
3.10.2.2 XTT assay.....	70
3.10.3 Determining the effect of NPs on biofilm	72
3.10.4 Minimum inhibitory concentrations using XTT.....	72
3.10.4.1 Preparation of culture and biofilm formation	73
3.10.4.2 96-well plate setting and treatment.....	73
3.10.4.3 XTT reduction assay	74
3.11 Cytotoxicity Testing.....	75
3.12 Conclusion.....	77
CHAPTER 4.....	78
RESULTS AND DISCUSSION	78

4.1 UV–vis Spectrophotometer of Synthesized AgNPs.....	78
4.2 Dynamic Light Scattering (DLS) and Zeta Potential.....	83
4.3 High Resolution Transmission Electron Microscopy (HRTEM).....	86
4.4 Stability Testing of the Synthesized AgNPs	90
4.5 Dispersive X-ray Spectroscopy (EDX) Analysis and SAED.....	94
4.6 Fourier-transform Infrared Spectroscopy Analysis of the Biosynthesized Silver Nanoparticle and Plant Extract.....	94
ANTIMICROBIAL TESTING RESULTS	99
5.1 Modified Kirby-Bauer assay on <i>Candida albicans</i>	99
5.2 XTT Testing Results and Discussion.....	100
5.3 XTT: Minimum Inhibitory Concentration for AgNPs and Plant Extracts.....	103
5.4 MIC: Plant Extract	109
CYTOTOXICITY.....	112
LIMITATIONS.....	120
CONCLUSION AND FUTURE PROSPECTS.....	120
APPENDICES.....	123
Appendix A:	123
Appendix B:	125
Appendix C:	126
Appendix E:	127
Appendix F:.....	128
Appendix G:	129
BIBLIOGRAPHY	130



LIST OF FIGURES

Figure 1. Classification of nanoparticles	23
Figure 2. Biological synthesis of nanoparticles.....	26
Figure 3. Screening of <i>Berzelia lanuginosa</i> (WK 13) to biosynthesis silver NPs at 70 °C	78
Figure 4. Screening of <i>Helichrysum cymosum</i> (WK 18) to biosynthesis silver NPs at 70 °C.....	78
Figure 5. Screening of <i>Searsia crenata</i> (EL 4) to biosynthesis silver NPs at 70 °C	78
Figure 6. The UV absorption band of silver nanoparticle from serially diluted <i>Berzelia lanuginosa</i> shows that it was concentration dependent and the absorption at 0.25 mg/mL reflected a good peak symmetry suggesting the existence of good silver nanoparticles at that concentration	80
Figure 7. The UV absorption band of silver nanoparticle from serially diluted <i>Helichrysum cymosum</i> shows that it was concentration dependent and the absorption at 0.25 mg/mL reflected a good peak symmetry suggesting the existence of good silver nanoparticles at that concentration	81
Figure 8. The UV absorption band of silver nanoparticle from serially diluted <i>Searsia crenata</i> shows that it was concentration dependent and the absorption at 0.25 mg/mL reflected a good peak symmetry suggesting the existence of good silver nanoparticles at that concentration	82
Figure 9. DLS WK 13 size distribution of 83.54 nm	83
Figure 10. DLS WK 18 size distribution of 98.91 nm	83
Figure 11. DLS EL 4 size distribution of 108.1 nm	84
Figure 12. Zeta potential distribution of WK 13 depicting a negative charge of -23.4mV	85
Figure 13. Zeta potential distribution of WK 18 depicting a negative charge of -18.8mV	85
Figure 14. Zeta potential distribution of EL 4 depicting a negative charge of -31.3Mv	85
Figure 15. a) WK13 TEM; b) WK 13 SAED; c) WK 13 Histogram depicting the average size; d) WK 13 TEM depicting lattice fringes	87
Figure 16. a) WK18 TEM; b) WK 18 SAED; c) WK 18 Histogram depicting the average size; d) WK 18 TEM depicting lattice fringes	88

Figure 17. a) EL 4 TEM; b) EL 4 SAED; c) EL 4 Histogram depicting the average size; d) EL 4 TEM depicting lattice fringes.....	89
Figure 18. <i>Searsia crenata</i> (EL 4) stability assay of the AgNPs observed from UV-vis spectra upon incubation with BSA media after 24 h.....	91
Figure 19. <i>Searsia crenata</i> (EL 4) stability assay of the AgNPs observed from UV-vis spectra upon incubation with cysteine media after 24 h.....	91
Figure 20. <i>Berzelia lanuginose</i> (WK 13) stability assay of the AgNPs observed from UV-vis spectra upon incubation with BSA media after 24 h.....	92
Figure 21. <i>Berzelia lanuginose</i> (WK 13) stability assay of the AgNPs observed from UV-vis spectra upon incubation with cysteine media after 24 h.....	92
Figure 22. <i>Helichrysum cymosum</i> (WK 18) BSA Stability assay of the AgNPs observed from UV-vis spectra upon incubation with BSA media after 24 h.....	93
Figure 23. <i>Helichrysum cymosum</i> (WK 18) stability assay of the AgNPs observed from UV-vis spectra upon incubation with cysteine media after 24 h.....	93
Figure 24. Infrared spectra of AgNPs, biosynthesized from <i>Searsia crenata</i> showed reduction of shift as the silver salt formed and a shift in transmittance intensity as well as wavenumber	96
Figure 25. Infrared spectra of <i>Searsia crenata</i> leave extract showed reduction of shift as the silver salt formed and a shift in transmittance intensity as well as wavenumber	96
Figure 26. Infrared spectra of AgNPs biosynthesized from <i>Berzelia lanuginose</i> showed reduction of shift as the silver salt formed and a shift in transmittance intensity as well as wavenumber	97
Figure 27. Infrared spectra of <i>Berzelia lanuginose</i> leave extract showed reduction of shift as the silver salt formed and a shift in transmittance intensity as well as wavenumber.....	97
Figure 28. Infrared spectra of AgNPs biosynthesized from <i>Helichrysum cymosum</i> showed reduction of shift as the silver salt formed and a shift in transmittance intensity as well as wavenumber.....	98
Figure 29. Infrared spectra of <i>Helichrysum cymosum</i> leave extract showed reduction of shift as the silver salt formed and a shift in transmittance intensity as well as wavenumber.....	98

Figure 30. a) Zone of inhibition for WK 13; b) Zone of inhibition for WK 18; c) Zone of inhibition of EL 4; d) Zone of inhibition of 0.2% Chlorexidine.....	100
Figure 31. XTT results for plant D, E and F at 0 hours: difference (256 – 630nm) and the confidence index.....	101
Figure 32. XTT results for plant D, E and F at 2 hours: difference (256 – 630nm) and the confidence index.....	101
Figure 33. XTT results for plant D, E and F at 4 hours: difference (256 – 630nm) and the confidence index.....	102
Figure 34. The growth pattern of <i>Candida albicans</i> when combined with AgNPs and XTT over 48 hours	103
Figure 35. All AgNPs at the 4 different time intervals at concentration SR 4 (6.25%)	104
Figure 36. All AgNPs at the 4 different time intervals at concentration SR 1 (50%) .	105
Figure 37. All AgNPs at the 4 different time intervals at concentration SR 5 (3.125%)	105
Figure 38. MIC percentage reduction for each concentration and time for each AgNP	106
Figure 39. All AgNPs at the 4 different time intervals at concentration SR 5 (3.125%)	107
Figure 40. All AgNPs at the 4 different time intervals at concentration SR 6 (1.562%)	108
Figure 41. All AgNPs at the 4 different time intervals at concentration SR 7 (0.78125%).....	108
Figure 42. All plant extracts at T1 (4 hours) at various concentrations	109
Figure 43. All plant extracts at T2 (6 hours) at various concentrations	110
Figure 44. All plant extracts at T3 (24 hours) at various concentrations	110
Figure 45. All plant extracts at T4 (48 hours) at various concentrations	111
Figure 46. The growth pattern of <i>Candida albicans</i> when combined with the plant extract and XTT over 48 hours.....	111

LIST OF TABLES

Table 1. Tissue conditioners modified with nanoparticles	48
Table 2. Denture acrylic modified with nanoparticles.....	50
Table 3. Green synthesis methods for silver nanoparticles using plants and their respective morphological description and inhibition test results	53
Table 4. List of the collected plant species	64
Table 5. Total sample size (n=72)	69
Table 6. 96-well plate setting and treatment.....	71
Table 7. 96-well plate setting.....	73
Table 8. Cytotoxicity layout	76
Table 9. Zones of inhibition at 400 μ L of WK 13, WK 18, EL 4 extract and AgNps and Chlorhexidine	99
Table 10. Indicates the nanoparticles and plant extract, showing their respective cell survival rate	112
Table 11. Difference between AgNPs sample 1 (WK 13 AgNPs) and plant extracts samples 4 (WK 13 Plant extract).....	113
Table 12. Difference between AgNPs sample 2 (WK 18 AgNPs) and plant extracts samples 5 (WK 18 Plant extract).....	114
Table 13. Difference between AgNPs sample 3 (EL 4 AgNPs) and plant extracts samples 6 (EL 4 Plant extract).....	114
Table 14. Difference in survival rate across concentrates of AgNPs samples.....	115
Table 15. Difference in survival rate between concentrates of AgNPs samples	116
Table 16. Difference in survival rate across concentrates of plant extract samples	117
Table 17. Concentrates of nanoparticles and plant extract together	119

ABBREVIATIONS

AgNPs	Silver nanoparticles
BSA	Bovine Serum Albumin
TiO²	Titanium dioxide
MgO	Magnesium oxide
ZnO	Zinc oxide
TEGMA	N,N-Dimethylaminoethyl methacrylate
HEMA	Hydroxyethyl Methacrylate
PMMA	Poly methyl methacrylate
NP	Nanoparticles
MIC	Minimum inhibitory concentration
ALS	Agglutinin-like sequence
PLB	Class B phospholipases
Saps	Secreted aspartyl proteinases
LGE	Linear Gingival erythema
HIV	Human Immunodeficiency Virus
ADDL	Amyloid-derived diffusible ligands
PMS	Phenazine methosulfate
PBS	Phosphate Buffered solution
SPR	Surface plasmon resonance
XTT	2,3-Bis-(2-Methoxy-4-Nitro-5-Sulfophenyl)-2H-Tetrazolium-5-Carboxanilide
UV	Vis ultraviolet-visible spectroscopy
FTIR	Fourier-transform infrared spectroscopy
HRTEM	high-resolution transmission electron microscopy
EDX	energy-dispersive X-ray spectroscopy
SAED	selected area electron diffraction
DLS	dynamic light scattering
3D	Three dimensional
AuNPs	Gold nanoparticles

SYMBOLS

Å	Non-SI unit ångström
λ	Wavelength
%	Percent
μm	Micrometre
μg/kg	Microgram/ Kilogram
μg/mL	Microgram/millilitre
μL	Microlitre
μg	Microgram
ml	Millilitre
nm	Nanometre
cm	Centimetre
°C	Degrees Celsius
eV	Electronvolt
g	Gram
g/mol	Grams per mole (molar mass)
keV	Kilo electron-volt
MM	Molar mass
®	Registered
Wt%	Weight percentage



CHAPTER 1

INTRODUCTION

1.1 Introduction to the study

According to Tsakos et al, people worldwide are living longer (Tsakos *et al.*, 2013). The world population over 60 years will almost double from 12% to 22%, between 2015 and 2050. The world's population aged 60 years and older is expected to increase from 900 million to 2 billion total 2 billion. It is now estimated that 125 million people are aged 80 years or older.

It is estimated that in 2050, 80% of these older people will be living in middle- and low-income countries. The population is ageing more rapidly than in the past (Tsakos *et al.*, 2013). These changes necessitate dentists adjust to the growing group of elderly patients and create ideas for the dental care of frail, dependent, and fit elderly people. In general, for the elderly, dental care should be based on their individual everyday life. Due to demographic changes, dentures, and denture cleaning, improved oral hygiene, tooth loss occurs predominantly in higher ages. This suggests that rehabilitation with removable dental prostheses is changing to a higher average age than ever before. Coupled with this is an increase in risk of oral health diseases (Nitschke *et al.*, 2021).

Oral diseases are widespread in South Africa, and they affect a large number of people in terms of pain, tooth loss, deformity, decrease or loss of function, and even death. Most of South Africans rely on the government for services related to oral health care. Already back in 2001, Naidoo *et al* reported that a large percentage of people (36%) were experiencing oral health problems in the country. This was mostly evident among higher age groups, where in their study reported that in some communities, almost one third of the participants were edentulous and 62% of the respondents had lost some of their natural teeth (Naidoo *et al.*, 2001).

The increased number of partial or completely edentulous, results in a need for improvements in the quality of life and health of the elderly. This requires the use of an

oral device like a dental prosthesis. A dental prosthesis replaces the missing tissue morphology and restores the functions of the affected maxilla and mandible (Miculescu F, Ciocan, L Toma, Miculescu M, Berbecaru A, Oliva J, Coma R, 2014). The presence of a prosthesis can alter the oral environment, which in turn may result in changes to the biological and physical characteristics of oral structures and saliva. The consequence of the latter is an imbalance in the local microbiota and thus a predisposition to fungal infections such as denture stomatitis (Bianchi *et al.*, 2016).

Denture stomatitis is the most common oral disease associated with denture wearers. It is commonly linked with atrophic osseous ridges and ill-fitting dentures. Dentures act as an environment for biofilm formation, which can harbour increased levels of yeasts and bacteria, particularly in patients with poor denture hygiene, poor oral hygiene, or those who wear dentures overnight. Dentures are said to serve as both reservoir and traumatic inducer for triggering a local microbial infection-mediated inflammatory response (Altarawneh *et al.*, 2013).

Candida species responsible for denture stomatitis are fungal pathogens that are known for their capability to induce systemic and superficial infections in human hosts. The fungal pathogens can persist inside the host due to the development of multidrug resistance characteristics and pathogenicity, which often leads to the failure of therapeutic strategies. A specific characteristic of *Candida* species pathogenicity is its capability to form biofilms, which defends them from antifungal drugs and the host immune system defences (Cavalheiro & Teixeira, 2018; Santos *et al.*, 2018). Treatment of denture stomatitis includes hard relines, tissue conditioners, local or systemic administration of antifungal drugs such as Nystatin, Amphotericin B, Fluconazole, Miconazole, Fluconazole, Itraconazole and Ketoconazole (Djordjevic *et al.*, 2017). Drug resistance to fungal pathogens is developing into a serious threat to healthcare and public health systems worldwide. These multidrug-resistant fungal pathogens are no longer vulnerable to conventional antifungal drugs, which thus makes the development of new antifungals for public health vital. By utilizing the information of plants as medicines, medically relevant plants can be incorporated into the drug delivery process, this could then be used

to aid in the fight against antimicrobial resistance. This warrants the need for further exploration of alternative antifungal therapies (Marquez and Quave, 2020).

The above supports the demand for an alternative, more effective treatment of multidrug resistant fungal pathogens. In this study, biosynthesized silver nanoparticles (AgNPs) were for the first time synthesized using *Berzelia lanuginosa*, *Helichrysum cymosum* and *Searsia crenata* and the antifungal properties of the obtained AgNPs were studied against *Candida albicans* (ATCC 90028) as well as their cytotoxic properties.



CHAPTER 2

LITERATURE REVIEW

2.1 Introduction

The previous chapter introduced the topic under investigation which seeks to explore the antifungal and cytotoxic potential of green synthesised AgNPs, as well as described the main elements of the research process, setting the stage for the rest of the study. The current chapter presents the literature review that reflects on existing scholarly literature and research to elucidate this topic further.

The structure of the chapter is as follows. The section following the introduction (section 2.1) discusses nanoparticles (NPs) (section 2.2), giving particular attention to the classification (sub-section 2.2.1), synthesis (sub-section 2.2.2), and general and biomedical applications for NPs (sub-section 2.2.3). Thereafter, NPs in dental applications are explored further (section 2.3), along with the cytotoxicity of NPs (section 2.4). The focus then shifts to the toxicity of NPs in dental materials (section 2.5). Of particular interest to this study is AgNPs, this forms the focus of sub-section 2.6. Lastly, a brief conclusion wraps up the chapter (section 2.7).

The literature and scholarly views on NPs are reviewed next.

2.2 Nanoparticles (NPs)

NPs are 1-100 nanometres in size and consists of metal, carbon, or organic matter or metal oxides (Hasan, 2014). NPs are complex molecules that consist of three layers, namely: (1) the core, (2) the shell layer, and (3) the top or surface layer (Khan, Saeed and Khan, 2017). NPs have distinctive physical, biological, and chemical properties at a nanoscale when compared to their individual particles at increased scales (Ealias and Saravanakumar, 2017). This is attributed to a greater mechanical strength, volume to surface area, and improved stability in a chemical process. As a result of these properties, NPs have been used in various applications (Ealias and Saravanakumar, 2017).

NPs differ in shape and size. They can either be (a) *zero-dimensional*, such as nano-dots, where the height, length, and breadth is secure at a single point; (b) *one-dimensional*, for example, graphene, which only has one parameter; (c) *two-dimensional*, for example, carbon nanotubes, where it has breadth and length; or (d) *three-dimensional*, such as gold nanoparticles, which includes all the parameters, i.e. length, breadth, and height (Pareek *et al.*, 2017).

NPs have many regular and irregular shapes, e.g. cylindrical, spherical, tubular, hollow core, conical, flat, and spiral, etc. (Hasan, 2014). Their surfaces can have irregular discrepancies or be uniform, some are amorphous or crystalline with multi or single crystal solids either unattached or agglomerated (Khan, Saeed and Khan, 2017).



2.2.1 Classification of NPs

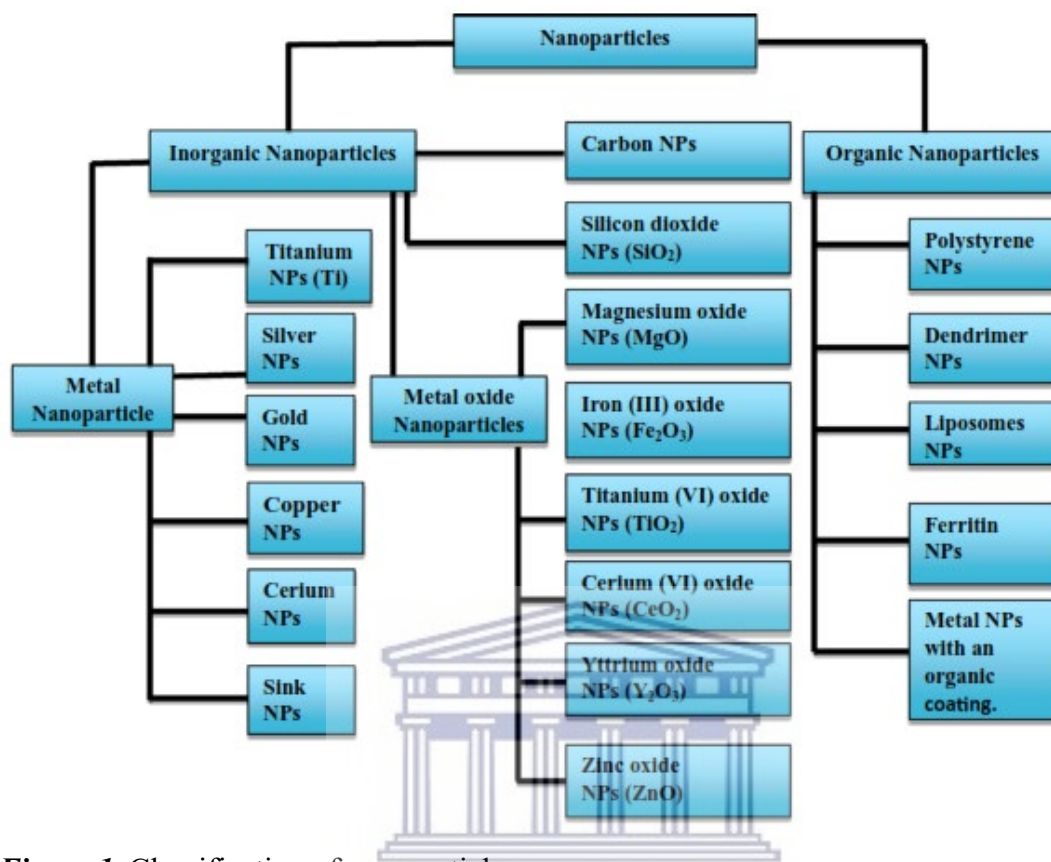


Figure 1. Classification of nanoparticles

(source: Maharramov *et al.*, 2019)

In general, NPs are classified into *organic*, *inorganic*, and *carbon-based*, as illustrated in Figure 1 above. These categories are discussed in more detail in the sections below.

2.2.1.1 Organic NPs

Liposomes, micelles, ferritin and dendrimers are the most known organic NPs (Shah *et al.*, 2015). These NPs have unique characteristics, such as being non-toxic and biodegradable, which make them ideal for drug delivery (Ealias & Saravanakumar, 2017). Besides the usual characteristics like surface morphology, size, and composition, etc., their area of application and their efficiency is also determined by its delivery systems and stability, the drug carrying capacity, either absorbed drug or entrapped drug system. These NPs are extensively utilised in the biomedical field as they can be injected into certain areas of the body, also known as targeted drug delivery, and they are highly effective (Singh, Yu Jin Kim *et al.*, 2016a)

2.2.1.2 Inorganic NPs

These NPs are not composed of carbon. Generally, inorganic NPs are categorised as metal and metal oxide-based NPs (Hasan, 2014).

2.2.1.3 Carbon-based NPs

Carbon based nanoparticles are made up of carbon and can be further divided into carbon black, graphene, carbon nano tubes, fullerenes and carbon nanofibers (Pareek *et al.*, 2017).

Graphene

Graphene is an allotrope of carbon. They are hexagonal structures of honeycomb lattice composed of carbon atoms in a two-dimensional planar surface. In general, 1nm is the normal thickness of a graphene sheet (Hasan, 2014).

Carbon Nano Tubes

A graphene nanofoil that contains a honeycomb lattice consists of carbon atoms which are looped into hollow cylinders, forming nanotubes. The diameter for each nanotube ranges from 0.7 nm per single layer and 100 nm for a multi-layered carbon nano tube. The lengths of these nanotubes range from micrometres to millimetres. The ends of the Carbon nano tubes may either be found closed or hollow by a half fullerene molecule (Khan, Saeed and Khan, 2017).

Fullerenes

Fullerenes are carbon molecules which are composed of carbon atoms held together by trigonal hybridization. They are spherical in shape. 28 to 1500 carbon atoms form the spherical structure with diameters of 4 to 36 nm for multi-layered fullerenes and up to 8.2 nm for a single layer fullerenes (Ealias and Saravanakumar, 2017).

Carbon black

Carbon black comprises of an amorphous material composed of carbon, with diameters varying from 20 to 70 nm and spherical in shape. The contact between particles is so great

that they're bound in aggregates resulting in about 500 nm agglomerates forming (Ealias and Saravanakumar, 2017).

Carbon Nanofiber

Carbon nanofibers are produced by the same graphene nanofoils as carbon nano tubes but instead of a regular cylindrical tube they are wound into a cup or cone shape (Ealias and Saravanakumar, 2017).

2.2.2 Synthesis of NPs

NPs are synthesized via different methods which are divided into bottom-up or top-down methods.

2.2.2.1 Bottom-up method

It is the accumulation of material from atoms to clusters to NPs. The most commonly used methods in the synthesis of AgNPs is the sol-gel, spinning, pyrolysis, chemical vapour deposition and biosynthesis methods (Ealias & Saravanakumar, 2017).

2.2.2.2 Top-down method

This method is also known as the destructive method and decreases the bulk material to nano-metric scale size particles. The various synthesis methods include nanolithography, mechanical milling, laser ablation, thermal decomposition, and sputtering (Ealias & Saravanakumar, 2017).

2.2.3 General and biomedical applications of NPs

NPs could be used for potential applications, such as bio-medical, catalysts for bacterial biotoxin elimination, biosensors, and lower cost electrodes (Rizk, 2014; Sharma, Kanchi & Bisetty, 2019).

NPs are also good candidates for applications such as medical, electrochemistry, trace-substance detection, catalysis, and biotechnology (Sharma, Kanchi & Bisetty, 2019).

Biotechnology and biomaterial advances gave rise to the development of a new field called “nanomedicine”, which was discovered in 1993 by Robert A. Freitas Jr (Abiodun Solanke, Ajayi & Arigbede, 2014). Nanomedicine is the science of using NPs to prevent, diagnose, and treat disease (Abiodun Solanke, Ajayi & Arigbede, 2014). Nanomedicine includes several applications, such as tissue scaffolds based on nanotechnology design, which leads to tissue formation, nanospheres with drug release, nanorobots for diagnostics and therapeutic purposes, as seen in Figure 2 below.

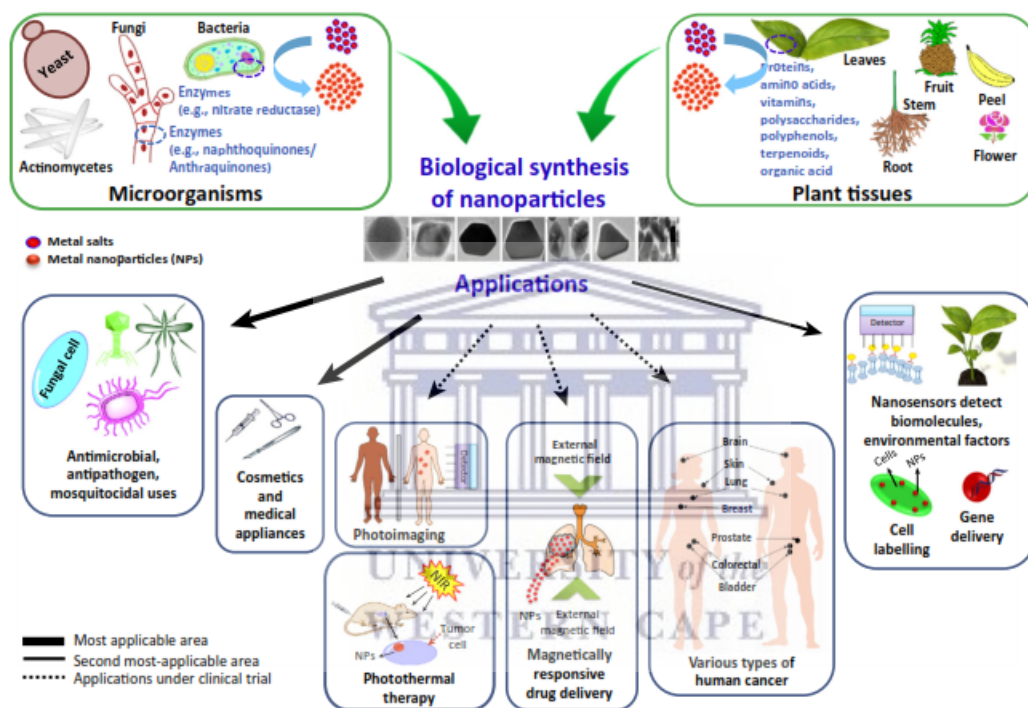


Figure 2. Biological synthesis of nanoparticles
(source: Singh, Yu Jin Kim *et al.*, 2016b)

2.2.3.1 Types of NPs

Gold NPs are utilised in the diagnosis of genetic disorders, tumour detection, photo imaging, angiogenesis, genetic disease, and photo thermal therapy (Singh, Yu Jin Kim *et al.*, 2016b). *Iron oxide NPs* are used in hyperthermia due to cancer therapy, tissue repair, drug delivery, cell labelling, targeting immunoassays, decontamination of biological fluids, magnetic resonance imaging and magnetically responsive drug delivery therapy (Pareek *et al.*, 2017). *AgNPs* have various antimicrobial uses, and are used in wound treatment, anticancer, and anti-inflammatory applications (Singh, Yu Jin Kim *et al.*,

2016b). Similarly, *zinc and titanium NPs* are applied in biomedical, cosmetic, and ultraviolet blocking agents, as well as in many other processing applications (Singh, Yu Jin Kim, *et al.*, 2016). *Palladium and copper NPs* have also been used in polymers, batteries, plastic, optical limiting devices, and plasmonic waveguides (Pareek *et al.*, 2017).

2.2.3.2 Drug delivery through the use of nanorobots

Undesirable adverse effects in untargeted regions may be caused by drug molecules travelling throughout the body via the circulatory system. Nanorobots can identify diseased cells and can locate and destroy them wherever they are situated. In cancer treatment, drug delivery to the specific target is of utmost importance in order to avoid harming healthy cells and at the same time destroying all the cancer cells. Placing the required drug dosage in the required area significantly lowers the total drug consumption (Ealias & Saravanakumar, 2017). This method in turn reduces the side effects and cost of the drug dosage (Ealias & Saravanakumar, 2017).

2.2.3.3 Anti-cancer treatment

Due to their size and unique properties, NPs have the ability to accumulate in tumours. Thus, NPs can be utilised in thermal treatment procedures. As mentioned before, NPs can be utilised as carriers for targeted delivery of anti-cancer drugs. This will improve delivery, as well as minimise side effects and treatment durations (Shah *et al.*, 2015).

2.2.3.4 Tissue engineering

Organ transplants and artificial implants can be substituted by tissue engineering, e.g. Carbon nanotube scaffolds aid in the growth of bones (Pareek *et al.*, 2017). Nanotechnology may be used to reproduce tissue and repair damaged tissue (Pareek *et al.*, 2017).

2.2.3.5 Antibacterial agents

NPs have been shown to be excellent antibacterial agents and are effective against many pathogenic microorganism strains (Singh, Yu Jin Kim, *et al.*, 2016). NPs are used as an

alternative to antibiotics to aid in targeting bacteria (Wang, Hu & Shao, 2017a). Applications include the use of NPs in antibacterial coatings for implant devices, as well as medicinal materials used to inhibit infections and to aid in wound healing; in systems to detect bacteria in order to generate microbial diagnostics; to treat diseases in antibiotic delivery systems; and to control bacterial infections in antibacterial vaccines (Wang, Hu & Shao, 2017b). The antibacterial mechanisms of NPs are not fully understood. The currently accepted mechanisms include non-oxidative mechanisms, metal ion release, and oxidative stress induction (Cheloni, Marti & Slaveykova, 2016). It is difficult for bacterial resistance to occur with the use of NPs due to multiple simultaneous mechanisms of action against microbes requiring multiple simultaneous gene mutations in the same bacterial cell for antibacterial resistance to develop (Cavassin *et al.*, 2015).

Having provided a general background and understanding of NPs in the sections above, the following section looks at dental applications of nanotechnology.

2.3 NP Dental Applications

A new field called “nanodentistry” is emerging due to the increased interest in dental applications of nanotechnology. The treatment opportunities in dentistry include applications of nanotechnology in diagnosis and treatment (sub-section 2.3.1); nanoshells (sub-section 2.3.2); bionanosurface technology and dental implants/nanocoatings (sub-section 2.3.3); and nanoanaesthesia (sub-section 2.3.4). In addition, sub-section 2.3.5 describes dental materials.

2.3.1 Applications of nanotechnology in diagnosis and treatment

Nano diagnostic devices are used at the molecular and cellular levels for identification of early disease (Shetty, Swati & David, 2013). Nanotechnology is used to diagnose and treat oral cancer by using saliva markers. These markers have been researched by utilising NPs in atomic force microscopy (Shetty, Swati & David, 2013). Diagnostic methods for oral cancer include oral fluid nanosensor tests, nanoelectromechanical systems, and optical nanobiosensors (AlKahtani, 2018). Nanosized particles replace micro sized particles, and this changes the conventional biosensor to a nanobiosensor. The benefit of

this is that the biological tissues are targeted at a molecular level. This improves the performance of biosensors; and also creates an opportunity to manufacture nanobiosensors which are small in size and can either be implanted or worn when compared to larger sized conventional biosensors that cost more to manufacture and are not feasible (AlKahtani, 2018). Metallic NPs are generally incorporated in nanobiosensor transduction systems. Without affecting their activity, these nanobiosensors are rapidly able to react with most biological molecules (Neel *et al.*, 2015).

2.3.2 Nanoshells

Chemotherapy is one of the main treatment modalities of cancer. However, it often fails because of its insufficient tumour killing capabilities and severe systemic side effects which result from the unavoidable drug resistance and nonspecific action on the normal cells and tumour cells. Non-invasive photothermal therapy based on gold nanomaterials has been intensively investigated for improving cancer treatment via the use of gold nanoshells (Wang *et al.*, 2016).

Gold nanoshells, which are composed of a concentric gold layer and a dielectric core, have been comprehensively researched because of their tunable plasmonic properties (Gao *et al.*, 2016). Gold nanoshells have a great potential for contrast enhancement in surface-enhanced Raman spectroscopy and fluorescence-based bio-imaging by controlling the distance between the fluorophore and NP, thus allowing applications for both in vivo therapy and diagnosis (Gao *et al.*, 2016). These nanoshells are also utilised in the treatment of oral cancer due to their ability to leave normal cells unharmed and excellent selectivity in destroying cancer cells by virtue of their metallic layers (Abiodun Solanke, Ajayi & Arigbede, 2014).

2.3.3 Bionanosurface technology and dental implants/nanocoatings

Osteoblast proliferation is induced through the creation of nano-size particles on the implant surface. Due to the nanoscale surface morphology augmenting the area, it provides a greater surface area on the implant, which then reacts with the biologic environment (Abiodun Solanke, Ajayi & Arigbede, 2014).

An *in vitro* study conducted by Almaguer-Flores *et al.*, (2010) explored the application of an amorphous carbon membrane measuring 40-60 nm in size with AgNPs. The purpose of this study was to evaluate the influence of the culture media, surface chemistry, and roughness on the bacterial colonisation process (Almaguer-Flores, Ximénez-Fyvie & Rodil, 2010). Nine strains were used on each surface, namely: *Actinomyces israelii*, *Aggregatibacter actinomycetemcomitans serotype b*, *Eikenella corrodens*, *Campylobacter rectus*, *Parvimonas micra*, *Fusobacterium nucleatum subsp. nucleatum*, *Prevotella intermedia*, *Porphyromonas gingivalis*, and *Streptococcus sanguinis*. When compared to standard titanium the results showed a substantial reduction in biofilm formation (Almaguer-Flores, Ximénez-Fyvie & Rodil, 2010).

2.3.4 Nanoanaesthesia

Nanotechnology may also be used to produce anaesthesia. A colloidal suspension containing millions of micron-sized dental robots is inserted into the gingiva of patients by the dentist to obtain anaesthesia (Bhavikatti, Bhardwaj and Prabhuji, 2014). These wandering dental robots reach the pulp via the gingival sulcus, lamina propria, and dentinal tubules (Gupta *et al.*, 2013). Results indicate a fast acting reversible anaesthesia which has no side effects (Bhavikatti, Bhardwaj and Prabhuji, 2014).

2.3.5 Dental materials

This sub-section describes several dental materials incorporated with NPs.

2.3.5.1 Prosthodontics

In one study, 0.4% Titanium oxide (TiO₂) NPs were incorporated into a three-dimensional (3D) printed poly-methyl methacrylate (PMMA) denture base. Improvements were reported in the structural and chemical properties as well as its antibacterial effects against the *Candida* species (Totu *et al.*, 2021). Similar research was also conducted on the behaviour of a heat cure PMMA incorporated with 7 wt% nano-zirconium oxide. Results showed the addition of NPs improved fracture toughness, flexural strength, and hardness levels (AlKahtani, 2018).

Luting cements impregnated with NPs have proven to have an increased effect on the bond strength to dentine and enamel as they are very small in size and can penetrate deeper into dentinal tubules. This results in an increased elastic modulus and a reduction in polymerisation shrinkage when compared to conventional luting cements (AlKahtani, 2018).

By impregnating magnesium oxide (MgO) and zinc oxide (ZnO) NPs into zinc polycarboxylate cement, it has been shown to significantly increase the tensile and compressive strength. Similarly, adding fluoroapatite or nano-hydroxyapatite particles to glass ionomer cements increases biaxial flexural, tensile, and compressive strength when compared to conventional glass ionomer cements (AlKahtani, 2018).

2.3.5.2 Nanocomposites artificial teeth

Nanocomposite denture teeth with homogenously distributed polymethylmethacrylate and nanofillers, have a high polishability and durability, superior aesthetics, increased shear strength, and increased abrasion resistance (Coutinho, Aras & D'souza, 2018).

2.3.5.3 Endodontics

The application of NPs in endodontics includes the impregnation of the bio-ceramic nanoparticles, i.e., glass ceramics, zirconia, and bioactive-glass in endodontic sealants. The incorporation of NPs into endodontic sealers improves the adaptation of the adhesive to nano-irregularities, faster setting time, insolubility in tissue fluid, dimensional stability, osseointegration, and chemical bond to the tooth structure (Utneja *et al.*, 2015). Lee *et al.*, (2015) carried out a study to advance gutta-percha by integrating nano-diamond particles. The modified gutta-percha functionalised with amoxicillin showed superior chemical properties, mechanical properties, biocompatibility, excellent adaptation to the canal walls, and minimal development of voids (Lee *et al.*, 2015). AgNPs have also been used as a coating for gutta-percha in an attempt to decrease the rate of micro leakage (Vahabi and Mardanifar, 2014).

The long-term and short-term effects of calcium hydroxide impregnated with AgNPs into intracanal medicaments have been investigated by Afkhami *et al* in 2015. Long-term

effects show no significant antibacterial effect when compared to the other materials. However, good short-term efficacy against *Enterococcus faecalis* was discovered when compared to calcium hydroxide incorporated with chlorhexidine and conventional calcium hydroxide (Afkhani *et al.*, 2015).

2.3.5.4 Nanocomposite

The production of nano-dimensional filler particles was enabled through nanotechnology (Jung, Sehr and Klimek, 2007). These nanocomposites have superior aesthetic features that have a high degree of strength, are easy to mould, and its resistance to abrasion is very high (Abiodun Solanke, Ajayi and Arigbede, 2014).

Examples of various types of NPs incorporated into composites are as follows (Vahabi and Mardanifar, 2014):

- Quaternary ammonium NPs due to their antibacterial agent, hydrophobic nature, and positive charge.
- Zinc NPs allow for a decrease in bacterial activity and prolong the life span of the composite restoration.
- Titanium dioxide NPs increase the hydrophilic activity of composites and prevent adhesion of microorganisms and biofilm formation.
- Nano-silica increases the strength and thermal stability and decreases shrinkage of composites.

The development of composite resin filled with rechargeable nano-amorphous calcium phosphate showed remineralising properties and the constant release of calcium and phosphate, and therefore inhibited the development of secondary caries (Xie *et al.*, 2016).

Cross-linked quaternised polyethyleneimine NPs in resin composites have been found to have long-term antibacterial effects, are stable in the matrix, and do not leak into the nearby environment (Shvero *et al.*, 2015).

2.3.5.5 Tooth whitening agents

To improve whitening efficiency and decrease the side effects, whitening agents were nano-modified. Deeper penetration of the calcium peroxide NPs into micro and nano cracks of the tooth structure lead to longer surface contact, which increases efficiency. Longer action time occurs as there is deeper penetration into the tooth structure which leads to an improvement in aesthetics (AlKahtani, 2018).

2.3.5.6 Nanosolutions

Nanosolutions are used in bonding agents such as Adper Single Bond 2 and Adper Single Bond Plus (3M ESPE) (Coutinho, Aras and D'souza, 2018). Dentine bonding agents manufactured from nanosolutions contain stable NPs homogenously spread throughout the solution. The NPs do not cluster as they are stable (Rao *et al.*, 2013). Nano adhesives have a longer shelf life, increased bond strength to enamel and dentine, durable marginal seal, and no separate etching is required (Coutinho, Aras & D'souza, 2018).

2.3.5.7 Impression materials

Nanofillers are incorporated into polyvinylsiloxanes, which produces a siloxane impression material with superior flow, better hydrophilic properties, and improved precision detail (Coutinho, Aras & D'souza, 2018). These nanofilled silicone impression materials have shown a high degree of fluidity. It is manufactured to give a snap set with less errors caused by micromovements (Coutinho, Aras & D'souza, 2018).

2.3.5.8 Dentine hypersensitivity treatments

Hydrodynamically transmitted changes in pressure to the pulp may cause hypersensitivity (Gupta *et al.*, 2013). Gold nanoparticles (AuNPs) are quickly adsorbed on the inner dentinal tubule walls and the use of silver staining was then utilised to help reduce dentin hypersensitivity by occluding the open tubules (Neel *et al.*, 2015). After the opened tubules were brushed with highly concentrated gold nanoparticles, the aggregation of NPs by laser irradiation was used to occlude the exposed tubules. Additionally, dental nanorobots offer a permanent and quick cure to dentin hypersensitivity by precisely and selectively occluding the tubules in minutes using biological materials (Neel *et al.*, 2015).

2.3.5.9 Orthodontic treatment

Orthodontic wires coated with fullerene-like tungsten disulphide inorganic NPs have been shown to reduce frictional force produced by orthodontic movement, thus reducing root resorption and a loss of anchorage (De Stefani *et al.*, 2020).

2.3.5.10 Nanotechnology for preventing dental caries

Detara *et al.*, (2018) investigated the effect of Siwak toothpaste and nano calcium carbonate on demineralised enamel surface roughness (Detara, Triaminingsih & Irawan, 2018). The study showed that both toothpastes resulted in a reduction of surface roughness of demineralised enamel (Detara, Triaminingsih & Irawan, 2018). Gold or colloidal silver can be used in between toothbrush bristles to prevent caries, periodontal disease, and gingivitis (Vahabi & Mardanifar, 2014). In addition to increased mechanical plaque removal, it also has antibacterial effects (Vahabi & Mardanifar, 2014).

Products to improve oral hygiene, such as mouth washes and toothpastes, were also modified. These are called “dentifrobots” (AlKahtani, 2018). Dentifrobots are able to clean organic residues left on occlusal surfaces of teeth (Imf, Dm & Ao, 2014). These dentifrobots can perform continuous calculus debridement and are self-deactivated when swallowed (Abiodun Solanke, Ajayi & Arigbede, 2014). Mouthwash products with added nano-calcium fluoride allowed for a reduction in dentine permeability, reduced caries activity, and increased labile fluoride concentration in the oral fluid (Danelon *et al.*, 2015).

Toothpastes containing 3% nanosized sodium trimetaphosphate and calcium carbonate NPs promote early caries lesion remineralisation when compared to conventional toothpastes (AlKahtani, 2018). When compared to normal toothpastes, toothpastes enhanced with nano-hydroxyapatite crystals resulted in enamel micro hardness increasing as shown in the results from the *in vitro* study (Ebadifar, Nomani and Fatemi, 2017). The reason for the higher reparative capacity of nanomaterials might be because the inorganic building blocks in enamel are 20-40 nm in size, thus there is a greater affinity to nanosized particles (AlKahtani, 2018).

The cytotoxicity and toxicity of NPs are described in the next two sections, respectively.

2.4 Biocompatibility of Nanoparticles

NP cytotoxicity is defined as the extent to which the interaction of NPs with cells interferes with processes essential for cell proliferation and survival and cellular structures (Yoda, 2012).

Due to a high number of potential applications, nanotechnology has been welcomed by industrial sectors. The application of NPs and nanomaterials are found in various fields including telecommunications, engineering, electronics, advertising, textiles, space and defence, medicine, and cosmetics (Hanan *et al.*, 2018). In the hopes of providing better treatments for combating diseases in medicine, nanotechnology is currently being utilised to create new anticancer and antibacterial agents (Hanan *et al.*, 2018). An ideal drug should be selective, potent, specific to the target site, safe, effective, have a convenient dosing frequency, have minimal food/drug interactions, and no requirement for blood level monitoring (Hanan *et al.*, 2018). These applications, however, have increasing concerns in relation to the biological impacts of the use of NPs on a large scale, and the risks to the environment and health (Sun *et al.*, 2011). It is therefore essential to systematically evaluate the beneficial and cytotoxic effects of NPs in biological systems (Sun *et al.*, 2011).

2.5 Toxicity of NPs in Dental Materials

The basis for risk assessment is the release and exposure of nanoparticles. With regards to the dental environment, possible exposure can occur in various places and under different circumstances (laboratory or dental office), namely:

2.5.1 Dental environment

These factors could include inhalation of generated dust (sub-section 2.5.1.1), ingesting these particles from removal of restorations during dental treatment (sub-section 2.5.1.2), or where these factors result in the release of titanium (sub-section 2.5.1.3) and silver

(sub-section 2.5.1.4) nanoparticles (patient) (Schmalz *et al.*, 2017). This is discussed in more detail below.

2.5.1.1 Inhalation/dust

Dust larger than 0.01 μm and smaller than 5 μm could be inhaled and can infiltrate deep into the alveolar areas of the lungs, outside the body's natural mechanisms of removal. Chronic inhalation of dust less than 5 μm in size (nanoparticles) may cause both systemic and local toxicity. Pneumoconiosis can be induced due to increased amounts and long-term exposure to dusts which are respirable (Napierska *et al.*, 2010). NPs less than 100 nm in size can be absorbed into the lymphatic system or the blood, leading to systemic toxicity (Napierska *et al.*, 2010). Schmalz *et al.*, (2017) concluded that there is a low to negligible health risk on dentists, patients, or dental personnel when polishing or grinding resin-based nanocomposites. No data was available for high risk patient groups, such as individuals with pulmonary disease or severe asthma (Schmalz *et al.*, 2017).

2.5.1.2 Ingestion of NPs

NPs are swallowed when restorations are worn down and, as a result, intestines are the main affected organ. Very little *in vivo* toxicity data exists for NPs from dental materials (Terzano *et al.*, 2010).

2.5.1.3 Titanium NPs from dental implants

The most biocompatible metal is titanium, due to its ability to develop an insoluble and stable protective oxide layer on its surface. Titanium is usually utilised in the manufacturing of endosseous dental implants. The properties of titanium implants can be enhanced by making use of titanium NPs (Schmalz *et al.*, 2017).

Although titanium-based implants are thought to be biocompatible, allergic reactions and hypersensitivity are side effects that have been found (He, 2016). Immuno-inflammatory reactions may also be caused by titanium-based materials. Titanium ions are released from titanium-based implants due to wear or corrosion (He, 2016). Increased concentrations of metals derived from orthopaedic implants in body fluids may cause

chronic or acute effects which are toxic (He, 2016). The long-term effects from titanium implants are not completely understood, however, allergic reactions and hypersensitivity have been recorded. In a clinical study conducted by Schmalz (2018), the examination of patients and the anamnesis for the presence of titanium allergy was evaluated, as well as the use of epicutaneous and cutaneous testing in patients with dental titanium implants or those planning to receive dental titanium implants (Schmalz *et al.*, 2018). It was found that marrow necrosis, granulomatosis, and fibrosis could be formed from detached metal debris from implants. The highest titanium content found in human mandibular bone was 37,700 $\mu\text{g}/\text{kg}$ bone (Schmalz *et al.*, 2018). It is presumed that all titanium in the bone was nano-titanium and 1 kg bone in 1 litre of fluid, a nano-titanium concentration can be calculated as 37 $\mu\text{g}/\text{mL}$. The half maximal effective concentration (EC_{50}) value for nano-titanium in human cells is 2,800 $\mu\text{g}/\text{mL}$. Thus, it is expected that there might not be any toxicological clinical effect of titanium NPs released from dental implants (Schmalz *et al.*, 2018).

2.5.1.4 Toxicity of AgNPs in dental materials

The clinical complications related to AgNPs used in resin-based composites are colour change. A high amount of resin-based composite components released can occur due to the AgNPs affecting the polymerisation process (e.g. monomers) (Chladek *et al.*, 2011). The higher the amounts of elutable residual monomers, the lower the degree of conversion of monomers (e.g. CQ, TEGDMA, HEMA) from cured resin-based composites with the risk of causing allergic reactions or being metabolised to mutagenic epoxy compounds (Bakopoulou, Papadopoulou & Garefis, 2009). The real danger of the incorporation of AgNPs into resin-based composites is currently challenging to assess. Nevertheless, the possibility of adverse biologic effects of AgNPs when added to resin-based composites seems to become greater (Schmalz *et al.*, 2017).

2.5.1.5 Cytotoxicity

The mechanism of the cytotoxicity of AgNPs occurs in three stages: NPs accumulate on the surfaces of the cells and work together with the cell membrane; this results in an alteration in the permeability and charge of the membrane. It is then followed by the internalization of NP inside the cells via the pores in the cell membranes. Thereafter

changes in cellular physiological processes occur like the formation of reactive oxygen species as well as metabolic processes at the nuclear level occur; this leads to abnormalities and then cell death (Verma *et al.*, 2017).

The cytotoxicity of AgNPs is determined by the difference in the size of the particle. AgNPs have shown to have a vital effect on lactate dehydrogenase activity, cell viability, and reactive oxygen species generation in a size-dependent fashion in different cell lines (Akter *et al.*, 2018). Multiple studies have been carried out to determine the particle size effect of AgNPs on different cell lines and have come to the conclusion that the smaller the particle size the more cytotoxic the AgNP would be (Liu *et al.*, 2010, Wang *et al.*, 2014, Park *et al.*, 2010 and Greulich *et al.*, 2009).

The remainder of this chapter focuses on AgNPs in dentistry. The specific topics reviewed include a synthesis of AgNPs (sub-section 2.6.1); synthesis of AgNPs using chemical and physical methods (sub-section 2.6.2); biological approaches for the synthesis of AgNPs (sub-section 2.6.3); NP characteristics and its effects on cytotoxicity and antibacterial properties (sub-section 2.6.4); biomedical applications of AgNPs (sub-section 2.6.5); dental applications of AgNPs (sub-section 2.6.6); a biosynthesis of AgNPs using natural plant extract (sub-section 2.6.7). The final sub-section describes the advantages of biologically synthesised NPs over conventionally synthesised NPs (sub-section 2.6).

2.6 Silver Nanoparticles (AgNPs)

AgNPs are nanometre-sized particles of silver that are less than 100 nm in size (Kaur & Luthra, 2016). It has been found that AgNPs and silver compounds have antibacterial activity (Almatroudi, 2020). AgNPs have many dental and biomedical applications as AgNPs have shown unique interactions with fungi and bacteria species (Corrêa *et al.*, 2015). Besides AgNPs being an effective antimicrobial, they also have other advantages, such as long-term antibacterial activity, low toxicity, low bacterial resistance, good biocompatibility with human cells, and sustained ion release (Corrêa *et al.*, 2015).

2.6.1 Synthesis of AgNPs

Various methods have previously been utilised for the synthesis of AgNPs (Singh *et al.*, 2015). In general, conventional chemical and physical methods seem to be very hazardous and expensive when compared to biological methods. Biologically-prepared AgNPs show high yield, high stability, and solubility (Zhang *et al.*, 2016). When compared with numerous artificial methods for AgNPs, biological methods were found dependable, fast acting, non-toxic, and simple. The green methods can also result in well-defined morphology and size. It is shown that a green approach for the synthesis of AgNPs is very promising (Zhang *et al.*, 2016).

2.6.2 Synthesis of AgNPs using physical and chemical methods

NPs prepared via physical methods are prepared at atmospheric pressure by using a tube furnace via evaporation-condensation. Physical methods, such as pyrolysis and spark discharging, were used to synthesize AgNPs. The advantages of AgNPs synthesized by physical methods are that there are no dangerous chemicals involved, radiation, and speed; however, the disadvantages include increased solvent contamination, energy consumption, low yield, and decreased even distribution (Almatroudi, 2020).

AgNPs can be prepared via chemical methods where organic solvents or water is used. This process is achieved by the use of three important components, such as metal precursors, stabilising agents, and reducing agents. Two steps are used in the reduction of silver salts, namely: (1) nucleation, and (2) consequent growth (Zhang *et al.*, 2016).

The “top-down” and “bottom-up” methods may also be used to manufacture silver nanomaterials. The reduction of bulk metals through the process of mechanical grinding and stabilising it with the use of colloidal protecting agents, is known as the *top-down method*. The *bottom-up methods* involve sono-decomposition, electrochemical methods, and chemical reduction (Gudikandula & Charya Maringanti, 2016).

Chemical methods utilised processes that involve laser irradiation, laser ablation, chemical reduction, cryochemical lithography synthesis, electrochemical reduction, thermal decomposition, and sono-decomposition (Alaqad & Saleh, 2016). These methods

are costly. In addition, materials such as borohydride, citrate, 2-mercaptoethanol, and thio-glycerol used to synthesise AgNPs are hazardous and toxic (Zhang *et al.*, 2016). Besides these disadvantages, the surfaces of the manufactured particles were found to be sedimented with chemicals, and they were not of expected purity. It is challenging to prepare well-defined sized AgNPs as another step is required to prevent particle aggregation (Singh, Yu Jin Kim, *et al.*, 2016). Furthermore, it was also found that by using these methods a large number of hazardous and toxic by-products are removed (Zhang *et al.*, 2016).

2.6.3 Biological approach for the synthesis of AgNPs

Biological methods of synthesising NPs are dependable, economical, environmentally friendly, and simple (Almatroudi, 2020). AgNPs synthesised via the green approach is economical and does not require that toxic chemicals are used. Thus making the biological methods biocompatible (Ahmad *et al.*, 2019). Many bacteria, including *Escherichia coli* (*E. coli*), *Lactobacillus* strains, *Pseudomonas stutzeri* AG259, *Brevibacterium casei*, *Bacillus licheniformis*, fungi *Ganoderma neo-japonicum* Imazeki, and *Fusarium oxysporum*; and plant extracts, namely *Typha angustifolia*, *Artemisia princeps*, and *Allophylus cobbe* were utilised. Numerous biomolecules, such as fibrinolytic enzyme, biopolymers, starch, and amino acids were also used (Zhang *et al.*, 2016).

The type of biocompatible material, reducing agent, and the solvent determines the biological synthesis of NPs. The main benefit of utilising biological methods is the elimination of the additional step required to inhibit particle aggregation, the availability of amino acids, secondary metabolites, or proteins present in the synthesis process. An eco-friendly and pollution-free environment is established when synthesising AgNPs from biological molecules (Ahmad *et al.*, 2019). AgNPs synthesised using biological methods to produce controlled shape and size is important for numerous biomedical applications. The size, reducing agents, monodispersity, and shape of the NPs can be controlled by using plant extracts or bacterial protein (Ahmed *et al.*, 2016).

Additional benefits of biological methods include the wide variety of biological resources available, the ready solubility of prepared NPs in water, decreased time requirement, and stability (Aygün *et al.*, 2020). The biological activity of AgNPs is dependent on the structure and morphology of AgNPs, controlled by shape and size of the particles. With regard to shape and size, the truncated-triangular and smaller size NPs seem to have more superior and effective properties. Even though numerous studies have successfully synthesised AgNPs with various size and shape ranges, limitations are still present (Singh *et al.*, 2016, Zahir *et al.*, 2015, Poopathi *et al.*, 2015, Sadeghi, Rostami & Momeni, 2015).

When comparing chemical methods and biological methods, the latter allows for more effortless control of the distribution of nanoparticles, shape, and size by improving the synthesis methods, including temperature, number of precursors, pH, temperature, and the number of stabilising and reducing factors (Zhang *et al.*, 2016).

2.6.4 NP characteristics and effects on cytotoxicity and antibacterial properties

As previously indicated, the charge density is strictly related to size. The smaller the NPs the bigger the charge density (Monteiro *et al.*, 2015). This explains the relationship between small NPs and their agglomeration. The agglomeration of NPs allows for changes in their capability to work as a caring or their toxicokinetic characteristic (Athie-García *et al.*, 2018).

Synthesis methodology that improves these characteristics is the use of sub products from algae plants, fungi, bacteria, yeast, etc. (Durán, Nakazato & Seabra, 2016). The high content of reducing sugars, proteins, or anthocyanins, works as a reducing agent; additionally, some of these molecules are adhered in the NPs surface (Saratale *et al.*, 2018). This addition gives various characteristics to the NPs produced by chemical reduction. The NPs acquired with biogenic methods offer homogeneous NPs with antioxidant characteristics that allow the addition of other molecules and control their toxicity characteristics.

The inhibition of the *C. albicans* growth has proven to be efficient via the biogenic NPs production. The differences in the concentration required to inhibit their growth are

directly related the capping nature, to NPs size, and the microorganisms being evaluated (Monteiro *et al.*, 2012).

Diverse toxicity mechanisms have been suggested due to the NPs size (nanometre scale). This is due to the direct interaction of the cell membrane with the NP (Kim *et al.*, 2009). The interaction of NPs microorganism is accepted by the microorganism superficial charge and the NPs superficial charge (Dos Santos *et al.*, 2014). This interaction leads to interference of the cell wall and the leakage of ions and the intracellular material with the microorganism's death (Qasim *et al.*, 2015).

Subsequent to NPs dilution, another toxicity mechanism is the ion interaction with the cell. The ions are integrated into the cell, and then could work together with thiol groups of enzymes and proteins, which leads to the inhibition of vital biological activities (Cioffi & Rai, 2012). The NPs internalisation has also been reported on; it generates the interaction of ions with molecules and NPs of biological importance as enzymes or DNA (Hwang *et al.*, 2012). Inside of the cell, the ions or the NPs elicit a Fenton's type reaction. Because of this, the oxidative stress increases, and the DNA and proteins lipids release (Carlos *et al.*, 2017).

Membrane fluidity, ultrastructure morphology, cellular morphology and ergosterol content are altered (Radhakrishnan *et al.*, 2018).

2.6.5 Biomedical applications of AgNPs

AgNPs have anti-bacterial properties, and have been used widely in the health industry (Ahmed *et al.*, 2016). AgNPs can be used for multiple applications, namely, as antibacterial agents in healthcare, biomedical devices, orthopaedics; medical device coatings ; optical sensors, diagnostics, as anticancer agents in drug delivery ,the pharmaceutical industry , in household, commercial-related products; in consumer products; and cosmetics;; and the food industry; (Pareek *et al.*, 2017, Ge *et al.*, 2014, Midha *et al.*, 2017, Wei *et al.*, 2015).

The following sub-sections provide some examples of biomedical applications of AgNPs.

2.6.5.1 Wound dressings

Robert Burrell invented the world's first AgNP product which was made commercially available (Acticoat™; Smith and Nephew, London, UK). Acticoat™ is a form of silver antimicrobial barrier dressing. It has rapid and sustained bactericidal activity, and because of this, it reduces inflammation and promotes healing. Furthermore, it is used in the treatment of different wounds, ulcers, burns, pemphigus, and toxic epidermal necrolysis. It was observed that wound dressings impregnated with AgNPs significantly improved healing time by 3.35 days on average and increased the bacterial removal from septic wounds in comparison to silver sulfadiazine, with no complications of note (Neelakandan & Thomas, 2018). The AgNP wound dressing was shown to accelerate reepithelialisation but not angiogenesis (Xing *et al.*, 2014).

2.6.5.2 Cardiovascular implants

A prosthetic silicone heart valve impregnated with AgNPs was the first medical cardiovascular device designed to reduce inflammatory response and inhibit the silicone valve from bacterial infection (Burduşel *et al.*, 2018). Metal silver can cause inhibition of the normal function of fibroblast, hypersensitivity, and can result in paravalvular leakage. AgNP products are nontoxic and safer in medical devices, than metal silver (Burduşel *et al.*, 2018).

2.6.5.3 Drug delivery systems

AgNP based nano systems were assessed as ideal carriers of numerous therapeutic molecules, which includes antimicrobial, antioxidant, anti-inflammatory and anticancer bio substances (Burdusel *et al*, 2018). They are generally used due to their wide antimicrobial activity against various micro-organisms, their electrical conductivity, and localised surface plasmon resonance effect. They also play a vital role in many applications such as sensors, surface-enhanced Raman scattering, catalyst, antimicrobial, and biomedical applications.

2.6.5.4 Catheters

Catheters are susceptible to infections caused by bacteria by allowing for the rapid spread of bacteria to the wound and its surrounding areas, and can cause severe adverse effects (Wu *et al.*, 2015). Due to their lack of observed toxicity and superior antibacterial properties, AgNPs can reduce the occurrence of adverse effects and bacterial infections post operatively (Midha *et al.*, 2017).

In an animal model, plastic catheter tubes coated with AgNPs can prevent the *in vitro* growth of bacteria for at least of 72 hours, with no substantial toxicity. A pilot clinical trial of 19 patients who received catheters impregnated with AgNPs had no catheter-related ventriculitis (Xing *et al.*, 2014).

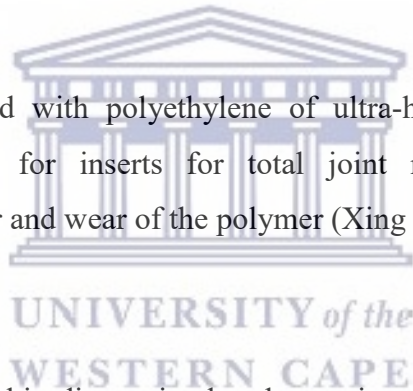
2.6.5.5 Bone cement

AgNPs were also combined with polyethylene of ultra-high molecular weight for manufacturing components for inserts for total joint replacement. The AgNPs significantly reduced the tear and wear of the polymer (Xing *et al.*, 2014).

2.6.5.6 Bio-diagnosis

NPs can also be utilised for bio-diagnosis, the plasmonic properties of AgNPs rely on dielectric medium, shape and size that surrounds it (Midha *et al.*, 2017). An AgNP array biosensor was developed by Zhou *et al.*, 2014 for diagnoses of serum p53 in head and neck squamous cell carcinoma (Midha *et al.*, 2017).

AgNPs can also be used to manufacture dual-imaging immune targeted nano shells in order to detect cancer cells. AgNPs can identify the interaction between the anti-ADDL antibody and amyloid-derived diffusible ligands (ADDL), which is associated with the development of Alzheimer's disease. Silver is oxidised easily and develops compounds in biological solutions like halides, which weaken the plasmonic efficacy of AgNPs (Burdusel *et al.*, 2018).



2.6.5.7 Other medical applications

AgNPs are also utilised for coating contact lenses in eye care products (Xing *et al.*, 2014).

2.6.6 Dental applications of AgNPs

The main reason for incorporating AgNPs into dental materials are to decrease or prevent biofilm formation and microbial colonisation (Jadhav *et al.*, 2016). The sub-sections below describe some dental applications that have incorporated AgNPs.

2.6.6.1 Dental composites

The antibacterial effects of AgNP impregnated restorative materials could reduce the formation of secondary decay, increase the life-span of restorations, and be efficient in reducing the bacterial biofilms formation on restorations and teeth, without compromising cytotoxicity and mechanical properties of composite resins (Corrêa *et al.*, 2015).

The addition of amorphous calcium phosphate and AgNPs of sizes ~3 nm and ~100 nm into a resin co-monomer blend resulted in a reduction of the colonisation of microorganism of lining materials, thereby increasing the antifungal efficacy against *C. albicans* (Chladek *et al.*, 2013).

2.6.6.2 Dental adhesives

Dental adhesives are required to bond composite to dentine (Noronha *et al.*, 2017). They require modification to prevent bacteria invading along the margins of restorations. Dental primers could also kill the remaining bacteria as it is in direct contact with the tooth surface (Kaur & Luthra, 2016).

The addition of AgNPs into orthodontic adhesives produces antibacterial remineralisation benefits as well as an increased shear bond strength (Kaur & Luthra, 2016).

A study done by Melo et al., (2013) evaluated the influence of the modified adhesive system on the bond strength to dental substrate with the addition of 0.1% of AgNPs into an adhesive system. The results showed that the AgNPs did not decrease the bond strength, when compared to the control group without AgNPs it was also revealed that there was a decrease in metabolic activity on biofilm (Melo *et al.*, 2013).

Similarly, Li et al., (2013) incorporated 0.05% of AgNPs into an adhesive system to assess bacterial contact-inhibition vs long-distance inhibition. It was reported that the AgNPs reduced lactic acid production on the biofilm, proving that AgNP containing adhesives facilitate long-distance antibacterial potential (Li *et al.*, 2013).

2.6.6.3 Root canal materials

The success of root canal treatment is dependent on the eradication of bacteria. It is therefore important that materials used in root canal treatment should have antibacterial properties to improve the lifespan of teeth which have been endodontically treated. The ideal filling material in endodontic treatment is gutta-percha (Bapat *et al.*, 2018). Nanosilver-gutta-percha was developed to try and improve the antibacterial effect. Nanosilver-gutta-percha is normal gutta-percha coated with AgNPs. Results has shown a significant effect against *C.albicans*, *Enterococcus faecalis*, *Escherichia coli*, and *Staphylococcus aureus* (Corrêa *et al.*, 2015). AgNP root canal irrigation solutions at 0.005% have been found to be equally as effective as 5.25% sodium hypochlorite, hence it could be utilised as an irrigant (Bapat *et al.*, 2018). In addition, research has shown that Mineral Trioxide Aggregate (MTA) containing AgNPs has a higher antimicrobial effect than MTA without AgNPs (Corrêa *et al.*, 2015).

2.6.6.4 Surgical implants

A common occurrence with implants is the formation of biofilm on the surface, which then leads to infection, inflammation, and implant rejection (Jadhav *et al.*, 2016). Coating AgNPs over the implant acts as an antimicrobial agent and reduces the risk of the implant failing (Corrêa *et al.*, 2015). The incorporation of silver also limits the amount of antibiotics patients require and provides protection from infection at the implant site (Kaur & Luthra, 2016).

2.6.6.5 Dental unit waterline

The dental water in waterlines, which are contaminated by microbial growth, are treated through a process of electrolysis or chemical additives which dose the water with silver nitrates (Kaur & Luthra, 2016).

2.6.6.6 Maxillofacial prosthesis

Maxillofacial prosthesis is used to replace missing facial structures (Jadhav *et al.*, 2016). These prostheses are prone to microbial growth and *Candida* infection. *Candida* causes damage to the prosthesis usually made of silicone as well as the surrounding tissues. Coating these prostheses with AgNPs could diminish the effect of fungal infections (Jadhav *et al.*, 2016).



2.6.6.7 Tissue conditioners

Table 1. Tissue conditioners modified with nanoparticles

Concentration of nanoparticles	Organism tested against	Tissue conditioner or denture acrylic	References
1%, 2.5%, 5% and 10% (AgNO ₃)	<i>C. albicans</i> , <i>P. aeruginosa</i> , <i>E. faecalis</i> , and <i>S. aureus</i> .	Tissue conditioner	(Kreve <i>et al.</i> , 2019)
0.625, 1.25, 2.5, 5, 10, 20 wt% of ZnOAgN.	<i>C. albicans</i>	Tissue conditioner	(Mousavi <i>et al.</i> , 2019)
0.1, 0.5, 2.0 and 3.0 wt % of AgNp	<i>S. aureus</i> , <i>S. mutans</i> , and <i>C. albicans</i>	Tissue conditioner	(Nam, 2011)
2% dry weight	<i>C. albicans</i> , <i>S. aureus</i> and <i>P. aeruginosa</i> .	Tissue conditioner	(Matsuura <i>et al.</i> , 1997)
1, 2, 3, 4 and 5 (wt/wt)%	<i>C. albicans</i>	Tissue conditioner	(Nikawa <i>et al.</i> , 1997)

Tissue conditioners are used to line dentures in patients with resorbed ridges or sharp alveolar ridges, or irritated inflamed and abused mucosa (Kaur & Luthra, 2016). The use of tissue conditioners allows the tissues to be repaired. Tissue conditioners are more susceptible to microbial colonisation as they degrade over time. Recent studies have reported on the incorporation of NPs into tissue conditioners as seen in Table 1. The integration of AgNPs into tissue conditioners could aid in reducing microbial colonisation (Jadhav *et al.*, 2016).

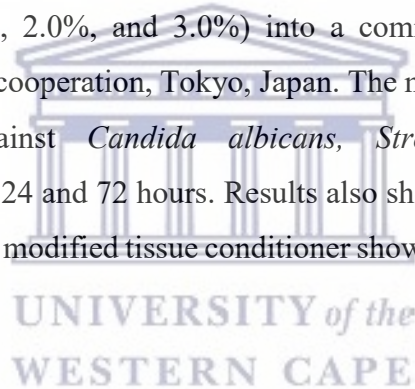
Kreve *et al.*, (2019) performed a diffusion study over a period of 24 hours where they investigated the effect of different concentrations of nanostructured silver vanadate incorporated with AgNPs (AgVO₃) on the antimicrobial activity against *Pseudomonas aeruginosa*, *Enterococcus faecalis*, *Staphylococcus aureus* and *Candida albicans* in a soft

denture liner (Trusoft). The outcome of the study showed that the liner had no antibacterial activity for *C. albicans* and *P. aeruginosa*, it was however effective at 5% and 10% for *P. aeruginosa*, the 10% showed higher efficacy. For *C. albicans*: 5% and 10% had a similar antimicrobial effect. All were effective in showing activity for *E. faecalis* and none were effective against *S. aureus* (Kreve & Dos Reis, 2019).

An *in vitro* study conducted by Mousavi et al., (2018) evaluated the antifungal properties of a tissue conditioner with AgNPs. Concentrations ranging from 0.625 to 20 wt% were tested. The results revealed an inhibition of *Candida albicans* at 5, 10 and 20 wt% (Mousavi *et al.*, 2019).

Ki-Young Nam (2011) investigated the incorporation of AgNPs at four different concentrations (0.1%, 0.5%, 2.0%, and 3.0%) into a commercial tissue conditioner, namely, GC Soft-Liner, GC cooperation, Tokyo, Japan. The modified tissue conditioners were then evaluated against *Candida albicans*, *Streptococcus mutans*, and *Staphylococcus aureus* after 24 and 72 hours. Results also showed that at concentrations as low as 0.1% and 0.5% the modified tissue conditioner showed antimicrobial properties (Nam, 2011).

Matsuura et al., (1997) reported on the incorporation of silver-zeolites into tissue conditioners and their antimicrobial effects were tested (Matsuura *et al.*, 1997). The findings indicated that the modified tissue conditioner possessed antibacterial properties and there was also evidence of long-term antimicrobial activity. Similarly, Nikawa et al., (1997) showed an improvement in the oral environment of denture stomatitis patients. The study suggested that a tissue conditioner incorporated with Zeomic (silver and zeolite) could be a potential aid in denture plaque control (Nikawa *et al.*, 1997).



2.6.6.8 Acrylic resin

Table 2. Denture acrylic modified with nanoparticles

Concentration of nanoparticles	Organism tested against	Tissue conditioner or denture acrylic	References
3, 3.5 wt%	<i>C. albicans</i>	<i>Denture acrylic</i>	(De Matteis <i>et al.</i> , 2019)
2, 5, 10 wt%	<i>C. albicans</i>	<i>Denture acrylic</i>	(Gligorijević <i>et al.</i> , 2017)
1, 2, 3 and 5% (w/w)	<i>C. albicans</i>	<i>Denture acrylic</i>	(Li <i>et al.</i> , 2016)
0.5, 1, 2.5, 5 and 10 % wt% AgNP PMMA	<i>C. albicans</i> and <i>S. mutans</i>	<i>Denture acrylic</i>	(De Castro, Valente, Agnelli, <i>et al.</i> , 2016)
0.3, 0.8 and 1.6 wt%	Tested <i>mechanical properties</i>	<i>Denture acrylic</i>	(KÖROĞLU <i>et al.</i> , 2016)
2.5, 5 and 10 wt%	<i>C. albicans</i>	<i>Denture acrylic</i>	(Ghahremanloo and Movahedzadeh, 2015)
24%/5% w/w	<i>C. Glabrata</i> and <i>C. albicans</i> .	<i>Denture acrylic</i>	(Kamikawa <i>et al.</i> , 2014)
Not mentioned	<i>C. albicans</i> and <i>C. Glabrata</i>	<i>Denture acrylic</i>	(Monteiro <i>et al.</i> , 2014)
The methyl methacrylate monomer was added with 1 µg/mL of AgNPs and 1% of benzoyl peroxide as an initiator before mixing with the PMMA powder.	<i>C. albicans</i>	<i>Denture acrylic</i>	(Acosta-Torres <i>et al.</i> , 2012)

Dentures are mainly constructed with PMMA resin. The denture fitting surface in contact with the oral mucosa is usually rough. This in conjunction with multiple factors such as xerostomia, poor oral hygiene, and immunocompromised conditions predisposes one to denture stomatitis (Corrêa *et al.*, 2015). *C. albicans* is one of the main opportunistic pathogens and is able to colonise the resin. Recent studies have reported on the incorporation of NPs into denture acrylic as seen in Table 2.

De Matteis *et al.*, (2019) explored the *Candida* colonisation of modified acrylic with (3 wt % and 3.5 wt %) of AgNPs. In PMMA impregnated with a higher concentration of AgNPs results showed that reduction of cell viability was more evident (De Matteis *et al.*, 2019).

Gligorijević *et al.*, (2017) conducted a lab study via disc diffusion to determine the antimicrobial effects of acrylic incorporated with AgNPs. The acrylic powder was modified with different concentrations of AgNP at 2%, 5%, and 10%. No *C. albicans* growth inhibition zones were seen, thus there was no proof of the fungicidal effect of AgNP (Gligorijević *et al.*, 2017).

Li *et al.*, (2016) conducted a lab study to determine the adhesion of *Candida* in AgNP solution and acrylic resin. The results indicated that *C. albicans* decreased with an increase in AgNP concentration (Li *et al.*, 2016). Similarly, Castro *et al.*, (2016) conducted a study to evaluate the antifungal efficiency of AgNPs in PMMA. Their results indicated a decrease in colony forming units as AgNP increases, especially in the 5 and 10 wt% groups (De Castro, Valente, Da Silva, *et al.*, 2016).

Koruglu *et al.*, (2016) studied the efficacy of AgNPs at three various concentrations of 0.3, 0.8 and 1.6 wt% on the elastic modulus, impact strength, glass transition temperature, and flexural strength, of microwave polymerised acrylic resin and conventional heat polymerised acrylic resin. The results showed that the impregnation of AgNPs did not affect the elastic modulus and flexural strength in the conventional heat-polymerised resin group. The values were reduced in microwave polymerised resin when 0.8 and 1.6 wt% AgNPs were added. The conventional resin group showed the greatest impact strength

without adding AgNPs. However, the microwave-resin group with 0.8 wt% AgNPs showed the lowest impact strength. The heat polymerised resin group showed the greatest glass transition temperatures, but when adding AgNPs, it resulted in a decrease of the glass transition temperatures of both groups. In both resin groups, no improvement in impact strength could be seen when AgNPs were added (KÖROĞLU *et al.*, 2016).

Ghahremanloo *et al.*, (2015) confirmed that acrylic with AgNPs has an effect on the inhibition of *C. albicans* (Ghahremanloo & Movahedzadeh, 2015).

Kamikawa *et al.*, (2014) evaluated an AgNP coating on a denture base. The results showed that over time *C. glabrata* and *C. albicans* adhered to the resin surface of the control, but the adhesion of both *C. glabrata* and *C. albicans* was significantly reduced to the AgNP-coated surface (Kamikawa *et al.*, 2014).

Monteiro *et al.*, (2014) revealed that pH and temperature variations of AgNPs did not affect their efficacy against the viable cells of *Candida* biofilms (Monteiro *et al.*, 2014). Oei *et al.*, (2012) studied the efficacy of AgNPs impregnated in polymethyl methacrylate on antimicrobial and mechanical properties. When incorporating AgNPs great improvement was seen in antibacterial and mechanical properties (Oei *et al.*, 2012).

Similarly, Acosta-Torres *et al.*, (2012) also reported the effect of AgNPs impregnated into PMMA and its subsequent biocompatibility and antifungal properties. The investigation showed no cytotoxicity, genotoxicity, and a reduced adherence of *C. albicans* (Acosta-Torres *et al.*, 2012). The results further revealed that the mechanical properties of the acrylic resin were not significantly affected, and it also led to prolonged antimicrobial properties of the resin. These results are vital in managing microbial colonisation in a denture base.

2.6.7 Biosynthesis of AgNPs using natural plant extract

A wide variety of plants have been used for the successful biosynthesis of AgNPs (Olusegun *et al.*, 2012). AgNPs synthesis via plant extract offers a new possibility as the

proteins, phenolic compounds, carboxylic acid, and anthocyanin work as a stabilising agent and reducing agent (Olusegun *et al.*, 2012).

The green silver synthesis of AgNPs using plant extracts such as extract from *Phoenix dactylifera* and the *Tulsi* leaf extract or and the plants mentioned in Table 3 has been proven. It has been confirmed that biosynthesis using natural plant extracts inhibit *Candida albicans* with different efficiencies.

Table 3. Green synthesis methods for silver nanoparticles using plants and their respective morphological description and inhibition test results

Plant used	Inhibition test	NPs size (nm)	Reference
<i>Cassia roxburghii</i> and <i>Ketoconazole</i>	18 mm (inhibition zone)	15-20	(Moteriya, Padalia and Chanda, 2017)
<i>Dodonaea viscosa</i> and <i>Hyptis suaveolens</i>	10 µg/mL (BIC)	40-55	(Muthamil <i>et al.</i> , 2018)
<i>Gracilaria corticata</i>	12 mm (inhibition zone with 30 µL of solution)	18-46	(Kumar <i>et al.</i> , 2013)
Tulsi leaf extract	60 µg/mL (MIC ₉₀) and 120 (MFC)	2-7	(Khatoon <i>et al.</i> , 2017)
<i>Phoenix dactylifera</i>	20 mm (inhibition zone with 80 µg/20 mL)	21.65-41.05	(Oves <i>et al.</i> , 2018)
Red cabbage	75 ppm reduce 83%/150 ppm (MFC)	70	(Ocsoy <i>et al.</i> , 2017)
Citrus lemon aqueous Juice and CTAB	40-60 µg/mL (MIC)	4-39	(Rahisuddin <i>et al.</i> , 2015)
Clove extract	10.8 ± 0.8 (inhibition zone)	12-85	(Parlinska-Wojtan <i>et al.</i> , 2018)
Flower broth of <i>Tagetes erecta</i>	21-12 cm in combination with	10-90	(Padalia and Chanda, 2017)

	antifungal (inhibition zone)		
<i>J. curcas</i>	12.14 µg/mL (MIC)	47.0 ± 2.0	(Kumar <i>et al.</i> , 2017)
<i>Ocimum sanctum</i> and CTAB	14 mm (inhibition zone)	5-10	(Aazam and Zaheer, 2016)
<i>Salvia africana-lutea</i> and <i>Sutherlandia frutescens</i>	1.5 to 0.012 mg ml ⁻¹ (MIC)	6-8 nm 15-20 nm	(Dube <i>et al.</i> , 2020)
<i>Pleurotus sajor-caju</i>	250 mg L ⁻¹ (MIC)	11.68 nm	(Musa <i>et al.</i> , 2018)
<i>Calotropis gigantea</i>	17.76 mm	10-70 nm	(Ali and Abdallah, 2020)
<i>Syngonium podophyllum</i>	15.60 mm	10.41 nm	(Musa <i>et al.</i> , 2018)
<i>Artemisia annua</i>	80-120 mg ml ⁻¹ (MIC)	7-27 nm	(Khatoun <i>et al.</i> , 2019)
<i>Mangifera indica</i>	0.016 mg/mL	65 nm	(Salati, Doudi and Madani, 2018)
<i>Fumaria officinalis L.</i>	17-18 mm	18-20 nm	(Milorad Cakić <i>et al.</i> , 2018)
<i>Zea Mays L.</i>	0.021 mg ml ⁻¹ (MIC)	12.63 nm	(Eren and Baran, 2019)

Clove extract was used in the production of AgNPs. Due to the high content of eugenol, flavonoids, triterpenoids, and many sesquiterpenes, allowed the clove to act as a reducing and capping agent in AgNPs synthesis. The AgNPs were the size of 12 and 85 nm. The AgNPs produced generated a complete inhibition of *Candida albicans* when a 40-fold dilution was applied. The results suggest that the functional groups' incorporation into the AgNPs generates a synergism between clove and NPs (Parlinska-Wojtan *et al.*, 2018).

The use of latex plants in the AgNPs green synthesis has also been explored. *J. curcas* and *L. grandis* extracts produced AgNPs with a size of 47 ± 2.0 nm and 7.6 ± 0.5 nm, respectively. The Fourier transform infrared (FTIR) spectra suggest the incorporation of phenolic OH, amides, amines, and aldehyde in the AgNPs as stabilising agents. The

smallest AgNPs showed a better effect in plankton and biofilms of *Candida albicans* than the bigger sized nanoparticles. The AgNPs synthesised proved to be efficient in the inhibition of biofilm formation, as changes in morphology and cell lysis were present when exposed to *Candida* (Kumar *et al.*, 2017).

2.6.8 Advantages of biologically synthesised NPs over conventionally synthesised NPs

The importance of *biological synthesis* is being emphasised globally over conventional methods of synthesis as the former is cheaper, non-toxic, eco-friendly, and has a high productivity rate (Hasan, 2014). It also doesn't require stabilising agents as the plants or microorganisms act as a capping and stabilising agent (Singh, Yu Jin Kim, *et al.*, 2016).

Both microorganisms and plants have long demonstrated the ability to absorb and accumulate inorganic metallic ions from their surrounding environments. These attractive properties make biological synthesis capable of significantly reducing environmental pollution and reclaiming metals from industrial wastes (Shah *et al.*, 2015). The surfaces of biological NPs absorb biomolecules when they come into contact with complex biological fluids, thus making them more effective in their pharmacological activity (Singh, Yu Jin Kim, *et al.*, 2016).

In addition to this, the time for biosynthesising NPs is significantly shorter than physiochemical methods. Biological NPs have also been shown to have better anticancer and antimicrobial applications due to the higher efficacy of biological NPs compared to physiochemical NPs (Singh, Yu Jin Kim, *et al.*, 2016). Moreover, biosynthesised NPs are more biocompatible than chemically synthesised nanoparticles.

NPs synthesised biologically are free from toxic contamination of by-products that become attached to the NPs during physiochemical synthesis, which then limits the biomedical applications of the formed nanoparticles. It is important to note the ability of a biological entity to use its own biochemical process to transform inorganic metallic ions into metal nanoparticles. However, biological synthesis is still a relatively new field of study and research is burgeoning.

In order to understand the effect of AgNPs on *Candida albicans* it is also important to understand the organism and its role in oral disease. The following section will summarize *Candida albicans* and its various forms.

2.6.8.1 *Candida albicans*

a) Description

Candida albicans is a multidrug-resistant fungal pathogen representing an important source of invasive disease in humans, generating high healthcare costs worldwide (Dadar *et al.*, 2018). *Candida albicans* is frequently found in different anatomical sites of healthy persons and could induce systemic and superficial infections under optimal environmental conditions. Clinical diagnosis of candidiasis could be difficult because of the lack of specific symptoms and clinical signs (Dadar *et al.*, 2018).

Candida albicans is part of the normal human microflora as a diploid polymorphic yeast of mucosal surfaces and is commonly found in the human gastrointestinal, respiratory, and genitourinary tracts. It is generally a harmless commensal fungus that can turn into an opportunistic organism in immunocompromised or immunologically deficient individuals (Neville, d'Enfert & Bounoux, 2015). In severely immunocompromised individuals, *Candida albicans* induces systemic infection and may turn from local opportunistic or commensal infections of the mouth, throat, and reproductive tract to a systemic invasive candidiasis affecting the circulatory system, bones, and brain (Kashem *et al.*, 2015). *Candida albicans* is the major species responsible for invasive candidiasis (46.3%), followed by *Candida glabrata* (24.4%) and *Candida parapsilosis* (8.1%). As a commensal pathogen, *Candida* can adapt to changes in the hosts' environment (Dadar *et al.*, 2018).

b) Pathogenesis and virulence of *Candida albicans*

Biofilms can also enhance systemic infection, and the presence of a *Candida albicans* biofilm structure has been implicated as a risk factor for increased patient mortality. A number of other properties and virulence factors possessed by *Candida albicans* are

known to promote its biofilm-forming ability and contribute to tissue damage and its persistence within the host (Tsui, Kong & Jabra-Rizk, 2016). First is the property of morphological switching as the distinct morphological states of *Candida albicans* dictate the phases of colonisation, growth, and dissemination. The yeast form has been associated with both initial attachment and dissemination, whilst the filamentous hyphal form enables *Candida albicans* to invade the host tissue and form a mature biofilm (Hanna, 2019). Hyphal morphogenesis can be triggered by a variety of factors such as amino acid availability, serum, temperature, and pH level. Notably, hyphal morphogenesis is a key mechanism for *Candida albicans* to evade killing by host phagocytic cells. Phagocytosis induces a switch in morphology from yeast to hyphae, which elongate and in time puncture the macrophage membrane. Thus, resulting in lysis and killing of macrophages, and allowing ingested *Candida albicans* to escape (Kong & Jabra-Rizk, 2015). Significantly, the ability of *Candida albicans* to adhere to host surfaces is essential for both successful colonisation and persistence during infection. The removal of loosely attached *Candida albicans* by flushing action and sloughing off of epithelial cells from mucosal surfaces are important factors in host defence against *Candida* overgrowth. Thus, an ability to avoid these removal mechanisms can be considered as a virulence attribute. The adhesion of *Candida albicans* to the host tissues is essential for infection (Chen, Li & Guo, 2013).

Attachment of *Candida albicans* to receptors on host tissues is assisted by the expression of a family of cell-wall adhesins known as agglutinin-like sequences (ALS) which have been shown to be differentially regulated in biofilm-grown cells. The ALS family of genes is comprised of eight genes of which *ALS3* is hyphal specific and is the most prominent (Verma-Gaur & Traven, 2016). *ALS3* is able to adhere to host cells and tissues and has also been associated with the adherence of *Candida albicans* to bacterial species. *Candida albicans* also produces several extracellularly released enzymes such as lipases and esterases, as well as hemolysins that are vital for host tissue invasion and nutrient acquisition (Verma-Gaur & Traven, 2016). These enzymes facilitate pathogenesis by aiding in the destruction of tissues, tissue barriers, and lysing host cells. Most important to note are the secreted aspartyl proteinases (Saps), a family of 10 proteinases with a certain degree of functional redundancy between them (Hanna, 2019). These enzymes

can directly induce damage to host cells, facilitate hyphal growth for invasion of tissue, increase adherence following exposure of receptor sites, and degrade antibodies and other host defence proteins (Wilson, Naglik & Hube, 2016). Phospholipases are another group of enzymes that contribute to the pathogenesis of *Candida albicans*; most notable are the class B phospholipases (*PLB*) which are secreted and act by disrupting host cell membranes. Accordingly, *PLB1* and *PLB5* deletions have been implicated in the decrease of systemic *Candida* infection (Tsui, Kong & Jabra-Rizk, 2016).

2.6.8.2 Oral candidiasis

a) Description

The oral cavity is at the intersection of medicine and dentistry, and is a window into general health (Kane, 2017). In the oral cavity, the oral mucosa is perhaps the most likely tissue to be compromised by systemic disease. Many diseases may initially present in the oral mucosa, and oral mucosal disorders may arise as a result of systemic diseases (Hu *et al.*, 2019). The most noteworthy of these is oral candidiasis, the most common fungal infection of the oral cavity in humans. Oral candidiasis normally reflects present or recent therapy with corticosteroids or other immunosuppressants, other immunodeficiencies or long-standing xerostomia (Hu *et al.*, 2019). While *Candida albicans* is the most common species associated with oral infection, accounting for more than 80% of clinical isolates, several other *Candida* species, such as *C. tropicalis*, *C. glabrata*, *C. krusei*, and *C. parapsilosis* may produce clinical infections, some of which can be resistant to antifungal therapy (Iqbal & Zafar, 2016). Furthermore, the presence of concomitant multiple *Candida* species in oral infections complicate the mycological features and enhance the clinical challenge (Iqbal & Zafar, 2016).

b) Clinical presentation

Oral candidiasis exists in many different clinical forms. These diverse clinical manifestations are often associated with different predisposing factors and symptoms. Below is a classification of the various clinical forms of oral candidiasis (Lalla & Dongari-Bagtzoglou, 2014).

c) Classification

- **Acute candidiasis**

1. Pseudomembranous candidiasis (oral thrush)
2. Erythematous (atrophic) candidiasis

- **Chronic candidiasis**

1. Erythematous (atrophic) candidiasis
2. Hyperplastic candidiasis (*Candida* leukoplakia)

- ***Candida*-associated lesions in oral cavity**

1. Angular cheilitis
2. Erythematous candidiasis (Denture related stomatitis)
3. Erythematous candidiasis (Median rhomboid glossitis)
4. Linear gingival erythema (Jabra Rizk, 2014).

2.6.8.3 Pseudomembranous candidiasis

Pseudomembranous Candidiasis is also known as thrush. This is the most widely recognised form of oral candidiasis. It appears as white or yellow pseudomembranes on the oral mucosal surface. These pseudomembranes are adherent but can be removed with some pressure (Fourie *et al.*, 2016). The underlying mucosa is typically erythematous and inflamed. The most common places it is found is on the buccal mucosa, tongue, soft palate and pharyngeal areas. Common predisposing factors include xerostomia and local or systemic immunosuppression (Vila *et al.*, 2020). Patients are usually unaware of the presence of pseudomembranous candidiasis as it is usually asymptomatic. In some cases, patients may report an alteration of taste or discomfort if larger areas are involved (Khan *et al.*, 2015).

2.6.8.4 Erythematous candidiasis

Erythematous candidiasis appears as red atrophic areas of the oral mucosa, without any white pseudomembranes. It may be clinically missed due to a less pathognomonic clinical appearance. It often occurs on the hard palate and the dorsum of the tongue (Fourie *et al.*, 2016). On the tongue, it appears as an atrophic, smooth-appearing dorsal tongue, with

loss of filiform papillae. The use of broad-spectrum antibiotics and the use of steroid inhalers are common predisposing factors for erythematous candidiasis (Vila *et al.*, 2020). A burning sensation is a common symptom of patients affected with erythematous candidiasis. Denture stomatitis is a form of erythematous candidiasis that occurs under a removable denture (Djordjevic *et al.*, 2017). The palatal surface is commonly affected under the maxillary denture, the boundaries of the lesion correspond to the tissue within the denture margins. Denture stomatitis is an inflammatory reaction that occurs in patients wearing dentures (Djordjevic *et al.*, 2017). A significant proportion of denture wearers (72%) are affected by this condition (Iqbal & Zafar, 2016). It is most commonly found in the palatal mucosa and the alveolar ridge, which makes direct contact with the base of dental prostheses (Djordjevic *et al.*, 2017). Denture stomatitis is asymptomatic in most cases; very few patients feel pain, tingling, and numbness, and the changes are initially diagnosed during the examination, when erythema or oedema can be observed, affecting the areas of the mucosa which is in contact with the prosthesis (Djordjevic *et al.*, 2017). Median rhomboid glossitis is a form of erythematous candidiasis that presents as a characteristic oval to rhomboid erythematous patch along the midline of the dorsum of the tongue (Khan *et al.*, 2015). The affected surface demonstrates loss of filiform papillae. Smoking and use of steroid inhalers are predisposing factors for Median rhomboid glossitis (Fourie *et al.*, 2016). Sometimes a similar erythematous lesion may present itself on the palate in the area contacted by the affected part of the tongue. Median rhomboid glossitis is asymptomatic and can persist chronically (Vila *et al.*, 2020).

2.6.8.5 Chronic hyperplastic candidiasis

Chronic Hyperplastic Candidiasis is the most uncommon form of oral candidiasis. It is characterised by the presence of a white hyperkeratotic plaque that cannot be wiped off. Furthermore, it is asymptomatic and clinically resembles an oral leukoplakia (Fourie *et al.*, 2016). When present, it affects the buccal mucosa and lateral borders of the tongue. Controversy surrounds the malignant potential of such lesions (Vila *et al.*, 2020).

2.6.8.6 Angular cheilitis

A mixed fungal and bacterial infection of the commissures of the mouth is referred to as *Angular cheilitis*. When affected, the mucosa is red, fissured, and sometimes crusted, also

affecting the adjacent skin at the corners of the mouth (Vila *et al.*, 2020). Predisposing factors include denture wearing, loss of vertical dimension, and vitamin deficiencies. Angular cheilitis may be seen in association with intraoral candidiasis, especially denture stomatitis, but may also occur alone. Patients may complain of discomfort when opening the mouth wide (Khan *et al.*, 2015).

2.6.8.7 Linear gingival erythema

HIV-gingivitis, now commonly referred to as *linear gingival erythema* (LGE), is the most common form of HIV associated periodontal disease in HIV-infected persons. It is considered resistant to conventional plaque-removal therapies, as it is considered to be a lesion of fungal aetiology (Jabra Rizk, 2014). It manifests itself as a red fired, linear band 2 to 3 mm wide on the marginal gingival accompanied by petechiae-like or diffuse red lesions on the attached gingival and oral mucosa, and may be accompanied by bleeding (Jabra Rizk, 2014).

Some concluding remarks follow next to wrap up the chapter.

2.7 Conclusion

Due to the increased number of partial or complete edentulous patients, oral devices like a dental prosthesis are required to improve the quality of life. However, the presence of a prosthesis can alter the oral environment, which in turn may lead to changes in the biological and physical characteristics of oral structures and saliva. The consequence of the latter is an imbalance in the local microbiota and thus a predisposition to fungal infections such as denture stomatitis. Denture stomatitis can persist inside the host due to the development of pathogenicity and multidrug resistance characteristics, which often leads to the failure of therapeutic strategies. These multidrug-resistant fungal pathogens are no longer susceptible to conventional antifungal drugs, and this warrants the need for further exploration of alternative antifungal therapies. The next chapter discusses research design and methodology of a possible alternative antifungal therapy.



CHAPTER 3

RESEARCH DESIGN AND METHODOLOGY

3.1 Introduction

The previous chapter explored AgNPs, focusing on their properties, benefits, and inclusion in dental applications. The current chapter describes the methodology employed to conduct this study. The methodology provides an overview of the experimental procedures that were followed to accomplish the aims and objectives of this study. The methodology includes: 1) plant collection and preparation of plant extracts; 2) biosynthesis of AgNPs; 3) characterisation of the NPs; 4) antifungal activity tests; and 5) cytotoxic potential of green synthesised AgNPs.

The structure of the chapter is thus as follows. Following the introduction (section 3.1), the chapter recaps the aim (section 3.2), objectives (section 3.3), and hypothesis (section 3.4) of the study. Thereafter, the study design (section 3.5) and materials and instruments (section 3.6) are described. Attention then shifts to plant collection (section 3.7), biosynthesis of AgNPs (section 3.8), characteristics of AgNPs (section 3.9) and analyses (section 3.10). The penultimate section focuses on cytotoxicity testing (section 3.11). Some concluding remarks follow next to wrap up the chapter (section 3.12).

3.2 Aim

The aim of the study was to explore the antimicrobial and cytotoxic potential of AgNPs synthesised from South African plant species, namely: *Berzelia lanuginose*, *Helichrysum cymosum*, and *Searsia crenata*.

3.3 Objectives

The objectives of the study were to:

- Synthesise and characterise AgNPs from South African plants, namely: *Berzelia lanuginose*, *Helichrysum cymosum*, and *Searsia crenata*.

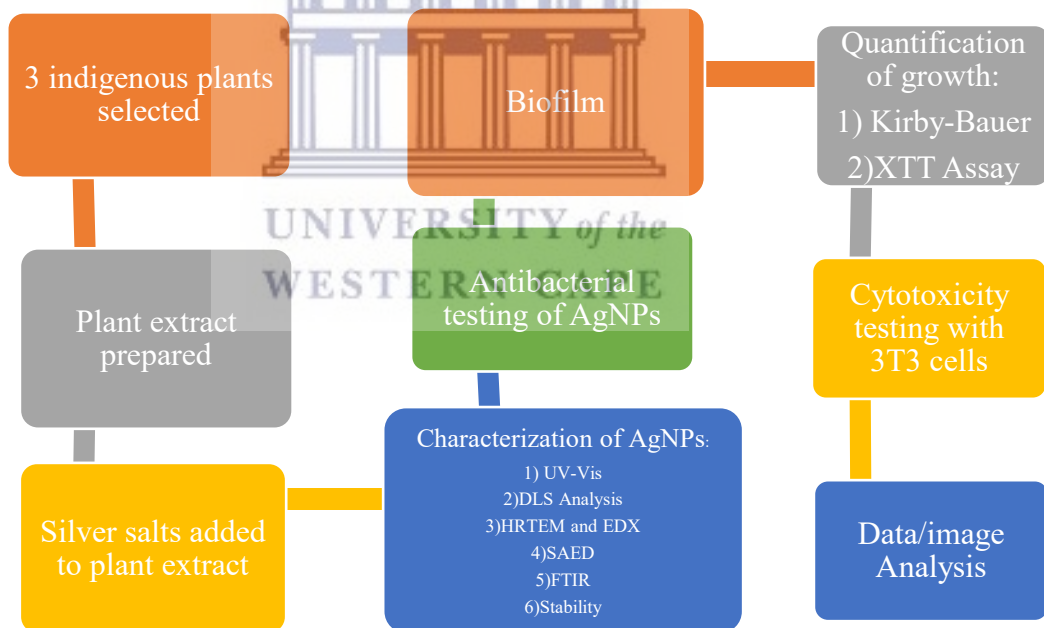
- Determine the antifungal action of the biosynthesised AgNPs against *Candida albicans*.
- Determine the biocompatibility of the biosynthesised AgNPs.

3.4 Null Hypothesis

- AgNPs synthesised from South African plants, namely *Berzelia lanuginose*, *Helichrysum cymosum*, and *Searsia crenata* will have no antifungal or cytotoxic properties.

3.5 Study Design

This was a descriptive *in vitro* experimental study. No patients or use of biological tissue was involved. Below shows a flow diagram of methods used.



3.6 Materials and Instruments

This section describes the materials and instruments used to carry out the research. Silver nitrate was purchased from Sigma Aldrich (Cape Town, South Africa) and 96-well microtiter plates were obtained from Greiner Bio-One GmbH (Frickenhausen, Germany). Centrifugation for the extracts was done using Allegra® X-12R (Beckman Coulter, Cape

Town, South Africa). The extracts were freeze dried using FreeZone 2.5 L (Labconco, Kansas City, MO, USA). UV-Vis (ultraviolet-visible) spectra were recorded using a SPECTROstar microplate reader (BMG Labtech, Cape Town, South Africa). The particle size, size distribution, and zeta potential measurements of the freshly synthesised NPs in the solution were analysed using Zeta Sizer (Malvern Instruments Ltd., Malvern, UK). The NPs were centrifuged using Centrifuge 5417R (Eppendorf AG, Hamburg, Germany). HRTEM analysis was done using Tecnai G2 F20 X-TWIN purchased from FEI in Eindhoven, Netherlands. The crystallographic properties were recorded by using results from SAED.

3.7 Plant Collection

This section describes the plant collection phase of the research. The topics discussed include *plant identification* and *preparation of the plant extracts*. These are discussed in more detail further below.

For the purpose of this study, the aerial part of three plant samples were randomly collected from two neighbouring sites in the Western Cape Province of South Africa, namely: from the grounds at CPUT Bellville and UWC Reserve, as indicated in Table 4 below.

Table 4. List of the collected plant species

Name of plant	Family	Code name	Collection Site
<i>Berzelia lanuginosa</i>	Bruniaceae	WK 13	The grounds at CPUT Bellville
<i>Helichrysum cymosum</i>	Asteraceae	WK 18	The grounds at CPUT Bellville
<i>Searsia crenata</i>	Anacardiaceae	EL 4	UWC Reserve

3.7.1 Plant identification

These plants were identified by the lecturers at the Horticultural Science Department, Cape Peninsula University of Technology (CPUT) namely Mr Gordon Dreyer, Mr

Terence Mabela, Mrs Deborah Erasmus, and Miss Carolyn Wilmot. These plants were then screened for their conservation status by Miss Z. Maphanga of the Cape Flats Nature Reserve.

3.7.2 Preparation of plant extracts

The plants were identified and collected; thereafter, the plant extracts were prepared according to Elbagory et al (2016). After drying the plant leaves were then grinded and extracted using boiled distilled water (50 mL of distilled water added to 5 g of each plant powder). A Büchner funnel was used to help with filtration. The plant leave decoctions were then centrifuged at 3750 rpm for 2 hours using an Allegra® X-12R centrifuge (Beckman Coulter, Cape Town, South Africa). The supernatant for each extract was then filtered through 0.45 µm filters (Elbagory *et al.*, 2016). Extracts were then kept overnight at -80°C and dried using FreeZone 2.5 L freeze dryer (Labconco, USA). A stock solution of (10 mg/ml) was freshly prepared for each extract before the screening step (Elbagory *et al.*, 2016).

3.8 Biosynthesis of AgNPs

In a 96-well plate, 250 µL of 1 mM silver salt was added to 50 µL of plant extracts stock solutions with increasing concentrations (0.007 to 16 mg/mL). The plates were then covered in foil and incubated at 70°C with shaking (40 rpm) (Elbagory *et al.*, 2016). After 1 hour of shaking, the surface plasma resonance of the AgNPs were then measured by recording the Ultraviolet-visible (UV-Vis) spectrum ranging from 300 nm to 800 nm. The machine used is called the SPECTROstar Nano by BMG Labtech. For further characterisation and stability evaluations, the synthesis of the AgNPs from the tested plant extracts was scaled up using the optimum concentration of the plant extracts (Elbagory *et al.*, 2016).

3.9 Characterisation of AgNPs

3.9.1 UV-Vis spectroscopy

UV-Vis spectroscopy is the most popular form of characterisation techniques to determine particle formation and its optical properties. It refers to absorption

spectroscopy or reflectance spectroscopy in the ultraviolet-visible spectral region. UV-Vis absorbance spectroscopy was carried out to monitor the formation of NPs (with a SPECTROstar Nano, BMG Labtech UV-Vis spectrophotometer). The UV readings were recorded immediately after the preparation (Elbagory *et al.*, 2016).

3.9.2 Dynamic light scattering (DLS) analysis

DLS was used to measure the hydrodynamic size and zeta potential of the synthesised NPs at 25°C by placing 1.0 mL in a cuvette. The measurement is done three times and the average was calculated for the size and the charge. These measurements were performed on all samples and selected concentrations (Elbagory *et al.*, 2016).

3.9.3 High Resolution Transmission Electron Microscopy (HRTEM) and Energy Dispersive X-ray Spectroscopy (EDX) analysis

To study the surface morphology of the AgNPs, samples were prepared by drop-coating one drop of each sample solution onto a holey carbon coated copper grid. This was then covered and dried under a Xenon lamp for 10 minutes, after which the sample coated grids were analysed under the microscope. Transmission electron micrographs were then operated in bright field mode at an accelerating voltage of 200 kV. The TEM analysis was done by monitoring TEM images and the size of the NPs was determined using ImageJ software (Elbagory *et al.*, 2016).

To prepare for energy dispersive X-ray spectroscopy analysis, 1 cm by 1 cm glass slides were used and cleaned with ethanol and water. They were then placed in a petri dish and labelled with the names of the various samples. Multiple drops of the AgNPs solution were placed onto the glass slides, which were then placed into the oven to dry at 70°C. This process was continued until each slide had a thick film of material (Elbagory *et al.*, 2016).

3.9.4 Stability testing of synthesised AgNPs

The in vitro stability of the synthesised AgNPs was measured by incubating the AgNPs with two aqueous buffer solutions namely: Cysteine and Bovine Serum Albumin (BSA). First, the synthesised AgNPs were centrifuged at 10,000 rpm for 5 min. The pellets were washed three times with distilled water to remove phytochemicals that are not capping the AgNPs. The NPs were re-suspended in 1 mL autoclaved distilled water. Thereafter, 100 μ L of the tested AgNPs solutions were incubated with equal volume of the buffer solutions in a 96-well plate. The final concentrations of the biological media in the final mixture were as follows: 0.5% cysteine, and 0.5% BSA. The stability of the AgNPs were evaluated by measuring the changes in UV-Vis spectra after 1, 4, 6, 12 and 24 h (Elbagory *et al.*, 2016).

3.9.5 Fourier-transform infrared spectroscopy analysis

Another essential technique used to characterise AgNPs is Fourier-transform infrared spectroscopy (FTIR). The distinctive vibrational spectroscopic approach of the FTIR technique results in qualitative as well as quantitative analysis for almost any form of a material sample (organic or inorganic). It is also an effective technique to determine and analyse the various functional groups of the material while showing the different chemical bonds in the material (Mourdikoudis, Pallares & Thanh, 2018). In this study, solid samples of AgNPs were then kept overnight at -80°C and dried using FreeZone 2.5 L freeze dryer (Labconco, USA). Prior to loading them into the machine, the freeze dried AgNPs and extract samples were ground down to confirm that they were dry and even. Then a pellet was formed using a standard clamp, and finally, the pellet was spectroscopically analysed.

3.10 Testing Antimicrobial Activity of AgNPs

This section tested the antimicrobial activity of the AgNPs. This entailed acquiring a yeast culture; testing the effects of the NPs on *Candida*; and then determining the effect of the NPs on biofilm.

3.10.1 Acquisition of yeast culture

Candida albicans (ATCC 90028) was acquired from UWC Oral and Dental Research Laboratory. Gram staining was done to confirm it is a gram-positive yeast. The culture was then streaked on Brain Heart Infusion (BHI) Agar and incubated for 24 hours at 37°C to check for its purity and to select isolates for further testing. These pure cultures were then streaked on fresh BHI agar plate, incubated for 24 hours at 37°C, and then kept aseptically at 4°C till needed for further experiments.

3.10.2 Testing the effect of the NPs on *Candida*

Initially the assumption was made that all the synthesised NPs had the same effect on *Candida albicans* (ATCC 90028). Two tests were done to determine the effect of the NPs on *Candida*, namely (a) Kirby-Bauer and (b) 2H-Tetrazolium-5-Carboxanilide (XTT) assays for unattached planktonic and sessile yeast.

3.10.2.1 Kirby-Bauer test

a) Preparation of discs

As indicated in Table 5, the total number of 72 discs were used and divided into 6 groups according to number of plants and nanoparticle treatments, resulting in 18 discs per treatment and plant. The 18 discs were placed into -3 subgroups according to the concentrations tested namely: 350µl, 400µl and 500µl. Each subgroup thus had 3 discs. Additional discs were assigned to the control group, 3 discs for chlorhexidine and 3-discs for the Negative control (CLSI, 2017).

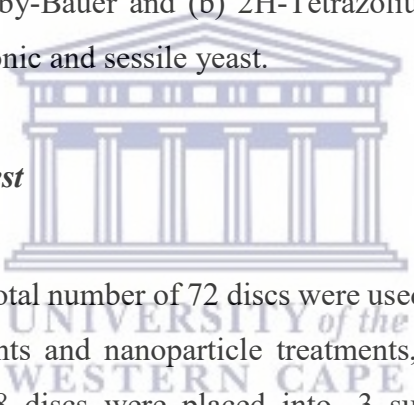


Table 5. Indicating the number of filtered discs and various concentrations used for the Kirby-Bauer test. Total sample size (n=72).

AgNPs	Extract/NP	Number of discs	Number of discs	Number of discs
		350 µl	400 µl	500 µl
WK13	Extract	3 discs	3 discs	3 discs
	Nanoparticle	3 discs	3 discs	3 discs
WK18	Extract	3 discs	3 discs	3 discs
	Nanoparticle	3 discs	3 discs	3 discs
EL4	Extract	3 discs	3 discs	3 discs
	Nanoparticle	3 discs	3 discs	3 discs
Control (Chlorexidine)		3 discs	3 discs	3 discs
Negative Control		3 discs	3 discs	3 discs
Total		24 discs	24 discs	24 discs

Filtered discs (Munktell) of 10 mm in diameter were aseptically infused with 400 µL of the NPs solution from different plants in a class II fume hood cabinet (Bio-Flow by Labotec). These discs were air dried at room temperature until they were completely dried. The discs were aseptically kept closed at room temperature until needed (CLSI, 2017).

b) Preparation of cultures

The inocula for the Kirby-Bauer testing were taken from the previously prepared cultures kept at 4°C. A single isolate was randomly selected and plated on a fresh BHI agar plate and incubated 24 hours at 37°C. Thereafter, the resultant isolate was picked and transferred in a test tube containing Phosphate Buffered Saline (PBS). The solution was adjusted to 0.5 McFarlands standards (McF) at room temperature using the DensiCheck (Biomérieux, INC) previously calibrated at 0.00, 0.50, 2.00 and 3.00 McF (CLSI, 2017).

c) Application of nanoparticles on cultures

A 100 µL of the adjusted yeast suspension was then pipetted onto a fresh Mueller-Hinton (MH) agar plate and evenly spread using a glass hockey stick. Thereafter, the infused

discs were aseptically placed onto the spread plate. The plates were then incubated at 24 hours at 37°C. After the lapse of the 24 hours, the diameters of the zones of inhibition were measured using electronic digital callipers. These zones of inhibitions were captured onto a spreadsheet and later analysed (CLSI, 2017).

3.10.2.2 XTT assay

To measure the effect of the treatment (NP) on the sessile yeast (biofilm), changes in the amount of live yeast were indirectly measured. This was observed both qualitatively and quantitatively on the machine (model SMR 16.1) from Biocom by noting changes in colour and optical densities (OD), respectively, across the samples.

a) Preparation of culture and biofilm formation

The inocula for the XTT assay were taken from the previously prepared cultures kept at 4°C. A single isolate was randomly selected and plated on a fresh BHI agar plate and incubated 24 hours at 37°C. Thereafter, the resultant isolate was picked and transferred in a test tube containing Phosphate Buffered Saline (PBS). The solution was adjusted to 0.5 McF at room temperature using the DensiCheck (Biomerieux, INC) previously calibrated at 0.00, 0.50, 2.00 and 3.00 McF (Balouiri, Sadiki and Ibsouda, 2016).

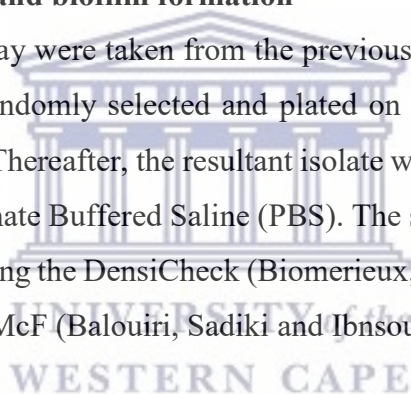


Table 6. 96-well plate setting and treatment

	1	2	3	4	5	6	7	8	9	10	11	12
B	Orange	Orange	Orange	Blue	Blue	Blue	Green	Green	Green	Red	Red	Yellow
C	Orange	Orange	Orange	Blue	Blue	Blue	Green	Green	Green	Red	Red	Yellow
D	Orange	Orange	Orange	Blue	Blue	Blue	Green	Green	Green	Red	Red	Yellow
E	Orange	Orange	Orange	Blue	Blue	Blue	Green	Green	Green	Red	Red	Yellow
F	Orange	Orange	Orange	Blue	Blue	Blue	Green	Green	Green	Red	Red	Yellow
G	Orange	Orange	Orange	Blue	Blue	Blue	Green	Green	Green	Red	Red	Yellow
H	Orange	Orange	Orange	Blue	Blue	Blue	Green	Green	Green	Red	Red	Yellow

Key:

Orange	– Treatment/plant 1 (WK 13)
Blue	– Treatment/plant 2 (WK 18)
Green	– Treatment/plant 3 (EL 4)
Red	– Blank
Yellow	– Untreated biofilm

As seen in Table 6, each 96-well plate was divided into 2 sections: columns 1–9 and columns 10–12, experiments and controls, respectively.

In total, 84 wells were used. For each treatment, 21 wells (n=21) were used, for example: for treatment 1 (WK 13), wells B1–H3 were used. The subsequent two sets of three columns were used for treatment 2 (WK 18), respectively. Wells B10–H12 were left for controls (14 blank and 7 wells for the untreated biofilm).

1. Fifty (50) microlitres of BHI and 150 microliters of 0.5 McF *Candida albicans* was pipetted into all the wells. The plate was then incubated for 48 hours at 37°C to fully develop the biofilms.
2. After incubation, the plate was then washed three times with sterile PBS. A hundred (100) microlitres of BHI was then added to each well; the biofilm was then allowed to acclimatise for 5 minutes.
3. A hundred (100) microlitres of the synthesised NPs was then added to each well of the experimental section. In the control section, 100 µL of sterile distilled water was pipetted.

4. The plate was then incubated for another 24 hours (Balouiri, Sadiki & Ibnsouda, 2016b).

3.10.3 Determining the effect of NPs on biofilm

The Cell Proliferation Kit II (Sigma Aldrich, South Africa) was used to visualise the effect of the treatments. The two components of the kit (XTT labelling reagent and electron-coupling reagent) were thawed at 37°C and mixed at a proportion of 5:0.1 (XTT to coupling agent) (Balouiri, Sadiki & Ibnsouda, 2016b). The 2,3-Bis-(2-Methoxy-4-Nitro-5-Sulphophenyl)-2H-Tetrazolium-5-Carboxanilide (XTT) assay is a colorimetric assay that detects metabolic activity by measuring the reduction of the tetrazolium salt reagent XTT.

1. After 24 hours of incubation, the treatment in the 96 well plate was washed using PBS three times and discarded each time. A hundred (100) microlitres of PBS was added into each well using pipette. Fifty (50) microlitres of XTT mixture was also added into each well.
2. The XTT plates were covered in foil and allowed to stand for 2 hours at room temperature.
3. After the 2-hour lapse, the plates were observed, and photos were taken.
4. Thereafter OD readings were taken on the spectrophotometer at wavelengths of 562 nm and 630 nm. This was recorded as T0.
5. Readings were taken again after 2 hours (T2) and 4 hours (T4) to observe if any changes occurred over time (Balouiri, Sadiki & Ibnsouda, 2016b).

3.10.4 Minimum inhibitory concentrations using XTT

In order to measure the effects due to the interventions, MICs were assessed both quantitatively and qualitatively by comparing the equivalence between colour change of experiments and controls for qualitative assessment. Comparison of OD readings was done for the quantitative assessment. The MICs were defined as the lowest intervention concentrations at which these equivalences occurred.

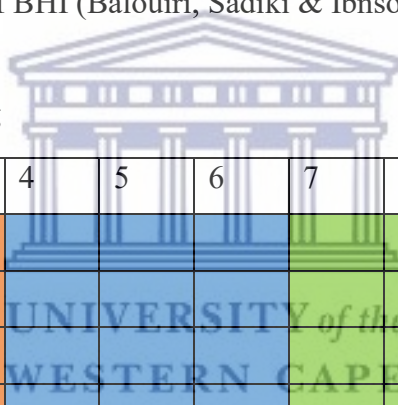
3.10.4.1 Preparation of culture and biofilm formation

The inocula for the XTT assay were taken from the previously prepared cultures kept at 4°C. A single isolate was randomly selected and plated on a fresh BHI agar plate and incubated for 24 hours at 37°C. Thereafter, the resultant isolate was picked and transferred in a test tube containing PBS. The solution was adjusted to 0.5 McF at room temperature using the DensiCheck (Biomerieux, INC) previously calibrated at 0.00, 0.50, 2.00 and 3.00 McF (Balouiri, Sadiki and Ibsouda, 2016).

3.10.4.2 96-well plate setting and treatment

As seen in Table 7, a 96-well plate was used: columns 1–3 used for one treatment/plant; 4–6 used for another; 7–9 used for another; column 10 blank; column 11 media; column 12 untreated 50 microlitres of BHI (Balouiri, Sadiki & Ibsouda, 2016b).

Table 7. 96-well plate setting



	1	2	3	4	5	6	7	8	9	10	11	12
B	Orange	Orange	Orange	Blue	Blue	Blue	Green	Green	Green	Red	Yellow	Grey
C	Orange	Orange	Orange	Blue	Blue	Blue	Green	Green	Green	Red	Yellow	Grey
D	Orange	Orange	Orange	Blue	Blue	Blue	Green	Green	Green	Red	Yellow	Grey
E	Orange	Orange	Orange	Blue	Blue	Blue	Green	Green	Green	Red	Yellow	Grey
F	Orange	Orange	Orange	Blue	Blue	Blue	Green	Green	Green	Red	Yellow	Grey
G	Orange	Orange	Orange	Blue	Blue	Blue	Green	Green	Green	Red	Yellow	Grey
H	Orange	Orange	Orange	Blue	Blue	Blue	Green	Green	Green	Red	Yellow	Grey

Key:

Orange	– Treatment/plant 1 (WK 13)
Blue	– Treatment/plant 2 (WK 18)
Green	– Treatment/plant 3 (EL 4)
Red	– Blank
Yellow	– Media
Grey	– Untreated

Each of the synthesised AgNPs were tested in triplicate over 4 timed intervals at 4, 6, 24, and 48 hours. A hundred and fifty (150) microlitres of the synthesised AgNPs were placed

into the entire A row and 100 microlitres of PBS into each of the other wells. A hundred (100) microlitres of the synthesised AgNPs were then taken from wells A into wells B and serial dilution was continued until row H. Fifty (50) microlitres of BHI was then added to all the wells. A hundred and fifty (150) microlitres of *Candida albicans* was added to each well (Balouiri, Sadiki & Ibensouda, 2016b).

3.10.4.3 XTT reduction assay

Materials

0.5 mg/ml XTT in PBS (XTT Sodium Salt, Sigma X4251)

0.32 mg/ml Phenazine methosulfate (PMS) in water Sigma P9625

Plate reader with optical density capabilities (492 nm) compatible with 96- or 384-well plate formats (Biocom- model SMR 16.1)

Procedure

1. Following cell density determination for overnight cultures, cells were added to wells at a final OD 600 = 0.5 (or equivalent to $\sim 1 \times 10^7$ cells/ml) in 200 μ l for 96-well plate assays or 1 μ l of overnight culture in 90 μ l.
2. The plates were sealed with Breathe-Easy® sealing membranes. Sealing the plates reduces evaporation and prevents cross-contamination between wells.
3. The plates were shaken at 37°C for 90 min at 250 rpm (96-well) in an incubator.
4. The membrane was removed, and the media was aspirated. The pipette tips on aspirator were changed between wells of different strains and/or conditions.
5. The wells were washed with 200 μ l of PBS. The PBS was aspirated.
6. Two hundred (200) μ l of fresh media was added to each well.
7. The plate was resealed with a new sealing membrane and shaken at 37°C for 24 hours at 250 rpm.
8. Roughly 15–30 min before the end of the 24-hour growth step, fresh XTT and PMS solutions were prepared. Centrifuging before use was done in order to remove any insoluble materials and transfer carefully to a new tube. Protected from light.
9. XTT and PMS were mixed at a ratio of 9:1 XTT: PMS. The solution was protected from light.

10. The membrane was removed from the plate and the media was aspirated from the wells.
11. A hundred (100) μ l of XTT: PMS mixture was added to the wells while taking care to avoid disrupting the biofilm.
12. The plate was then incubated for 30 min at 37°C in the dark.
13. The OD was measured on the Biocom plate reader (model SMR 16.1) (Gulati *et al.*, 2018).

The extracts were then tested for possible cytotoxicity. This procedure is described in more detail next.

3.11 Cytotoxicity Testing

In order to evaluate the possible cytotoxicity of the extracts, the MTT assay was followed. This widely used assay is a sensitive, quantitative, and most reliable colorimetric test that measures viability, proliferation, and activation of cells. The cells used were a Human Oral Fibroblast cell line (Buccal Mucosa Fibroblasts) established in the Oral and Dental Research Institute, University of the Western Cape, as these fibroblasts were well suited for the oral environment (van Wyk *et al.*, 1994). Stocks of these cells were kept frozen in liquid nitrogen and retrieved for use. Cells were maintained and cultured in standard conditions (37°C with 5% carbon dioxide and 95% humidity) in Dulbecco's Modified Eagles Medium (DMEM). The medium was supplemented with 10% fetal bovine serum, penicillin (10.000 U/ml) and streptomycin (10.000 μ g/ml) mix (Biochrom Ltd), changed every second day and cells sub-cultured using routine trypsin/EDTA procedures.

Table 8. Cytotoxicity layout

	WK 13		WK 18		EL 4	
	Extract	Nanoparticle	Extract	Nanoparticle	Extract	Nanoparticle
1%						
3%						
5%						
10%						
25%						
Control						

Three samples of the AgNPs and 3 samples of the extract were chosen, namely WK 13, WK 18, and EL 4, and tested, and a range of 5 concentrations (1%, 3%, 5%, 10% and 25%) used for each of the 6 samples (see Table 8).

1. In order to test the cytotoxicity towards the fibroblasts, the cells were first grown to near confluency.
2. Then the 3T3 cells were diluted to a final cell suspension containing approximately 3×10^4 cells/ml and plated out in 96 well plates.
3. A hundred (100) μ l of a range of concentrations for each of the 6 samples were plated out while 100 μ l normal DMEM acted as controls.
4. After 24 hours, the MTT assay was used to evaluate cell inhibition or stimulation of cell growth. This assay involves the ability of viable cells to use mitochondrial dehydrogenase enzymes to convert MTT (a soluble tetrazolium salt) to a blue/violet formazan end-product (Grobler *et al.*, 2014).
5. Ten μ l MTT (5mg/ml in phosphate-buffered solution) was added to each well and left for a further 3 hours to incubate at 37°C.
6. The medium was discarded afterwards to eliminate the MTT, and the precipitated formazan crystals were subsequently solubilised with 100 μ l/ well of dimethylsulfoxide (DMSO).
7. Absorbance was measured at wavelength 540 nm on a RT2100C spectrophotometer to determine the number of viable cells.

Some concluding remarks follow next to wrap up the chapter.

3.12 Conclusion

This chapter described the research design and methodology employed to explore the antimicrobial and cytotoxic potential of AgNPs synthesised from South African plant species, namely: *Berzelia lanuginosa*, *Helichrysum cymosum*, and *Searsia crenata*. The next chapter includes results and the discussion of the results obtained.



CHAPTER 4

RESULTS AND DISCUSSION

4.1 UV–vis Spectrophotometer of Synthesized AgNPs

The leaf extract from *Berzelia lanuginosa* (WK 13), *Helichrysum cymosum* (WK 18) and *Searsia crenata* (EL 4) showed rapid conversion of silver nitrate into silver nanoparticles which was indicated by distinct colour changes from clear to yellow to dark brownish yellow within few minutes of the extract addition in AgNO (1 mM) as shown in Figures 3, 4 and 5. The colour arises due to excitation of surface plasmon vibrations in the silver metal nanoparticles which is unique to metallic nanoparticles and gives a characteristic wavelength of certain metallic particles that depend on the shape and size of nanoparticles (Hein and Baxter, 2019).



Figure 3. Screening of *Berzelia lanuginosa* (WK 13) to biosynthesis silver NPs at 70 °C



Figure 4. Screening of *Helichrysum cymosum* (WK 18) to biosynthesis silver NPs at 70 °C



Figure 5. Screening of *Searsia crenata* (EL 4) to biosynthesis silver NPs at 70 °C

For *Berzelia lanuginosa* (WK 13) the UV absorption spectrum of silver nanoparticles as a function of reaction time is shown in Figure 6. There was maximum absorption between 400 and 500 nm with average maximum absorption at 430 ± 1.5 nm. For *Helichrysum cymosum* (WK 18) the UV absorption spectrum of silver nanoparticles as a function of reaction time is shown in Figure 7. There was maximum absorption between 400 and 500 nm with average maximum absorption at 440 ± 1.5 nm. For *Searsia crenata* (EL 4) the UV absorption spectrum of silver nanoparticles as a function of reaction time is shown in Figure 8. There was maximum absorption between 400 and 500 nm with average maximum absorption at 428 ± 1.5 nm. This absorption is known as surface plasmon resonance; it is a result of the conduction of electrons on the surface of AgNPs. With an increased gum concentration, there is an improvement in the nanoparticle synthesis. Metal nanoparticles have free electrons, which yield a surface plasmon resonance (SPR) absorption band, due to the mutual vibration of electrons of metal nanoparticles in resonance with light wave broadening of peak indicated that the particles are polydispersed (Hein and Baxter, 2019). The presence of the peaks show the characteristics of SPR of AgNPs (Anandalakshmi, Venugobal and Ramasamy, 2016). After adding the leaves extract in AgNO solution, the biomolecules become stabilized in the medium. The biomolecules interact with each other and with the silver salt. After the initial interaction, silver salt is then consumed, and the process of nucleation, reduction, and capping starts, leading to nanoparticles synthesis (Poopathi *et al.*, 2015). As mentioned, the peaks recorded in this study are as follows (*Berzelia lanuginosa* 430 ± 1.5 nm, *Helichrysum cymosum* 440 ± 1.5 nm and *Searsia crenata* 428 ± 1.5 nm), which was similar and within range of findings reported by several other studies namely 426 nm (Hein and Baxter, 2019), 450-500nm (Sadeghi, Rostami and Momeni, 2015), 435 nm (Bhat *et al.*, 2011), 420nm (Zahir *et al.*, 2015), 425 nm (Zafar and Zafar, 2019). A study done by Singh *et al* recorded a peak of 410nm which was outside of this range (Singh, Yeon Ju Kim, *et al.*, 2016). The specific plants tested were not studied prior to conducting this study.

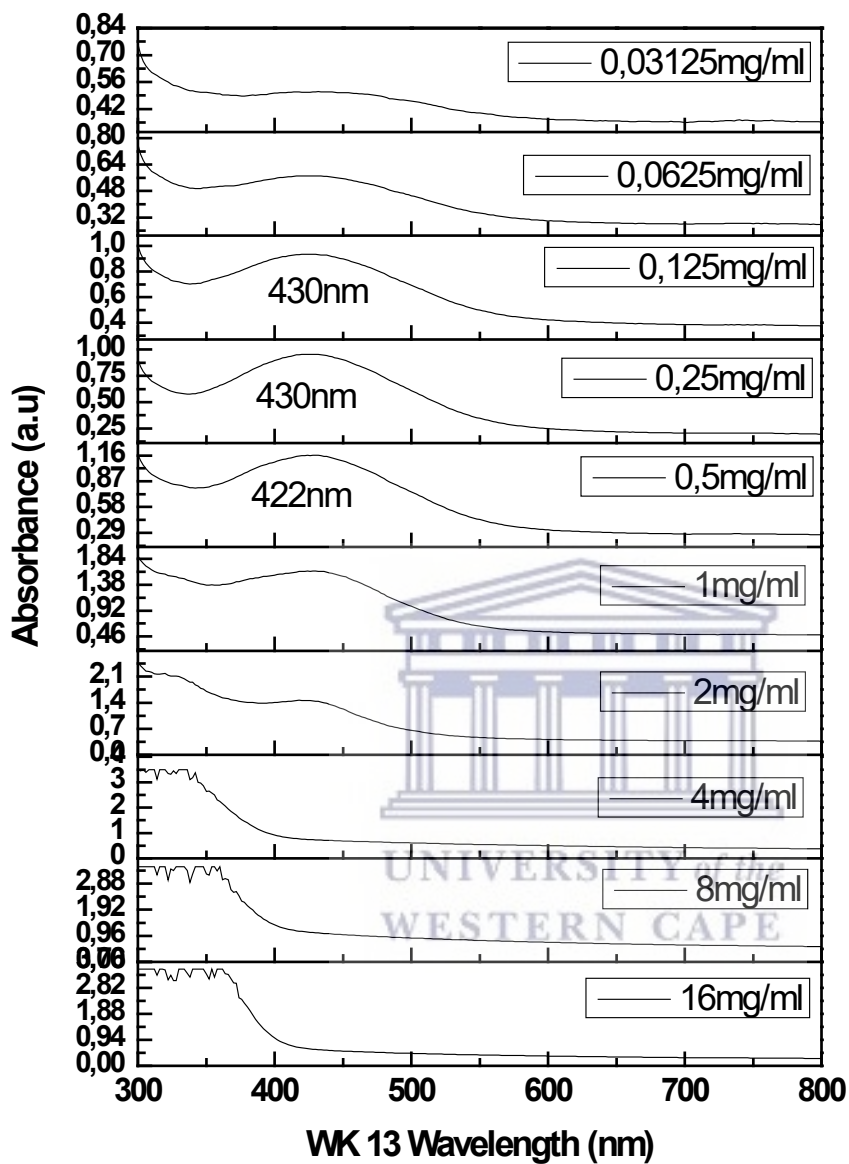


Figure 6. The UV absorption band of silver nanoparticle from serially diluted *Berzelia lanuginosa* shows that it was concentration dependent and the absorption at 0.25 mg/mL reflected a good peak symmetry suggesting the existence of good silver nanoparticles at that concentration

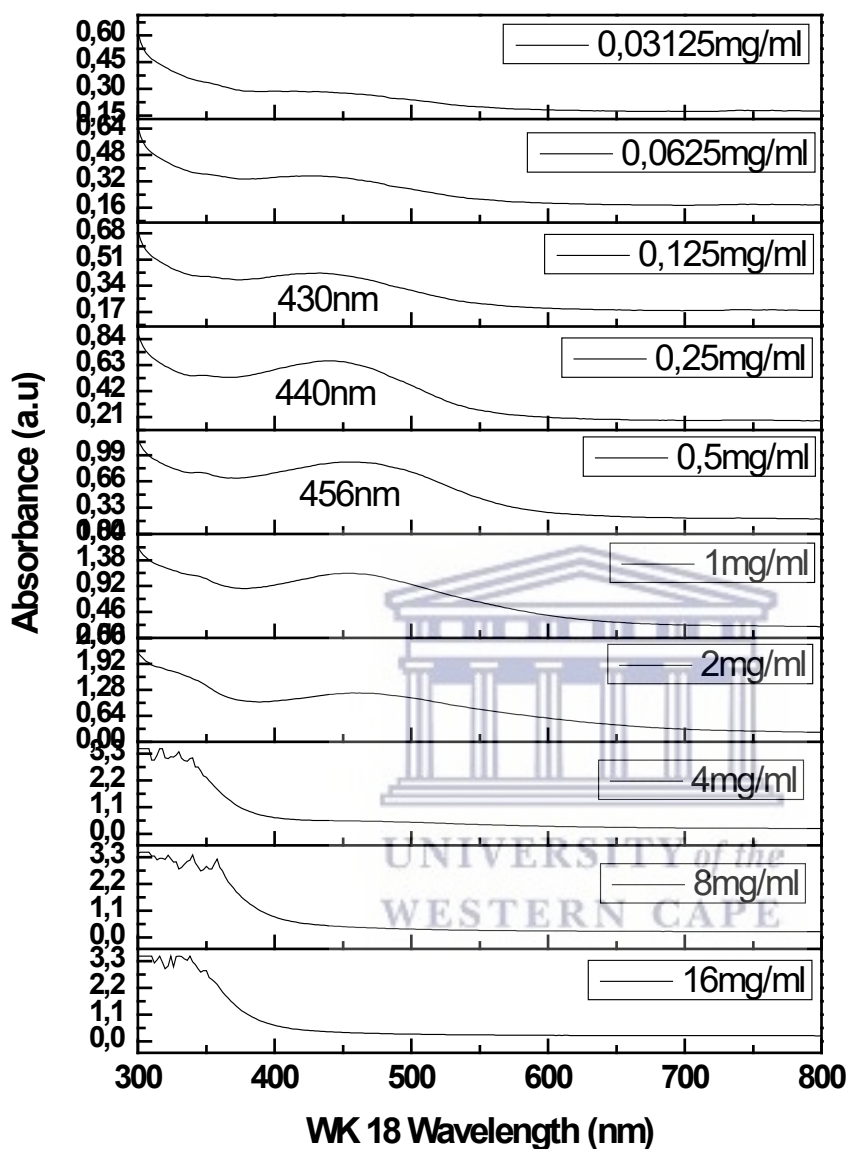


Figure 7. The UV absorption band of silver nanoparticle from serially diluted *Helichrysum cymosum* shows that it was concentration dependent and the absorption at 0.25 mg/mL reflected a good peak symmetry suggesting the existence of good silver nanoparticles at that concentration

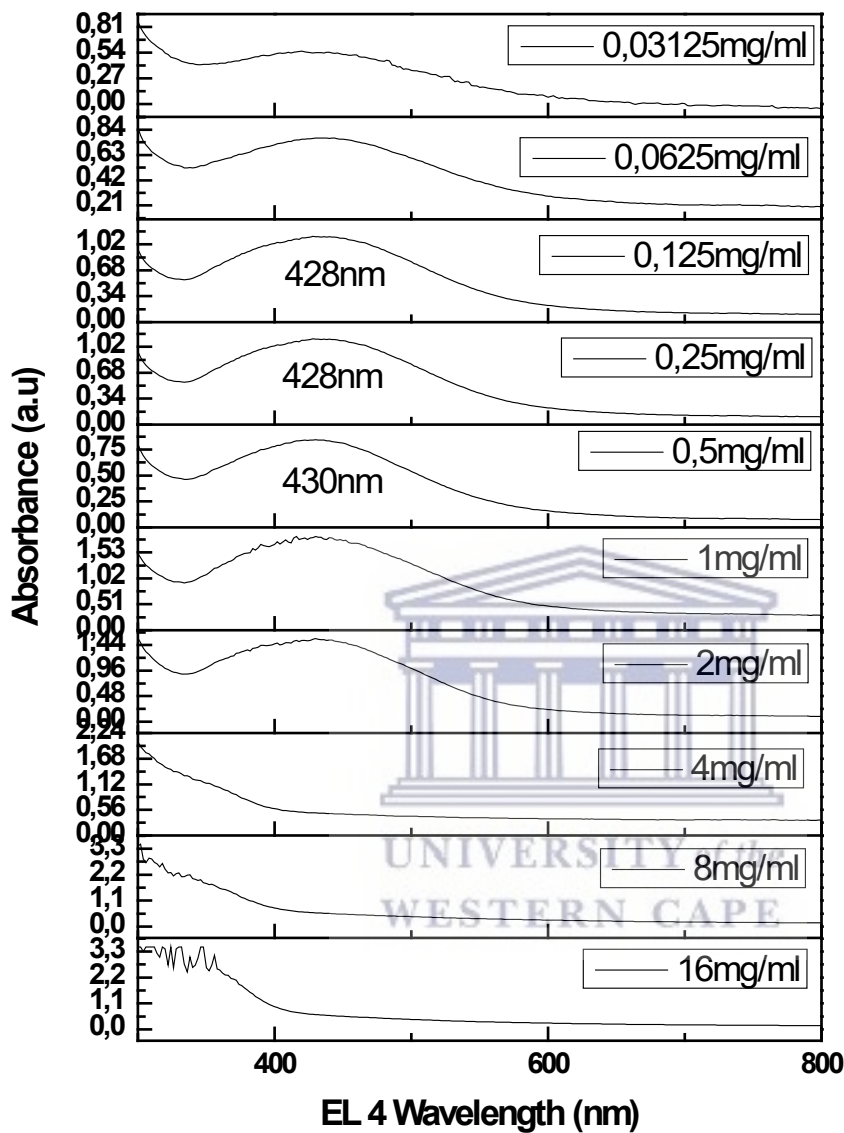


Figure 8. The UV absorption band of silver nanoparticle from serially diluted *Searsia crenata* shows that it was concentration dependent and the absorption at 0.25 mg/mL reflected a good peak symmetry suggesting the existence of good silver nanoparticles at that concentration

4.2 Dynamic Light Scattering (DLS) and Zeta Potential

Dynamic light scattering (DLS) was used to determine the size (average diameter) and zeta potential of the biosynthesized nanoparticles. The DLS size distribution image of the biosynthesized silver nanoparticles of WK 13, WK 18, and EL 4 is shown respectively in Figures 9, 10 and 11. It was found that the size distribution of AgNP of WK 13 is 83.54 nm, WK 18 is 98.91 nm, and EL 4 is 108.1 nm. The broad spectrum of DLS analyser confirms that the particle size is decreased when compared with the sharp SPR peak of WK 13 of 430 nm, WK 18 of 440nm and EL 4 of 428nm obtained in the UV–Vis spectra (Anandalakshmi, Venugobal and Ramasamy, 2016).

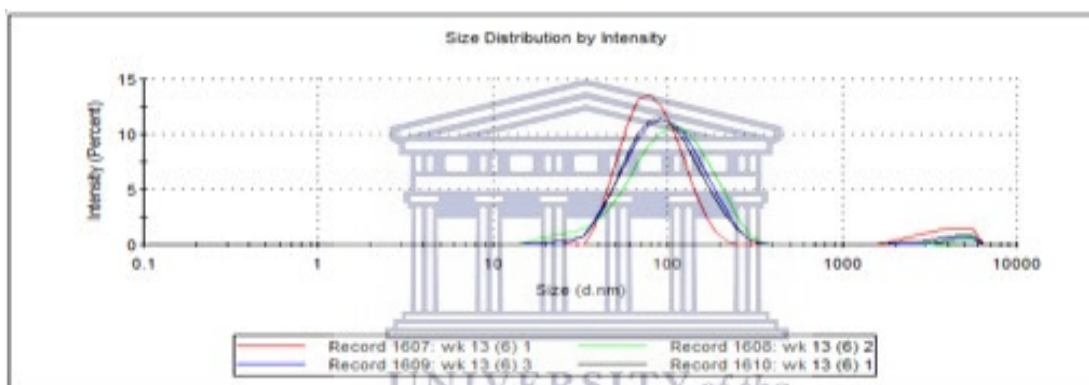


Figure 9. DLS WK 13 size distribution of 83.54 nm

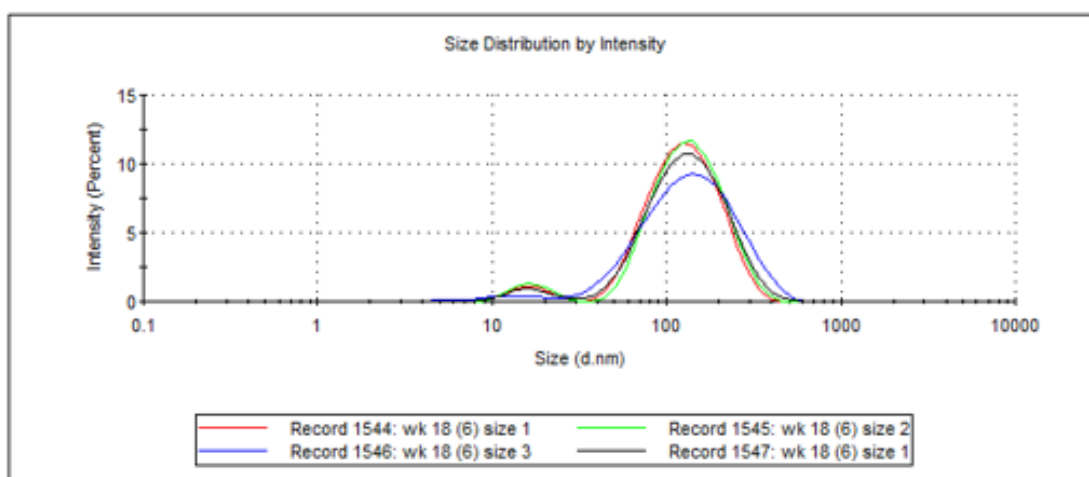


Figure 10. DLS WK 18 size distribution of 98.91 nm

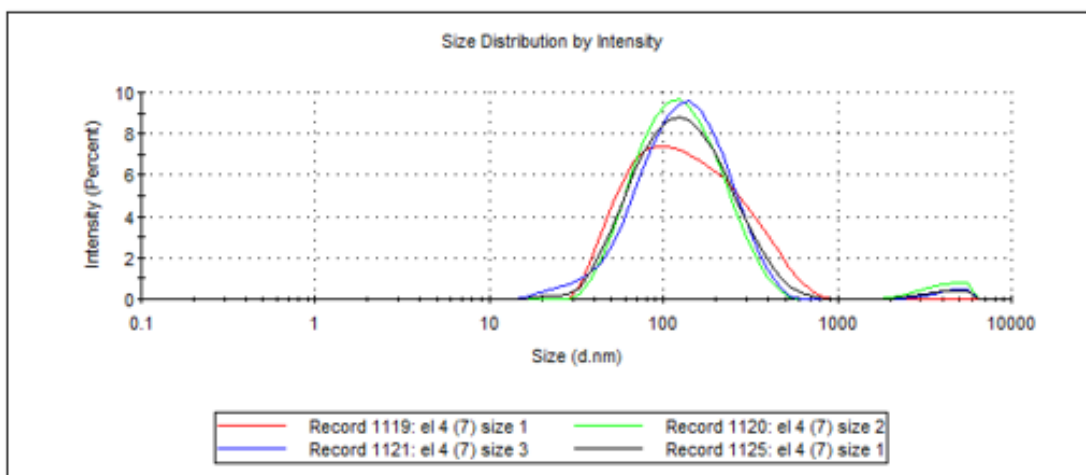


Figure 11. DLS EL 4 size distribution of 108.1 nm

The zeta potential is used to depict the surface charge and stability of AgNPs (Singh *et al.*, 2018). The mobility of the particle toward the electrode of the opposite charge is determined as the Zeta potential. Zeta potential is the measurement of the speed at which the ion travels to an electrode of an opposite charge, it is also a measure of stability of particles in solution. Particles of the same charge repel each other causing a layer around the electrode, the thickness of this layer and stability is then measured after repulsion. The more negative the particles charge is, the greater the repulsion and therefore the greater the stability. In general, zeta potentials can be used to predict the long-term stability of nanoparticles in a solution, where the volume of the charge reflects the forces of mutual antagonism between particles (Chanda *et al.*, 2011). Figure 12, shows that the biosynthesized AgNPs (WK13) had a negative charge with a zeta potential value of -23.4 mV this zeta potential value fall between -20 to -30 mV which falls in the range of moderately stable, Figure 13 shows WK 18 had a negative charge with a zeta potential value of -18.8 mV this zeta potential value fall between -10 to -20 mV which falls in the range of unstable and Figure 14 shows EL 4 had a negative charge with a zeta potential value of -31.3 mV this zeta potential value is $> \pm 30$ mV which falls in the range of highly stable (Kane, Mishra and Dutta, 2016).

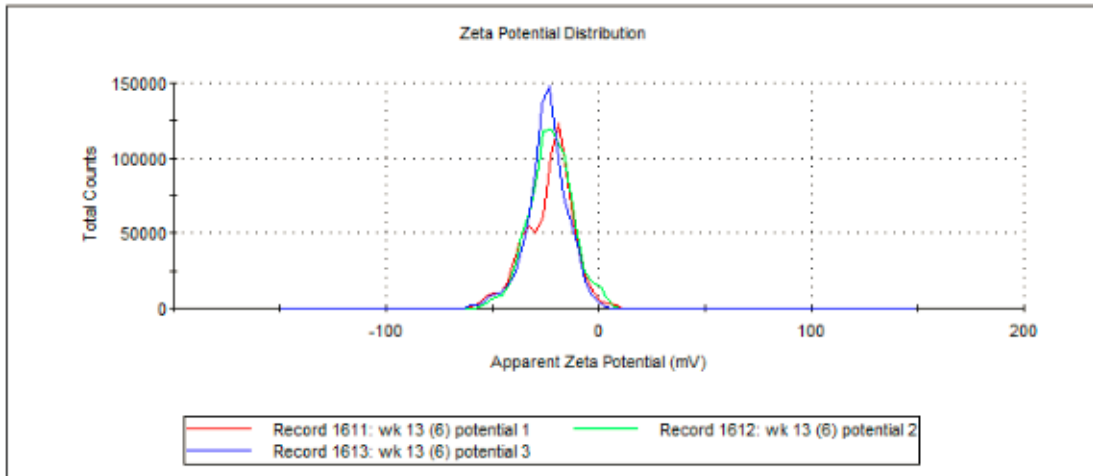


Figure 12. Zeta potential distribution of WK 13 depicting a negative charge of -23.4mV

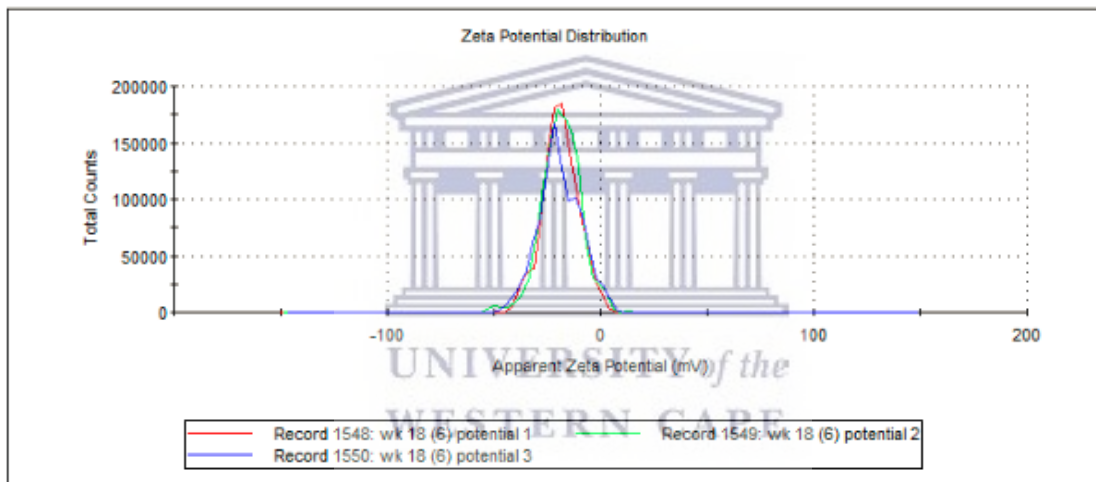


Figure 13. Zeta potential distribution of WK 18 depicting a negative charge of -18.8mV

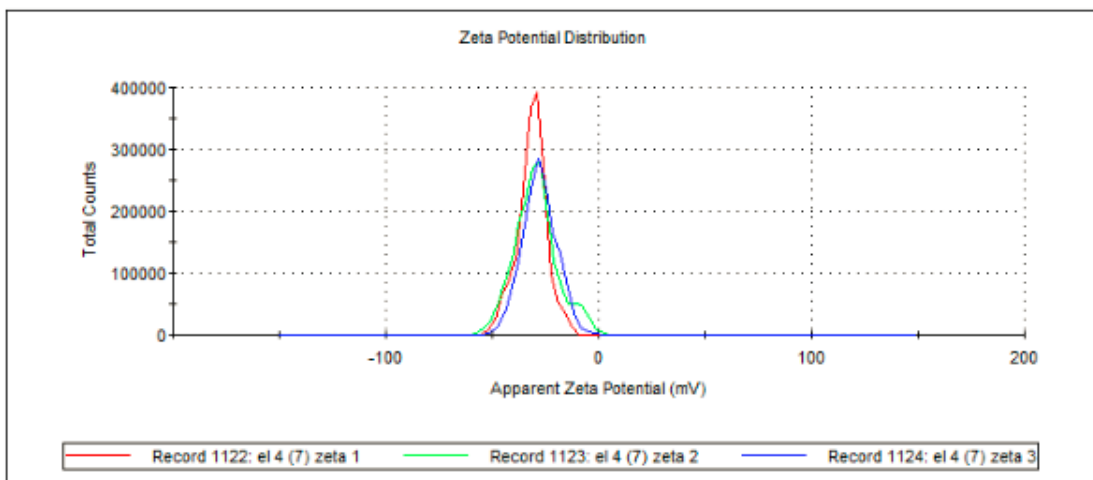


Figure 14. Zeta potential distribution of EL 4 depicting a negative charge of -31.3mV

4.3 High Resolution Transmission Electron Microscopy (HR-TEM)

High Resolution Transmission electron microscopy (HR-TEM) is one of the most improved techniques to study the shape, size and distribution of the NPs. In general, the size distribution of NPs is important as NPs display different chemical and physical properties depending on their size and shape (Protima Rauwel, Siim K  n  l, Stanislav Ferdov, 2014).

The HR-TEM image of the biosynthesized samples of WK13, WK 18, EL 4 are respectively shown in Figures 15a, 16a and 17a. The results show that the nanoparticles synthesized from the different plant extracts revealed various shapes and relative sizes as observed from the HR-TEM images in Figures 15a, 16a and 17a. AgNPs synthesized from WK 13 and EL 4 revealed spherical shapes of different sizes. These spherical shapes are a common feature in AgNPs as previously reported (Ahmed *et al.*, 2016, Murugan *et al.*, 2014, Anuj and Ishnava, 2013). WK 18 revealed a variety of shapes and sizes, namely: triangular, hexagonal, spherical, and pentagonal shapes. This was also observed by Kiran Kumar *et al.* (2014). It is believed that the shape anisotropy is due to a decrease in protective biomolecules which aids in the homogeneity of the shape during growth. This forces them to attain thermodynamic stability by acquiring shapes such as hexagons and triangles (Kiran Kumar *et al.*, 2014). The monodispersity of these nanoparticles is attributed to the capping layer of polyphenols which are known to reduce Ag^{+2} to Ag^{+0} and the oxidized polyphenol binds to the AgNPs via $-\text{C}=\text{O}$ bonds and concurrently stabilizes them (Protima Rauwel, Siim K  n  l, Stanislav Ferdov, 2014). It was also observed that AgNPs synthesized with plant extracts specifically in WK 13 and WK 18 are surrounded by a thin layer known as an aura from organic matter (Banerjee *et al.*, 2014, Shankar *et al.*, 2004, Song and Kim, 2009). Figures 15c, 16c and 17c depict the relevant histograms for WK 13, WK 18 and EL 4 and showed average sizes of 16-20nm, 31-60nm and 57-72nm respectively. These sizes are common as they were found in studies conducted by Murugan *et al.*, (2014, Khalil *et al.*, (2014, Anuj and Ishnava, (2013). The hydrodynamic size of the AgNPs was 83.54 d.nm, 98.91 d.nm and 108.1 d.nm, whilst the HR-TEM core size was 16-20nm, 31-60nm and 57-72nm for WK 13, WK 18 and EL 4 respectively. Differences between size determination done by DLS and HR-TEM have been reported previously (Elbagory *et al.*, 2016) . The confirmation of the presence of

crystallinity is seen via the lattice fringes present on the synthesized nanoparticles (Figures 15d, 16d, 17d). This was then further confirmed by SAED pattern observed (Figures 15b, 16b, 17b). The lattice fringe spacing was similar to that previously reported for AgNPs synthesized from *Murraya koenigii*, *Iresine herbstii*, *Pulicaria glutinosa*, *Medicago sativa*, *Salvia africana-lutea* and *Sutherlandia frutescens* (Lukman *et al.*, 2011; Philip *et al.*, 2011; Dipankar and Murugan, 2012; Khan *et al.*, 2013; Dube *et al.*, 2020).

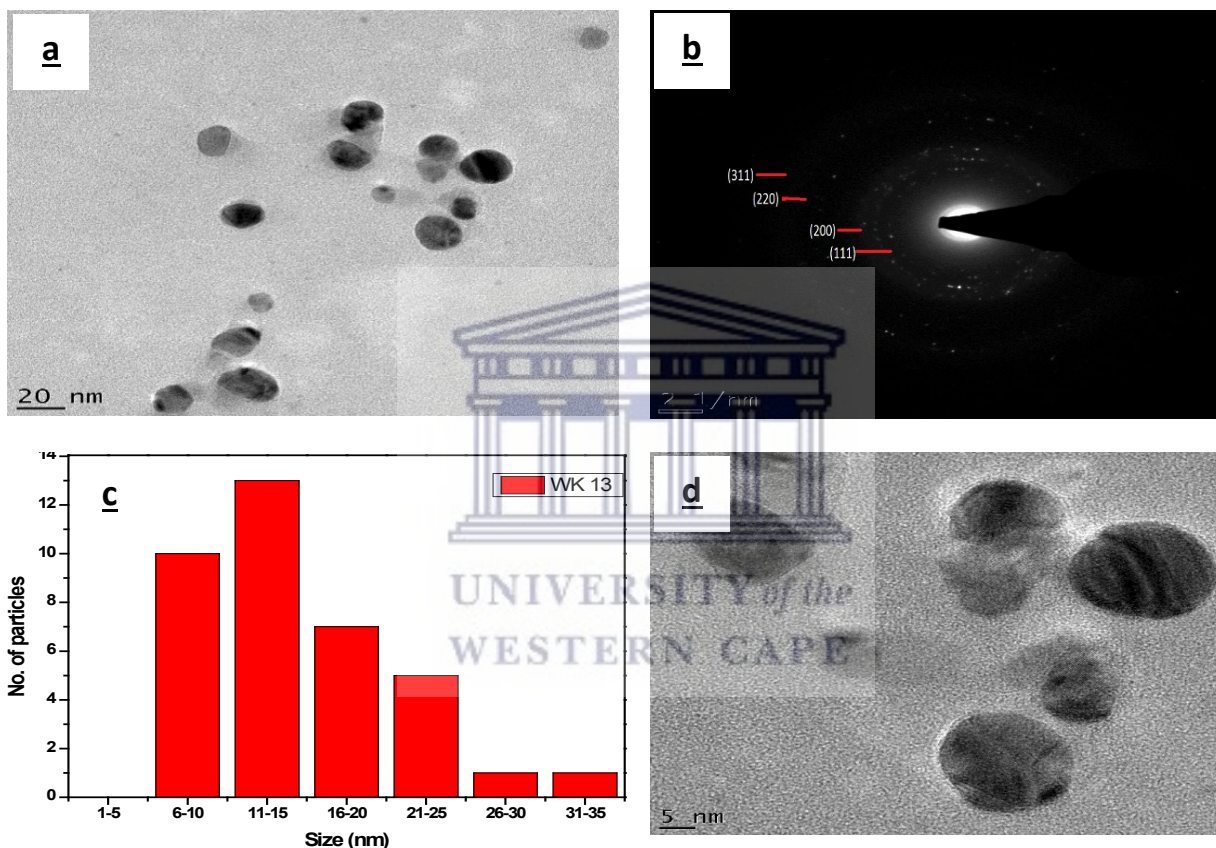


Figure 15. a) WK13 TEM; b) WK 13 SAED; c) WK 13 Histogram depicting the average size; d) WK 13 TEM depicting lattice fringes

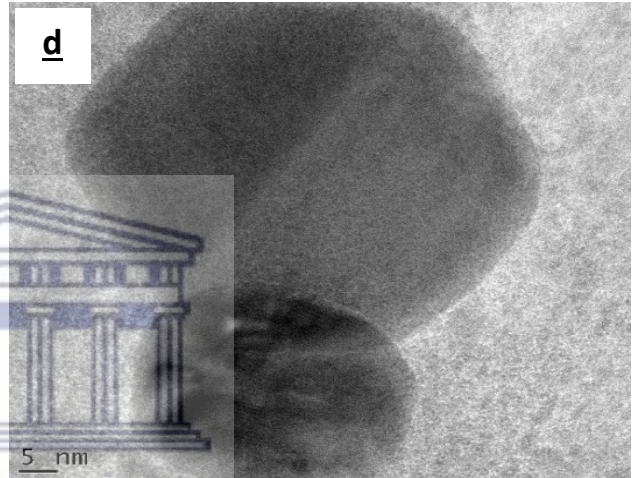
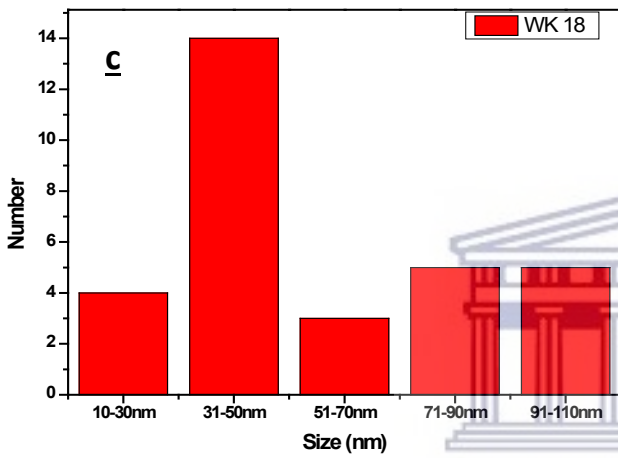
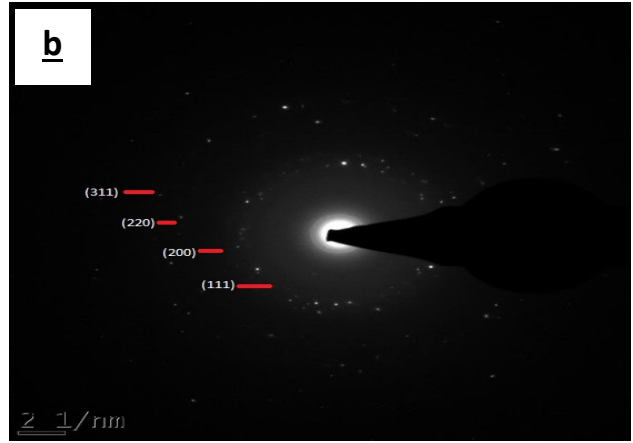
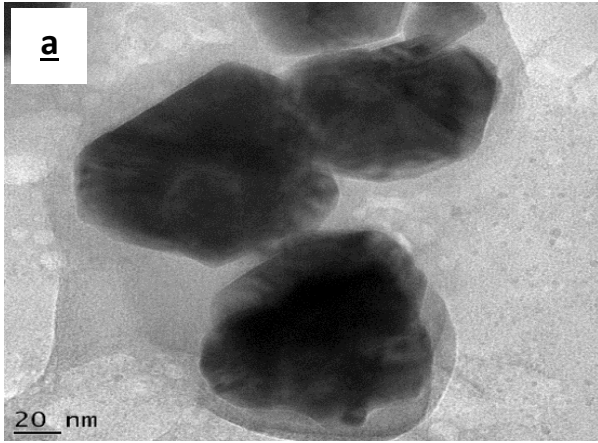


Figure 16. a) WK18 TEM; b) WK 18 SAED; c) WK 18 Histogram depicting the average size; d) WK 18 TEM depicting lattice fringes

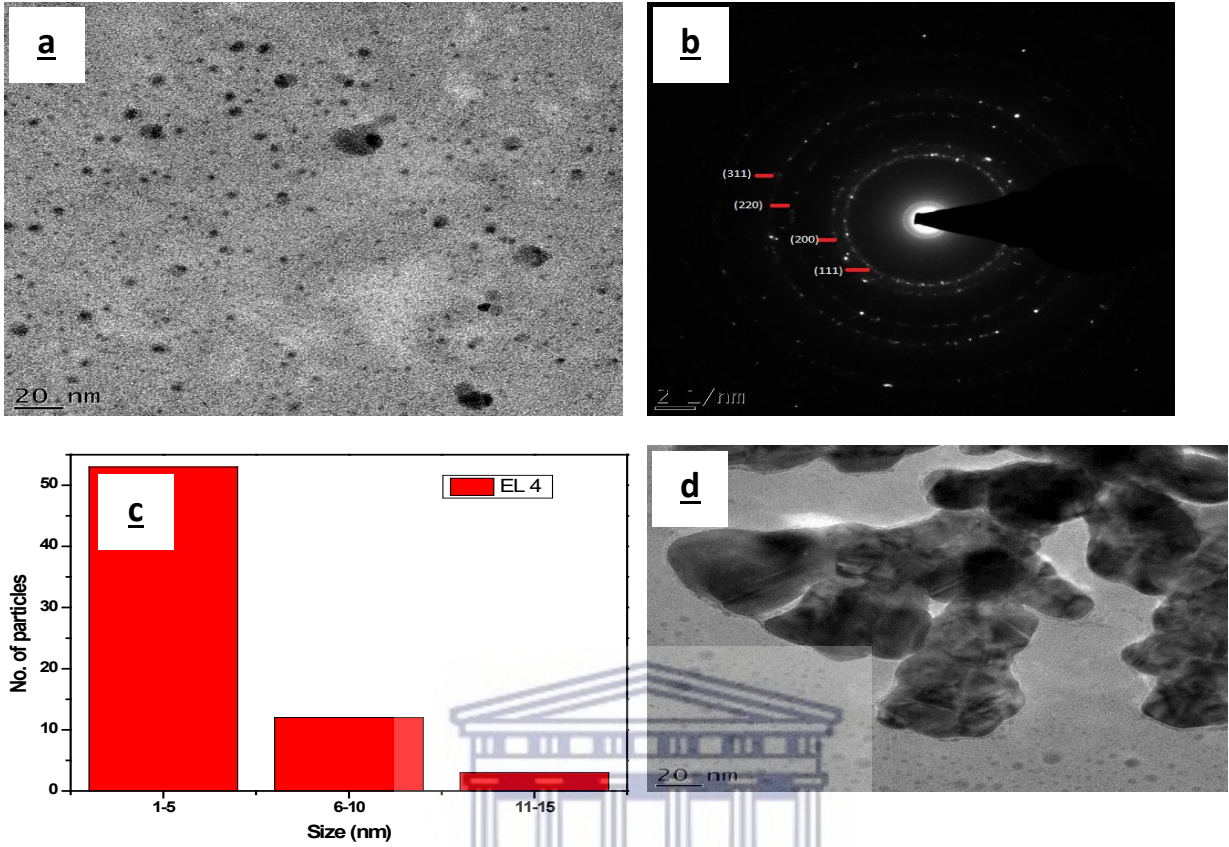


Figure 17. a) EL 4 TEM; b) EL 4 SAED; c) EL 4 Histogram depicting the average size; d) EL 4 TEM depicting lattice fringes

UNIVERSITY of the
WESTERN CAPE

4.4 Stability Testing of the Synthesized AgNPs

Stability testing was conducted to measure the effects of time on the functionality and structure of the AgNPs. The Zeta potential was completed to assess the stability of the biosynthesized AgNPs. As previously stated, all zeta potential results for the 3 biosynthesized silver nanoparticles were negative which indicated good stability. The stability of the NPs was recorded by UV-Vis spectra at different time periods namely: 2 hours, 4 hours, 6 hours, 12 hours and 24 hours and each were placed in two different mediums namely BSA and Cysteine.

According to the graphs indicated in Figures 20, 21, 22, and 23 *Berzelia lanuginosa* (WK 13) and *Helichrysum cymosum* (WK 18) showed that the NPs are biologically stable as there were minimal changes in UV-Vis spectra and by maintaining surface plasmon resonance in both mediums. According to Figures 18 and 19, results for *Searsia crenata* (EL4) indicated that there was a moderate shift in the UV-Vis spectra, there was also a decrease in surface plasmon resonance and thus absorbance indicating the formation of larger particles and a reduction in the number of nanoparticles (Ii *et al.*, 2012). These results indicate that these AgNPs have great potential in a biological application as their chemical and physical properties will be well-preserved in the biological environment (Sabuncu *et al.*, 2012).

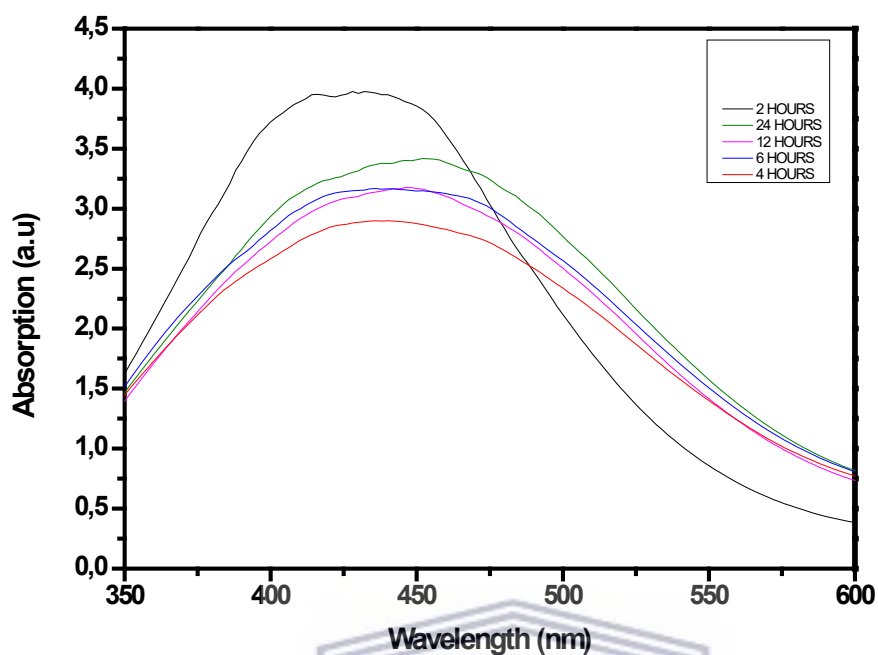


Figure 18. *Searsia crenata* (EL 4) stability assay of the AgNPs observed from UV-vis spectra upon incubation with BSA media after 24 h

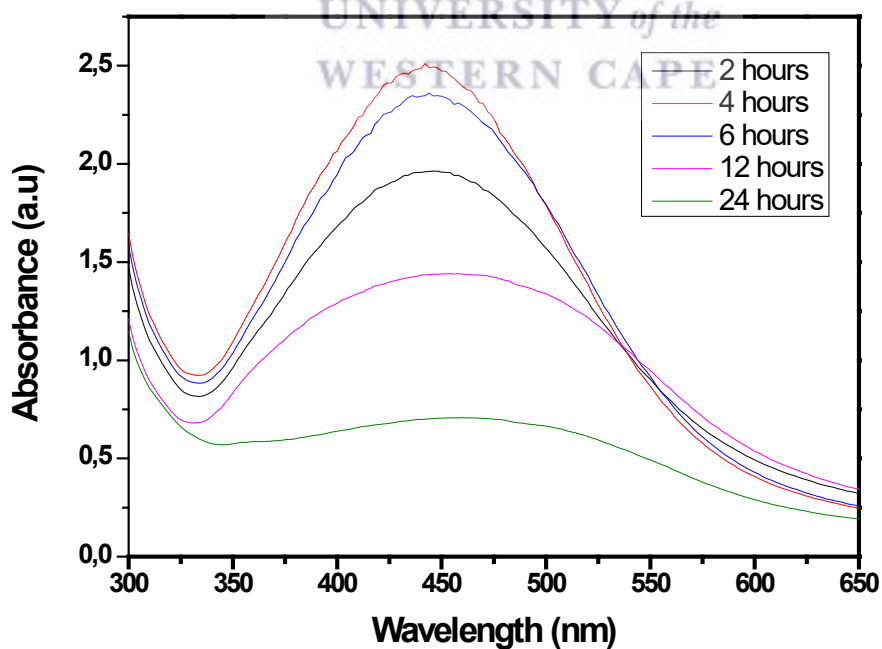


Figure 19. *Searsia crenata* (EL 4) stability assay of the AgNPs observed from UV-vis spectra upon incubation with cysteine media after 24 h

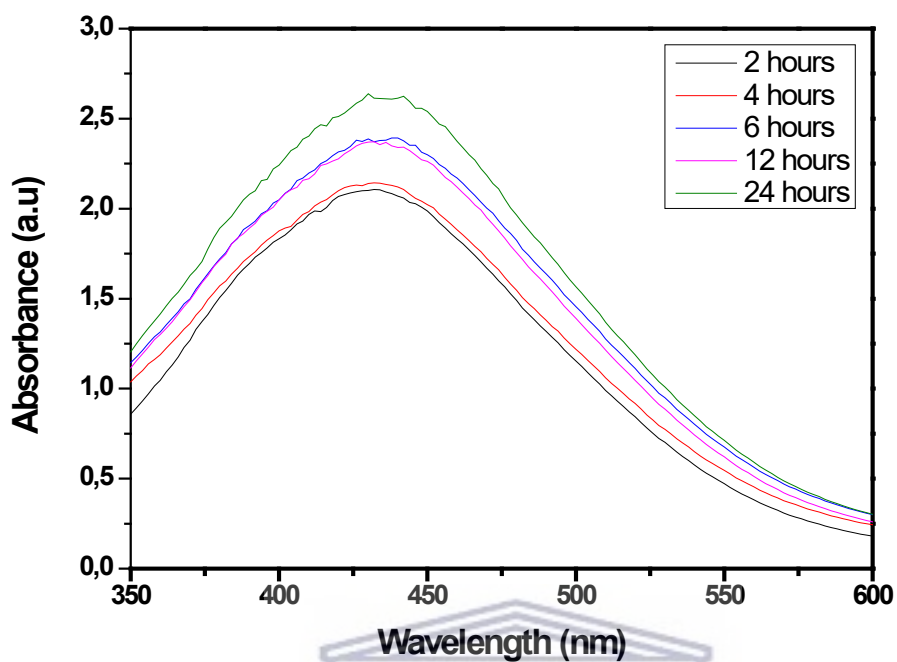


Figure 20. Berzelia lanuginose (WK 13) stability assay of the AgNPs observed from UV-vis spectra upon incubation with BSA media after 24 h

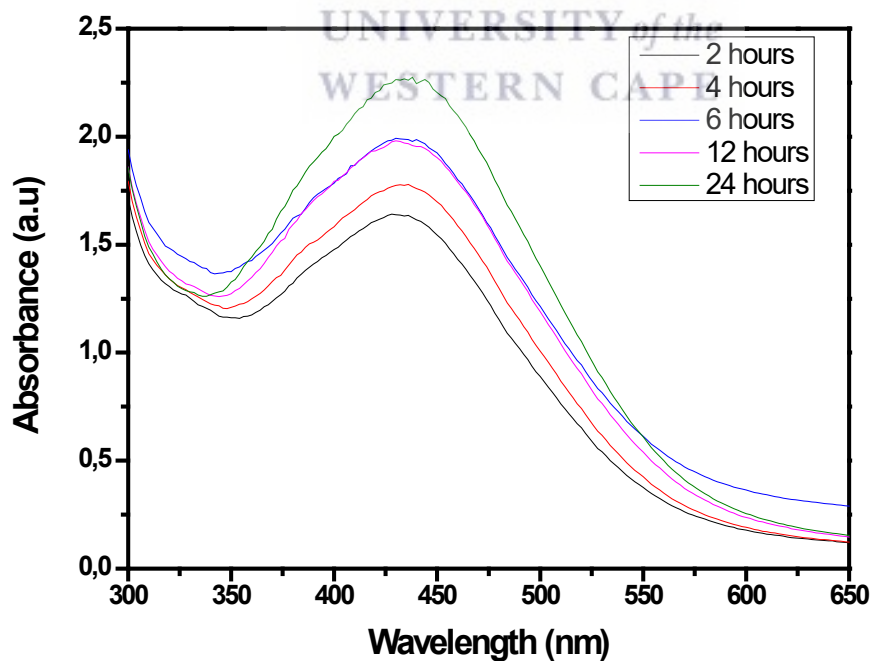


Figure 21. Berzelia lanuginose (WK 13) stability assay of the AgNPs observed from UV-vis spectra upon incubation with cysteine media after 24 h

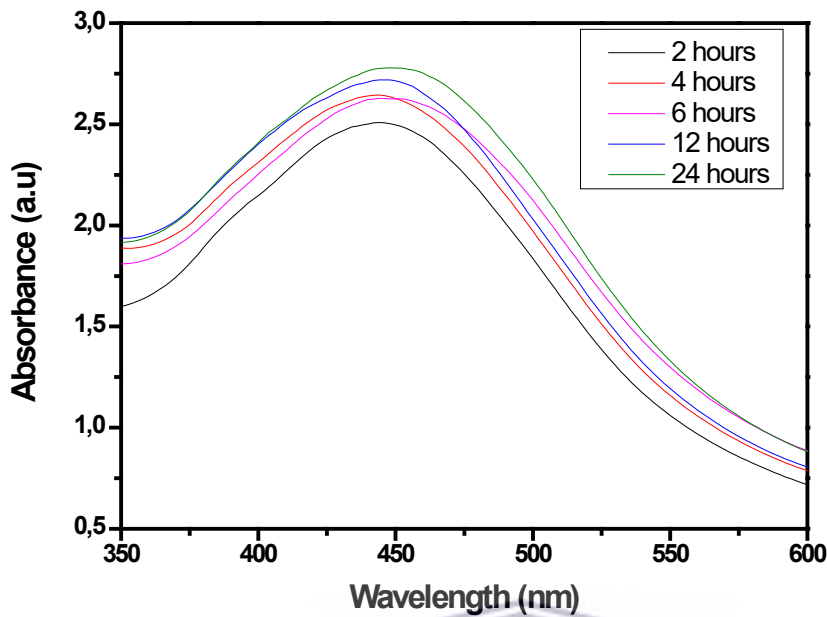


Figure 22. *Helichrysum cymosum* (WK 18) BSA Stability assay of the AgNPs observed from UV-vis spectra upon incubation with BSA media after 24 h

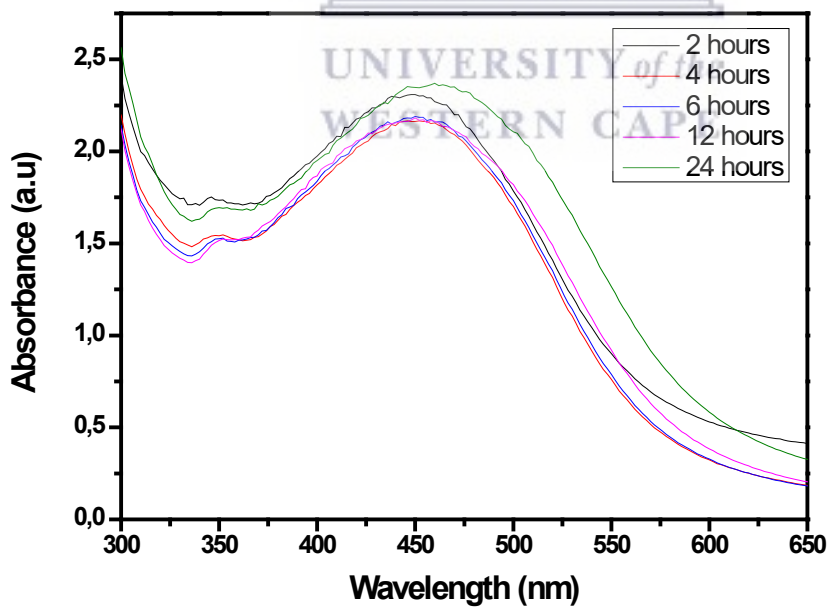


Figure 23. *Helichrysum cymosum* (WK 18) stability assay of the AgNPs observed from UV-vis spectra upon incubation with cysteine media after 24 h

4.5 Dispersive X-ray Spectroscopy (EDX) Analysis and SAED

The crystalline nature of synthesized nanoparticles was further evaluated through selected area electron diffraction (SAED) patterns (Figures 15b, 16b and 17b). The results for EL 4 displayed bright diffraction spots corresponding to 111, 200, 220 and 311 Bragg reflection planes (Das, Ghosh and Mandal, 2019; Aiswariya and Jose, 2021). The SAED pattern indicated that the crystals are mostly oriented on the 111 plane. Results for WK 13 and WK 18 did not show clear and distinct diffraction spots like EL 4, but diffraction spots were visible at 111, 200, 220 and 311. These indicated crystallinity was achieved (Nagar and Devra, 2019; Alahmad *et al.*, 2021).

4.6 Fourier-transform Infrared Spectroscopy Analysis of the Biosynthesized Silver Nanoparticle and Plant Extract

The FTIR measurements were carried out to assess the functional groups (capping biomolecules) responsible for the reduction, stabilisation, and production of the green AgNPs (Bagyalakshmi and Haritha, 2017). The IR spectrum of WK 13, WK 18, EL 4 and their relevant plant extracts were taken. In the present study, FTIR spectra of both the aqueous extract of WK 13, WK 18 and EL 4 and their corresponding synthesized AgNPs were recorded as seen in Figures 24- 29.

Results for AgNPs biosynthesized from EL 4 showed relevant peaks at 1627.96cm^{-1} , 1758.20cm^{-1} and 3448.08cm^{-1} . These results show the presence of C=C stretching bonds, C=O stretching bonds and O-H stretching bonds vibration of polyphenolic compounds or flavonoids respectively (Hashemi, Tasharrofi and Saber, 2020). As for the EL 4 extract there was a reduction of the shift as the silver salt formed and a shift in transmittance intensity as well as wavenumber. The Peaks were as follows, 1611.50cm^{-1} , 1448.91cm^{-1} and 3337.69cm^{-1} and these results showed the following, C=C stretching, O-H bending and O-H stretching bonds.

AgNPs biosynthesized from WK 13 showed relevant peaks at 1643.97cm^{-1} , 1761.15cm^{-1} and 3414.11cm^{-1} . These results showed the presence of C=C stretching, C=O stretching and O-H stretching vibration of polyphenolic compounds or flavonoids respectively.

Results for WK 13 extract showed values of, 1615.10cm^{-1} and 3363.74cm^{-1} representing C=C stretching and O-H stretching bonds. There was a reduction of the shift as the silver salt formed and a shift in transmittance intensity as well as wave number in extract results.

IR analysis for AgNPs biosynthesized from WK 18 showed relevant peaks at 1630.70cm^{-1} , 1710.88cm^{-1} , 1759.51cm^{-1} and 3398.98cm^{-1} . These results indicated the following bond groups respectively, C=C stretching, C=O stretching, and O-H stretching vibration of polyphenolic compounds or flavonoids. The IR analysis for the extract showed peaks at 1401.50cm^{-1} , 1605.50cm^{-1} and 3370.65cm^{-1} indicating O-H bending, C=C stretching and O-H stretching bond groups. There was also a reduction of the shift as the silver salt formed and a shift in transmittance intensity as well as wavenumber in extract results. A study conducted by Kartini et al in 2020 stated that the exact components and mechanism responsible for extract mediated green synthesis of nanoparticles remain uncertain. Primary metabolites such as proteins, vitamins, organic acid, and amino acids and secondary metabolites such as flavonoids, polyphenols, terpenoids and alkaloids have been shown to have significant contributions in metal salt reduction thus acting as stabilizing and capping agents for synthesized nanoparticles (Kartini *et al.*, 2020).

The chemistry and bond structure of these three plants have not yet been studied.

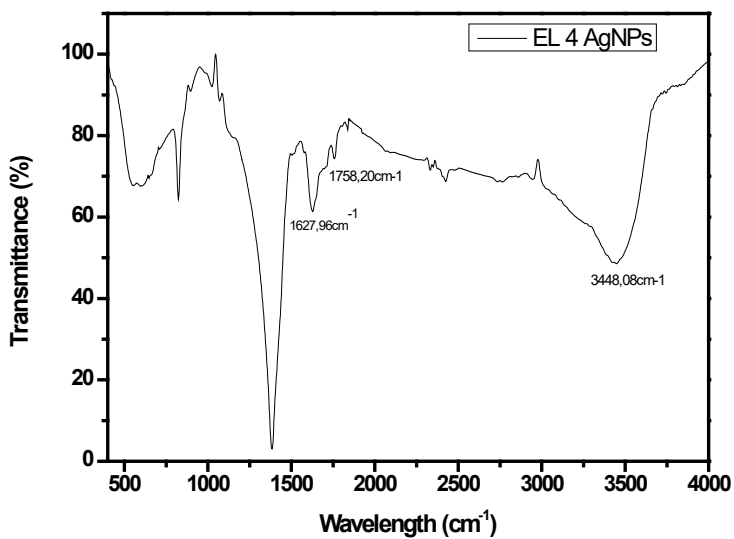


Figure 24. Infrared spectra of AgNPs, biosynthesized from *Searsia crenata* showed reduction of shift as the silver salt formed and a shift in transmittance intensity as well as wavenumber

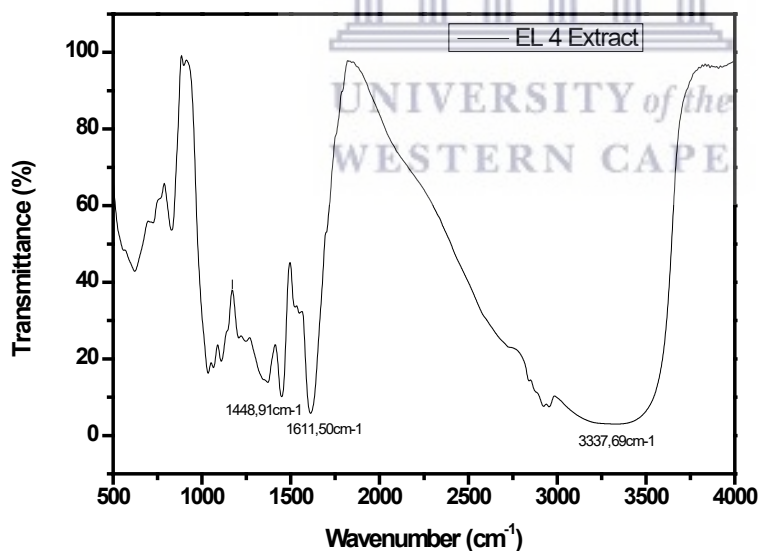


Figure 25. Infrared spectra of *Searsia crenata* leave extract showed reduction of shift as the silver salt formed and a shift in transmittance intensity as well as wavenumber

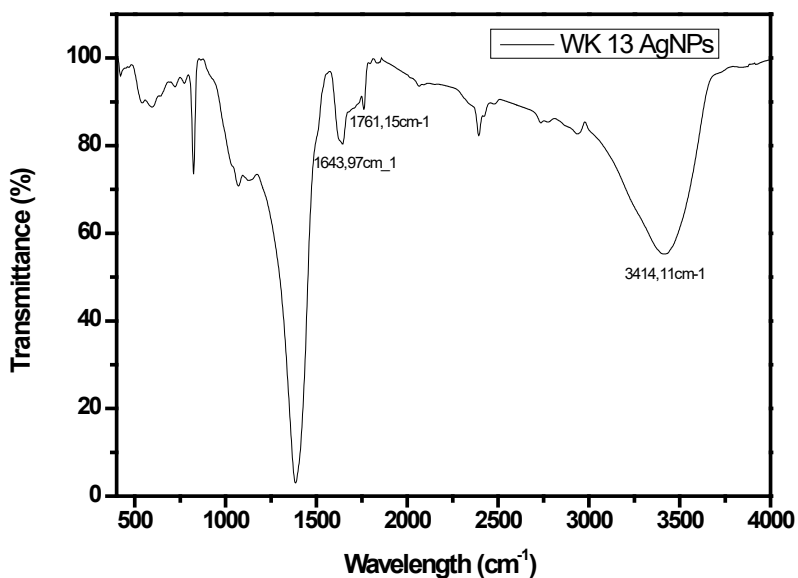


Figure 26. Infrared spectra of AgNPs biosynthesized from *Berzelia lanuginosa* showed reduction of shift as the silver salt formed and a shift in transmittance intensity as well as wavenumber

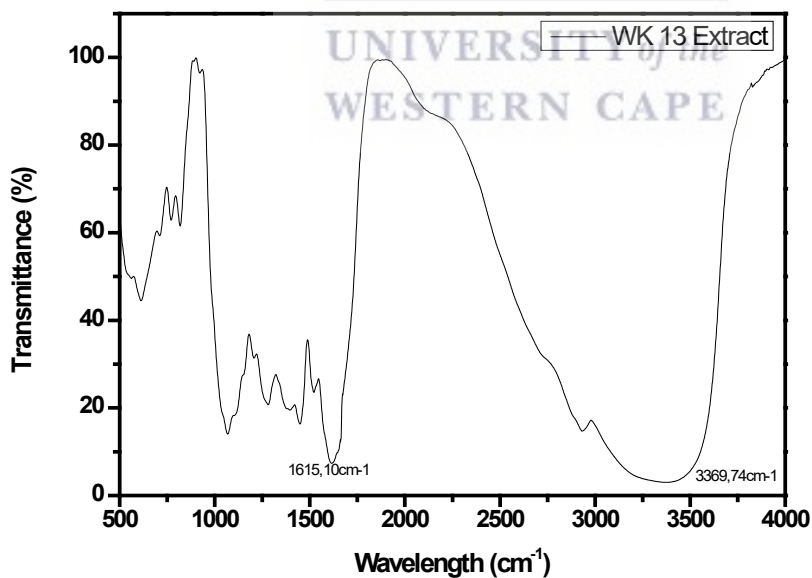


Figure 27. Infrared spectra of *Berzelia lanuginosa* leave extract showed reduction of shift as the silver salt formed and a shift in transmittance intensity as well as wavenumber

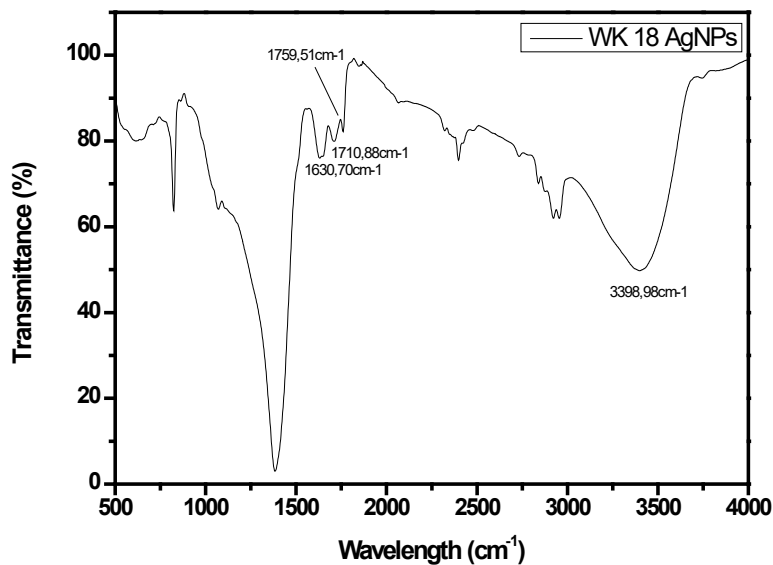


Figure 28. Infrared spectra of AgNPs biosynthesized from *Helichrysum cymosum* showed reduction of shift as the silver salt formed and a shift in transmittance intensity as well as wavenumber

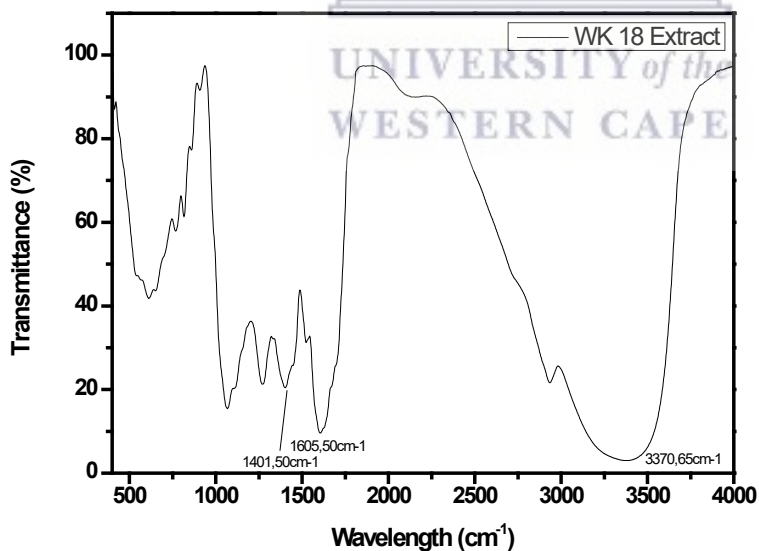


Figure 29. Infrared spectra of *Helichrysum cymosum* leave extract showed reduction of shift as the silver salt formed and a shift in transmittance intensity as well as wavenumber

ANTIMICROBIAL TESTING RESULTS

5.1 Modified Kirby-Bauer assay on *Candida albicans*

The antimicrobial activity of the aqueous extract and AgNPs of WK 13, WK 18 and EL 4 were investigated qualitatively and quantitatively against *Candida albicans* by determining the inhibition zones on agar plates and MIC values on micro plates. The water extract did not inhibit the *Candida albicans*. As shown in Table 9, the AgNPs had a moderate effect on the microorganisms when considering the standard antifungal agents. The same was noted in a study conducted by Geethalakshmi and Sarada in 2012 where *Candida albicans* was tested against AgNPs and results showed that the AgNPs had a moderate effect against *Candida albicans* when compared to its control and AuNPs (Geethalakshmi and Sarada, 2012). According to the disc diffusion method, AgNPs were shown to be more effective against the *Candida albicans* than their corresponding water extract.

The susceptibility of *Candida albicans* was tested against 0.2 % Chlorhexidine gluconate (control group), novel green AgNps WK 13, WK 18 and EL 4 (test group) and the relevant plant extract (negative control group). Each of the groups was studied using three samples (n=3 per volume tested) for each of the three different volumes: 350, 400 and 500 μ l. The zones of inhibition were then measured using a Vernier calliper as shown in Figure 30 (a - d) below.

Table 9. Zones of inhibition at 400 μ L of WK 13, WK 18, EL 4 extract and AgNps and Chlorhexidine

Plant	400 μ L	Inhibition zone diameter	Inhibition zone diameter	Inhibition zone diameter
WK 13	Extract	0mm	0mm	0mm
	AgNps	18mm	17mm	19mm
WK 18	Extract	0mm	0mm	0mm
	AgNps	19mm	19mm	18mm
EL 4	Extract	0mm	0mm	0mm
	AgNps	18mm	19mm	18mm
Control (Chlorhexidine)		26mm	28mm	27mm

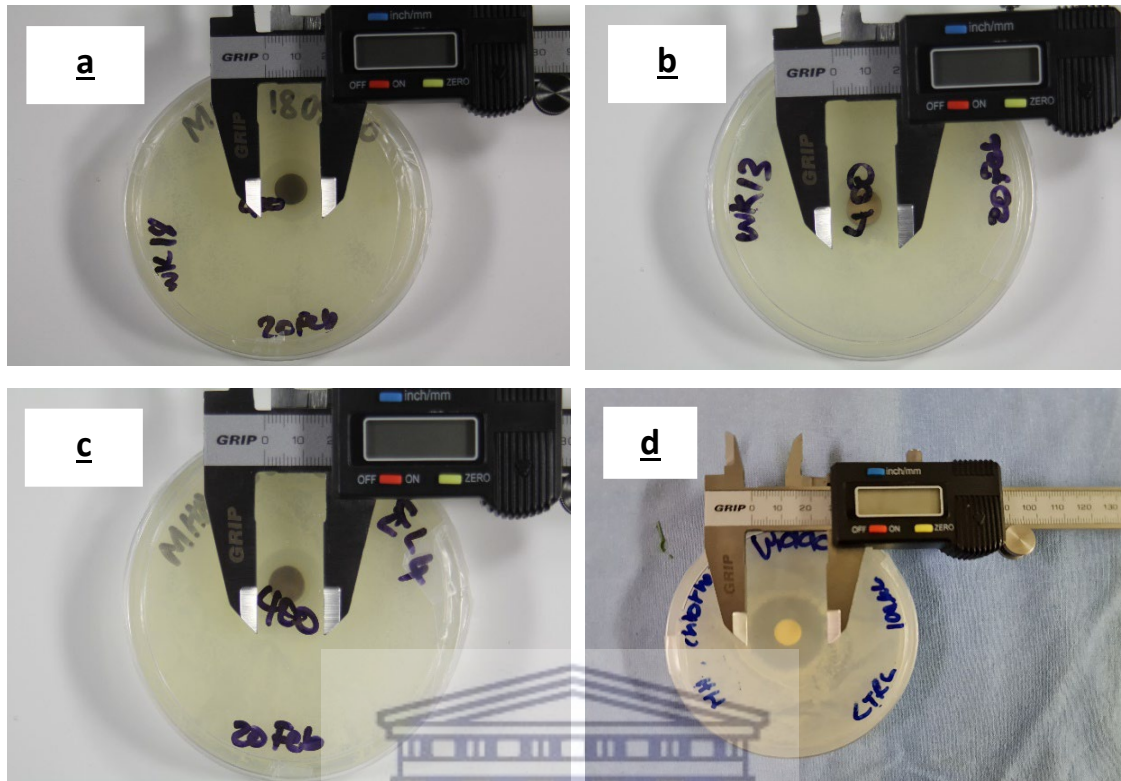


Figure 30. a) Zone of inhibition for WK 13; b) Zone of inhibition for WK 18; c) Zone of inhibition of EL 4; d) Zone of inhibition of 0.2% Chlorhexidine

5.2 XTT Testing Results and Discussion

XTT assay:

Key:

WK 13- Plant D	T0 = 0 hours
WK 18- Plant E	T2 = 2 hours
EL 4- Plant F	T3 = 3 hours

The normal doubling time for untreated *Candida albicans* is 1 hour (Anand and Prasad, 1991). Results shown in Figures 31 and 32 showed that plants D and F (WK 13 and EL 4) extended the lag phase past 2 hours, OD = ± 0.02 at λ (562-630nm). In as much as plant E (WK 18) lowered the doubling time compared to the untreated doubling time, by T2 *Candida albicans* had reached double its concentration at T0 (from OD= ± 0.025 to ± 0.055 on average at 562nm-630nm).

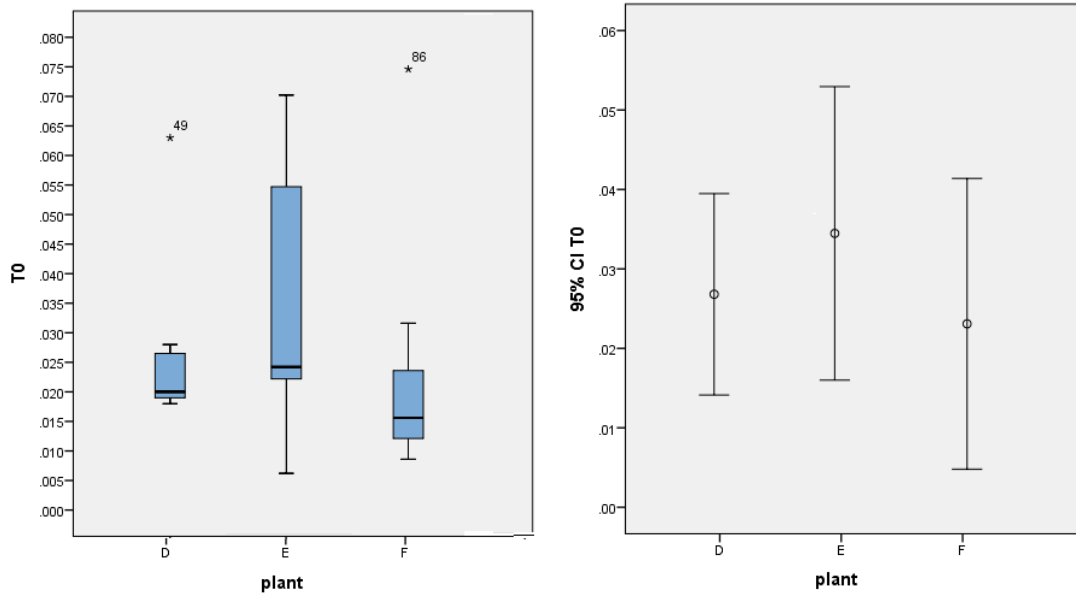


Figure 31. XTT results for plant D, E and F at 0 hours: difference (256 – 630nm) and the confidence index

Key:

WK 13- Plant D T0 = 0 hours
 WK 18- Plant E T2 = 2 hours
 EL 4- Plant F T3 = 4 hours

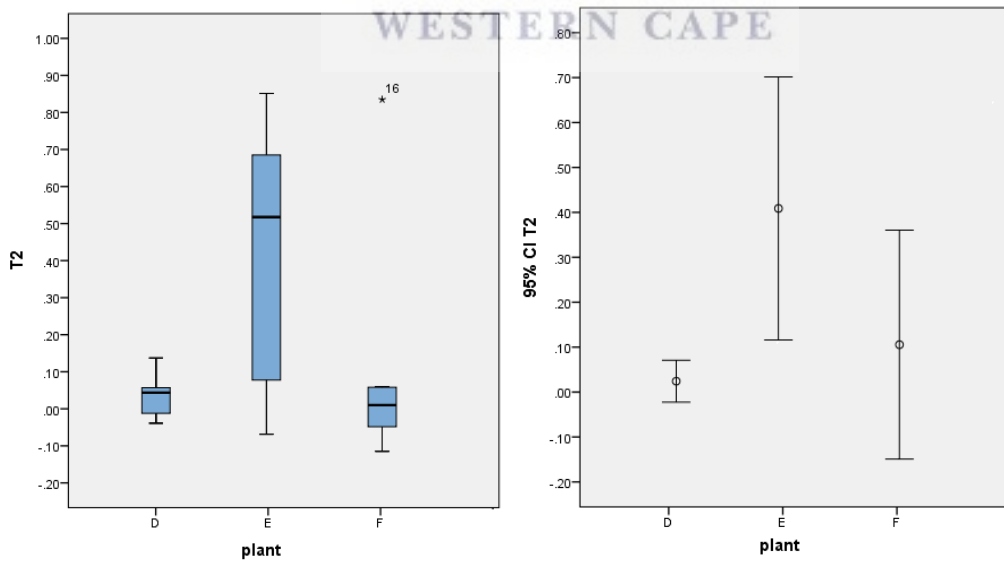


Figure 32. XTT results for plant D, E and F at 2 hours: difference (256 – 630nm) and the confidence index

Key:

WK 13- Plant D T0 = 0 hours
WK 18- Plant E T2 = 2 hours
EL 4- Plant F T3 = 4 hours

Over the observed time of 4 hours, plant E showed consistently higher growth than the other 2 plants (OD at 562-630nm) plant D lowered the fungal growth the most across the observed time as reflected in Figure 33. A study conducted by Li et al in 2014 agreed that the addition of AgNPs inhibits the formation of biofilm formation although Li et al determined that the higher the concentration of the AgNPs, the greater the effect on the biofilm (Li *et al.*, 2016).

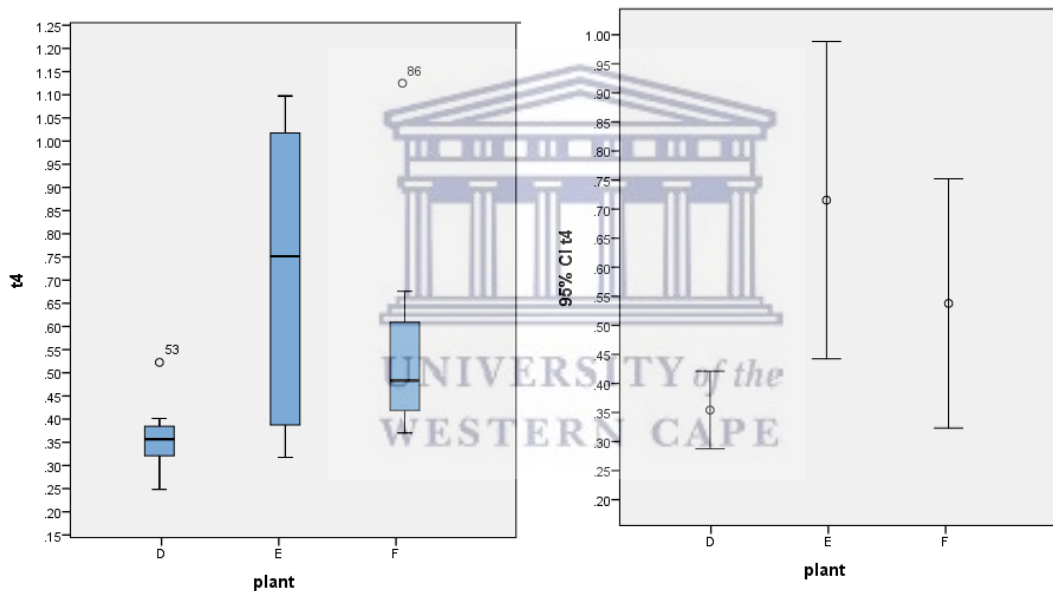


Figure 33. XTT results for plant D, E and F at 4 hours: difference (256 – 630nm) and the confidence index

Key:

WK 13- Plant D T0 = 0 hours
WK 18- Plant E T2 = 2 hours
EL 4- Plant F T3 = 4 hours

5.3 XTT: Minimum Inhibitory Concentration for AgNPs and Plant Extracts

Minimum inhibitory concentration (MIC) over time was done to determine the effect of the concentration on *Candida albicans* over time. MICs are usually studied as an endpoint in 24 or 48 hours, and it is not well documented what happens between the time of administration of treatment and the end point mark.

The MIC₅₀ is defined as the concentration required to inhibit the growth of 50% of bacterial/fungal isolates tested (Leite *et al.*, 2018).

The MIC for AgNPs and plant extract were tested separately to determine and compare their efficacy against *Candida albicans*.

Figure 34 demonstrated the growth pattern of the AgNPs over 48 hours and it reflected a qualitative reduction in *Candida albicans* growth where the lighter colour indicated lower growth and the deeper colour indicated higher growth. The colour development from clear to yellow is in an opposite gradient to the treatment where row B had 100% treatment concentration diluted two folds with each subsequent row from B to H as previously indicated in the methodology (Table 7). The MIC seemed to be between rows G and H for all the treatments after 4 hours exposure. The yeast appears to adjust and grow between the first 4 and 24 hours. This may indicate that all treatments were not fungicidal/or were fungistatic and the yeast recovered. This effect in 4 hours seems to indicate that the treatment could enable the immune system to combat the injured yeast.



Figure 34. The growth pattern of *Candida albicans* when combined with AgNPs and XTT over 48 hours

OD readings were taken at 4 different times and for the different concentrations of AgNPs namely, T1- 4 Hours, T2- 6 hours, T3- 24 hours, T4- 48 hours and SR 1- 50%, SR 2- 25%, SR 3- 12.5%, SR 4- 6.25%, SR 5- 3.125%, SR 6- 1.5625% and SR 7- 0.78125%.

T1 and 2 showed peak growth and between T2 and T3 showed a decrease in growth. At T3 and T4 there was a lower growth rate than between T1 and T2.

In Figure 35 (SR 4) all treatments caused a reduction in *Candida albicans* growth. The MIC₅₀ for all the treatments were observed to be below the concentration of SR 4. The yeast was reduced for all treatments from the original inocula.

Key:

- | | | |
|-----------------|-----------------|-------------------|
| SR 1 – 50% | Plant 4 – WK 13 | Time 1 – 4 hours |
| SR 2 – 25% | Plant 5 – WK 18 | Time 2 – 6 hours |
| SR 3 – 12.5% | Plant 6 – EL 4 | Time 3 – 24 hours |
| SR 4 – 6.25% | | Time 4 – 48 hours |
| SR 5 – 3.125% | | |
| SR 6 – 1.5625% | | |
| SR 7 – 0.78125% | | |

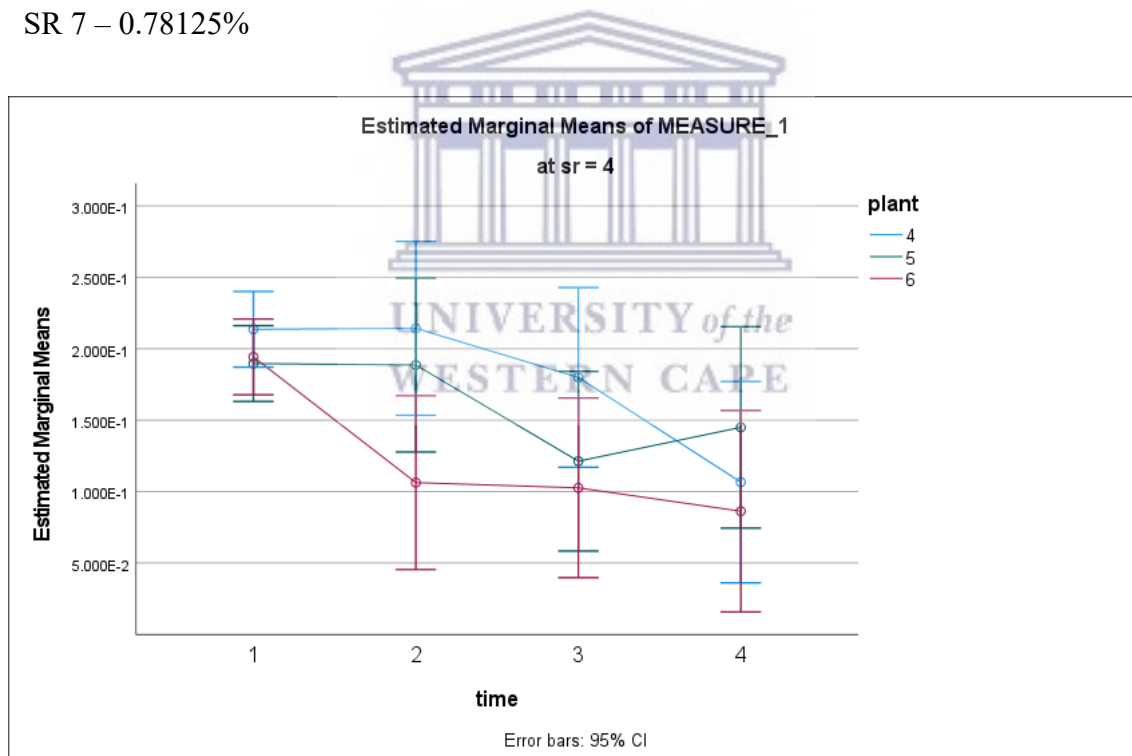


Figure 35. All AgNPs at the 4 different time intervals at concentration SR 4 (6.25%)

In this in vitro study it was observed that *Candida albicans* seemed to grow and stagnate erratically over time as seen in SR 1 and SR 5. *Candida albicans* seems to work differently for the different concentrations.

Key:

SR 1 – 50%

SR 2 – 25%

SR 3 – 12.5%

SR 4 – 6.25%

SR 5 – 3.125%

SR 6 – 1.5625%

SR 7 – 0.78125%

Plant 4 – WK 13

Plant 5 – WK 18

Plant 6 – EL 4

Time 1 – 4 hours

Time 2 – 6 hours

Time 3 - 24 hours

Time 4 – 48 hours

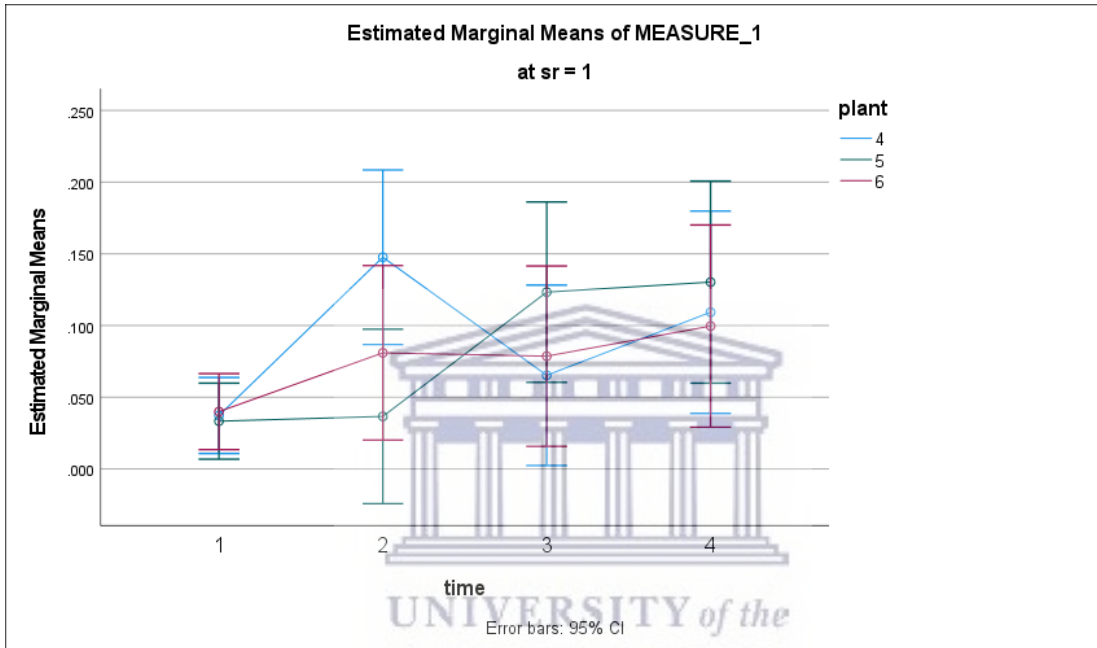


Figure 36. All AgNPs at the 4 different time intervals at concentration SR 1 (50%)

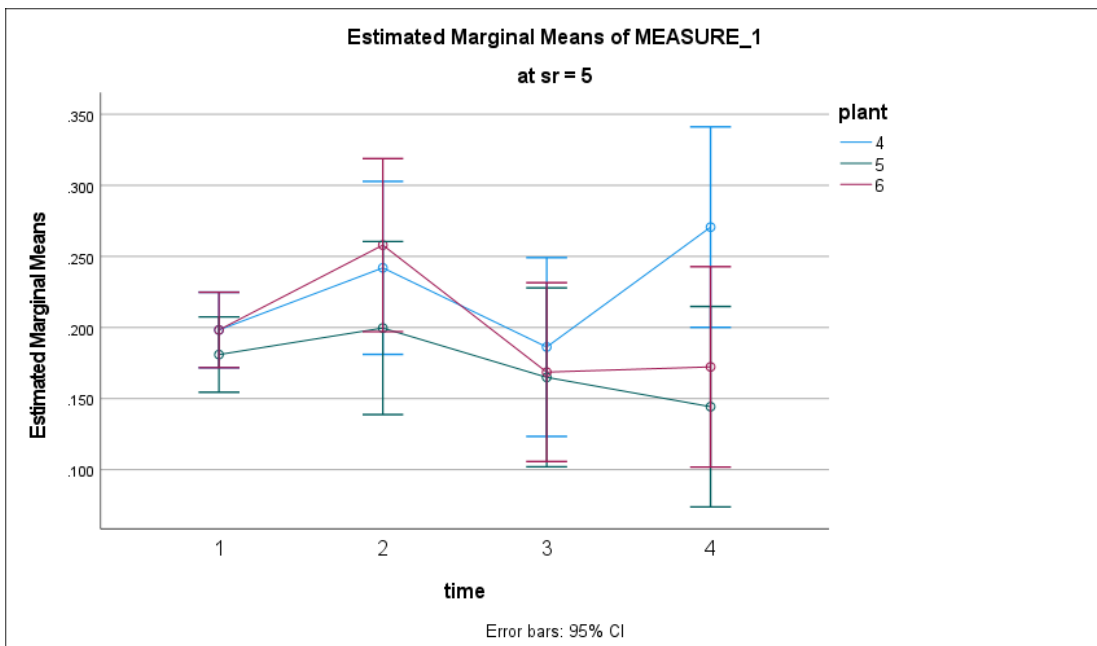


Figure 37. All AgNPs at the 4 different time intervals at concentration SR 5 (3.125%)

In Figures 36 and 37, Plant 4 showed an initial growth between 4-6 hours and a decrease between 4-24 hours, thereafter the yeast seemed to recover. The OD readings are a qualitative assessment where the colour of XTT began to develop for each treatment compared to that of the untreated sample. This indicates that the activities of the extracts began to weaken. Given that MICs are defined as the lowest concentration of an antimicrobial that will inhibit the visible growth of a microorganism overnight incubation. Hence, the lowest concentrations enabling this was considered the MIC concentration. The MBC were not calculated as this necessitated plating inocula from the dilution above MIC.

In order to determine the MIC percentage reduction was calculated for each concentration and time as seen in Figure 38.

Percentage reduction was calculated as:

$$\% \text{ reduction of sample} = \frac{(OD \text{ sample treated} - OD \text{ sample untreated at } 0.5 \text{ McF})}{OD \text{ sample untreated at } 0.5 \text{ McF}} \times 100$$

The reduction of 90% of the yeast population occurred between SR 2 and SR 3 for all the plants at 4 hours as seen in Figure 38.

calculated percentage changes in biofilms from baseline (untreated) after the intervention

Serial dilut	WK 1	WK 1	WK 1	WK 2	WK 2	WK 2	WK 3	WK 3	WK 3	EMPTY	EMPTY	Untreated	4 hours
average co	47,04492	48,93617	49,17258	47,75414	45,86288	46,3357	48,93617	48,69976	45,86288	84,39716	82,2695	0	
Serial dilut	WK 13	WK 13	WK 13	WK 18	WK 18	WK 18	EL 4	EL 4	EL 4	EMPTY	EMPTY	Untreated	4 hours
average co	46,60422	51,52225	51,52225	53,16159	51,99063	52,69321	52,9274	52,45902	10,77283	81,96721	81,96721	0	
Serial dilut	WK 1	WK 1	WK 1	WK 2	WK 2	WK 2	WK 3	WK 3	WK 3	EMPTY	EMPTY	Untreated	6 hours
average co	50,74627	43,07036	41,57783	44,98934	43,4968	45,41578	43,71002	49,46695	53,09168	83,79531	84,00853	0	
Serial dilut	WK 13	WK 13	WK 13	WK 18	WK 18	WK 18	EL 4	EL 4	EL 4	EMPTY	EMPTY	Untreated	6 hours
average co	-2,32019	-4,64037	49,41995	53,13225	51,50812	48,7239	8,352668	22,73782	49,88399	81,67053	82,13457	0	
Serial dilut	WK 1	WK 1	WK 1	WK 2	WK 2	WK 2	WK 3	WK 3	WK 3	EMPTY	EMPTY	Untreated	24 hours
average co	-2,08333	-21,5278	-30,2083	11,80556	-37,8472	-33,3333	25,34722	-6,25	-3,125	76,04167	78,125	0	
Serial dilut	WK 13	WK 13	WK 13	WK 18	WK 18	WK 18	EL 4	EL 4	EL 4	EMPTY	EMPTY	Untreated	24 hours
average co	40,75067	3,217158	-28,9544	24,93298	47,18499	2,680965	20,10724	3,485255	5,630027	82,30563	79,35657	0	

Figure 38. MIC percentage reduction for each concentration and time for each AgNP

As seen in Figure 39 and 40, the MIC₅₀ across all the times observed except 48 hours were consistently between SR 5 and SR 6. After 48 hours the AgNPs show inconsistencies whereby plant 4 (WK 13) had an MIC₅₀ between SR 4 and 5. Plant 5 and 6 (WK 18 and EL 4) were between SR 5 and SR 6. Figure 41 indicates all 4 different time intervals at SR 7 (0.78125%)

Key:

- | | | |
|-----------------|-----------------|-------------------|
| SR 1 – 50% | Plant 4 – WK 13 | Time 1 – 4 hours |
| SR 2 – 25% | Plant 5 – WK 18 | Time 2 – 6 hours |
| SR 3 – 12.5% | Plant 6 – EL 4 | Time 3 – 24 hours |
| SR 4 – 6.25% | | Time 4 – 48 hours |
| SR 5 – 3.125% | | |
| SR 6 – 1.5625% | | |
| SR 7 – 0.78125% | | |

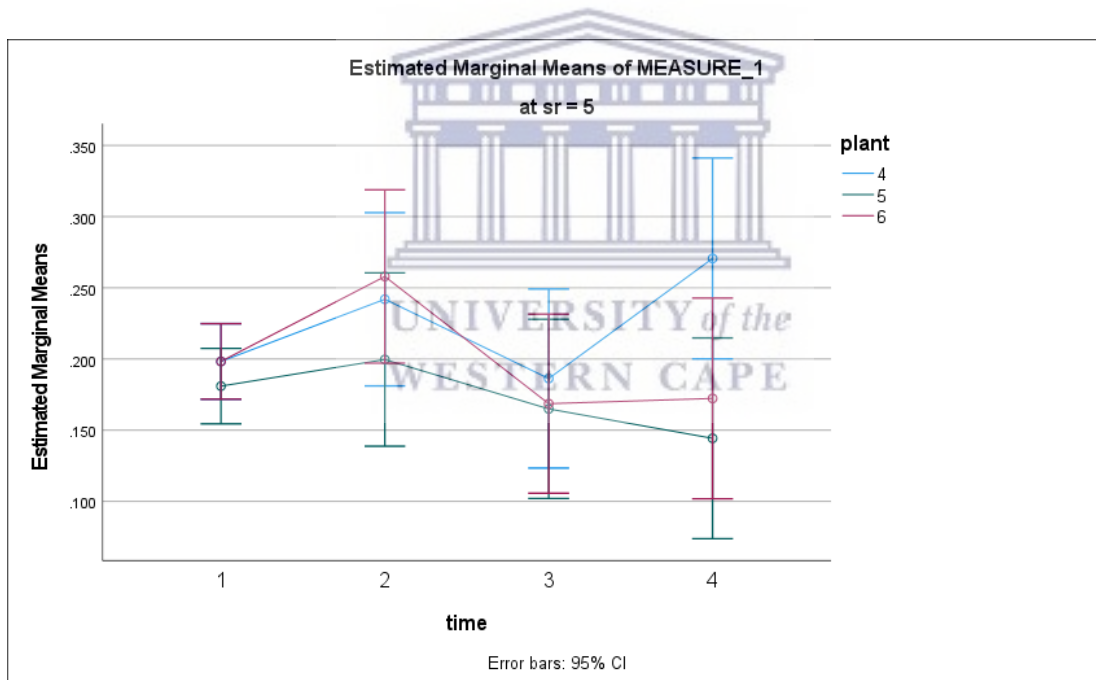


Figure 39. All AgNPs at the 4 different time intervals at concentration SR 5 (3.125%)

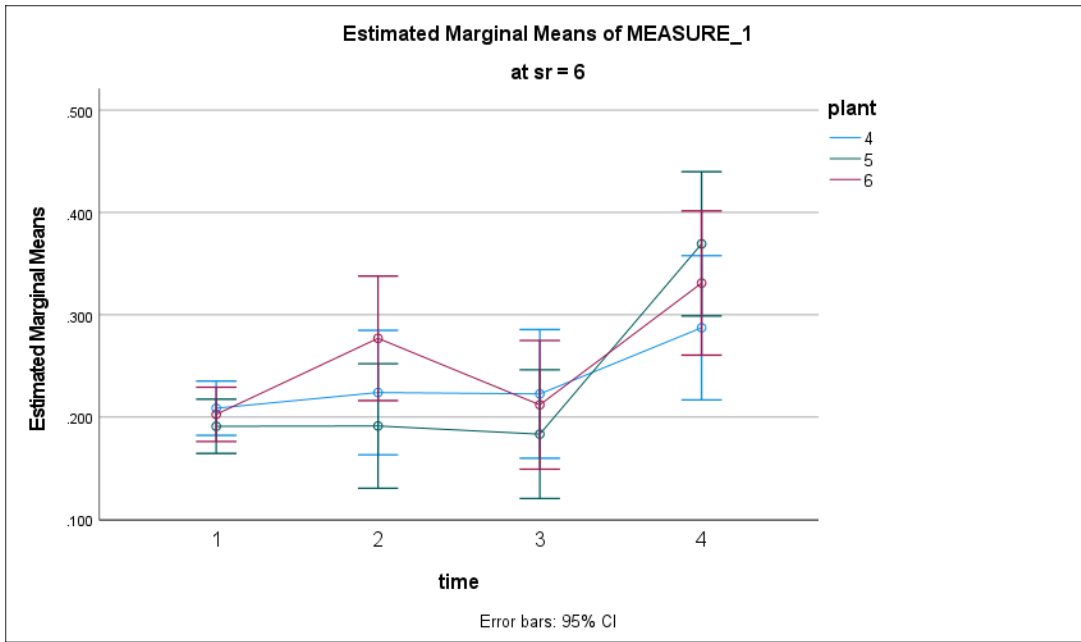


Figure 40. All AgNPs at the 4 different time intervals at concentration SR 6 (1.562%)

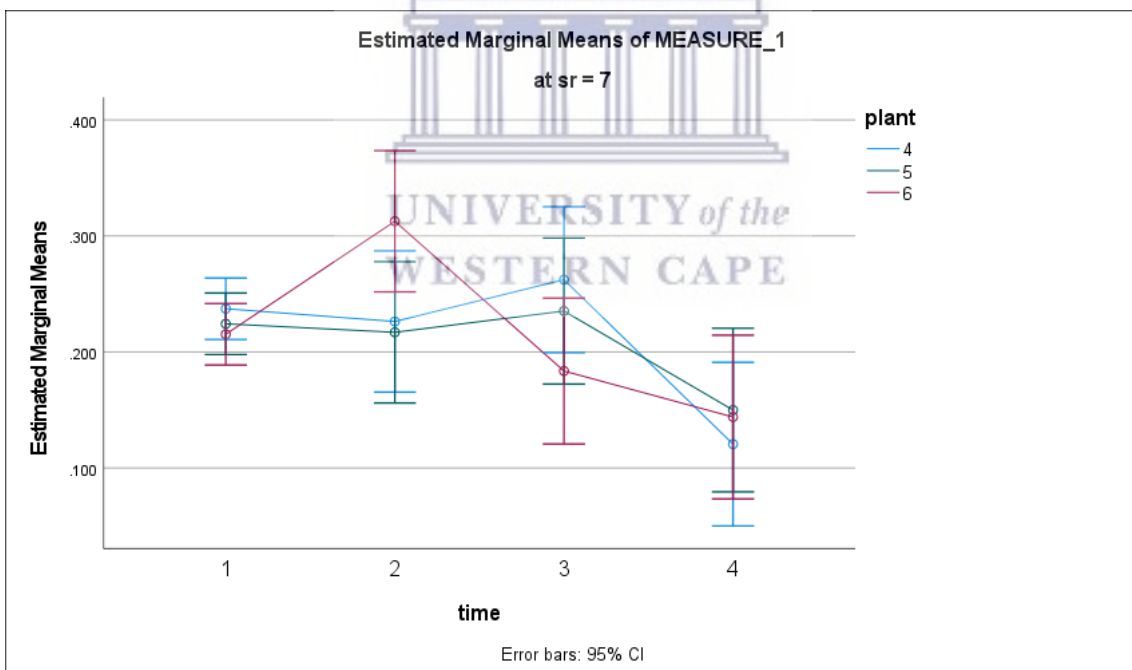


Figure 41. All AgNPs at the 4 different time intervals at concentration SR 7 (0.78125%)

5.4 MIC: Plant Extract

This section covers testing of MIC using XTT of plant extracts. The plant extracts seemed to have a lower effect in 4-24 hours when compared to their respective AgNPs with OD readings consistently above 0.5 for the plant extract. This indicates that synthesizing AgNPs from the plant extract may increase the potency of the plant extracts as shown below in Figures 42, 43, and 44.

Key:

T1 – 4 Hours
T2 – 6 hours
T3 – 24 hours
T4 – 48 hours

Plant 4 – WK 13
Plant 5 – WK 18
Plant 6 – EL 4

Concentration B – 50%
Concentration C – 25%
Concentration D – 12.5%
Concentration E – 6.25%
Concentration F – 3.125%
Concentration G – 1.5625%
Concentration H – 0.78125%

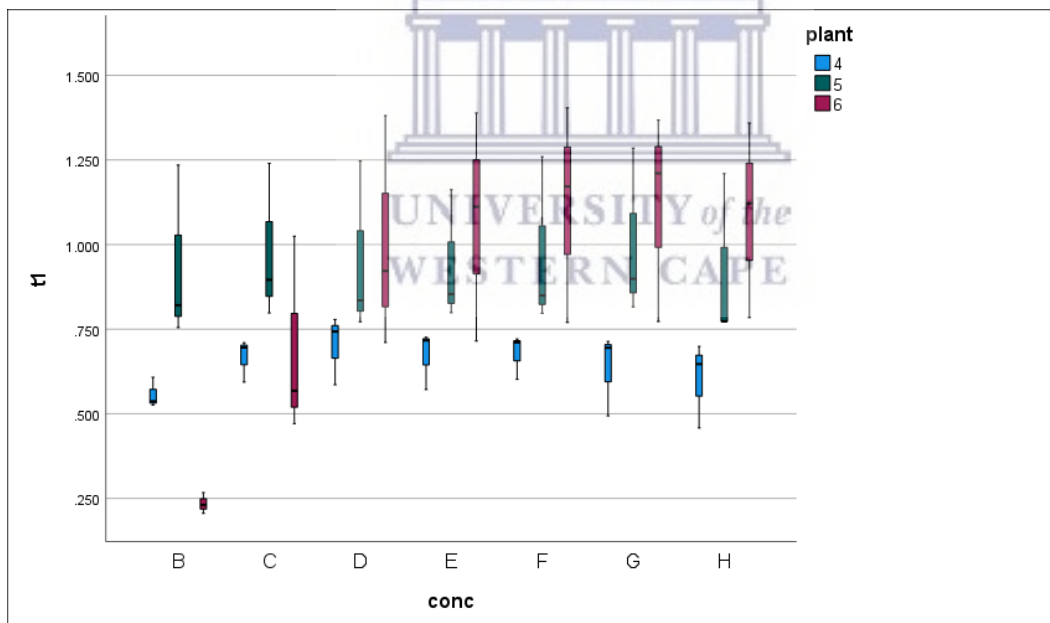


Figure 42. All plant extracts at T1 (4 hours) at various concentrations

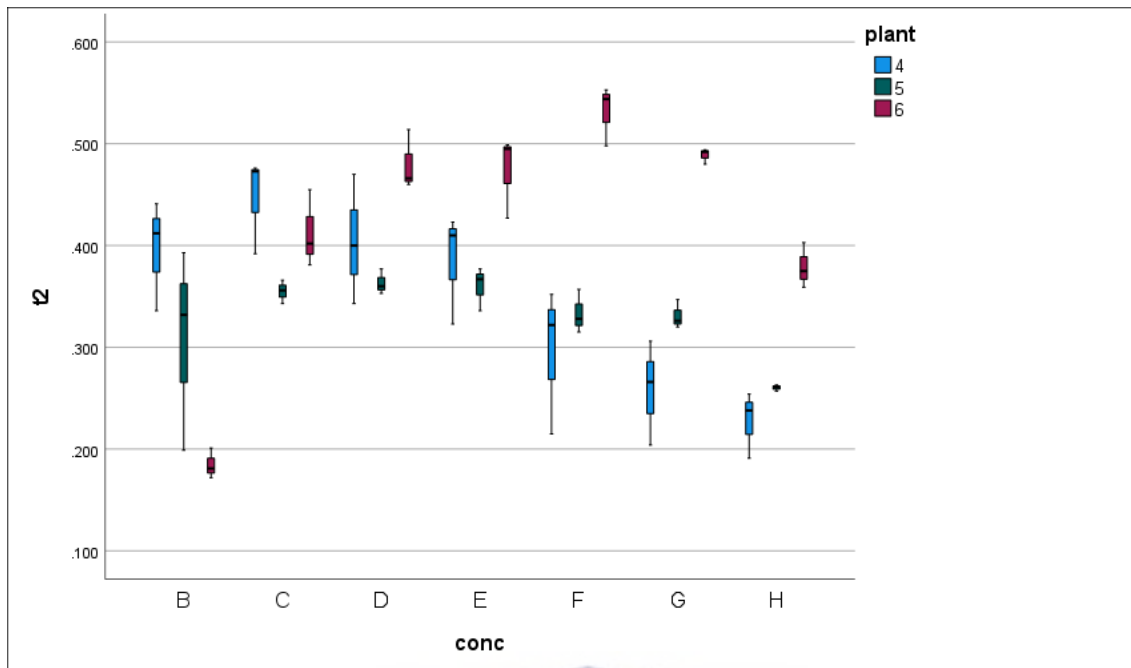


Figure 43. All plant extracts at T2 (6 hours) at various concentrations

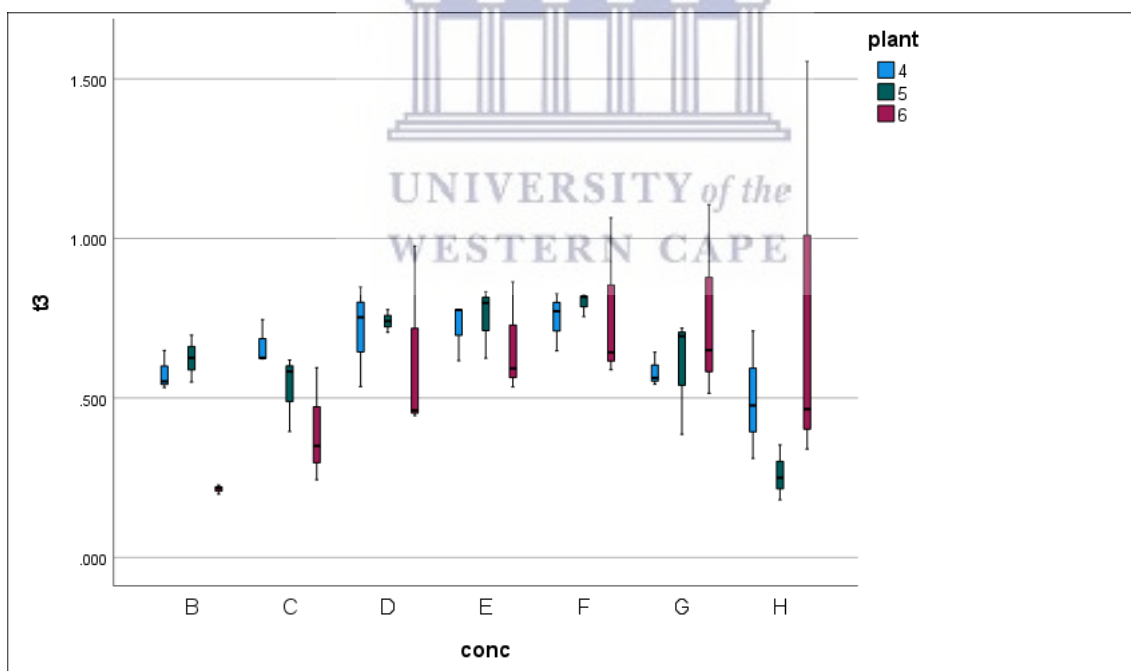


Figure 44. All plant extracts at T3 (24 hours) at various concentrations

However, after 24 hours as seen in Figure 45, the plant extracts seemed to be more potent than their AgNPs counterparts. This may indicate that the plant has a delayed effect.

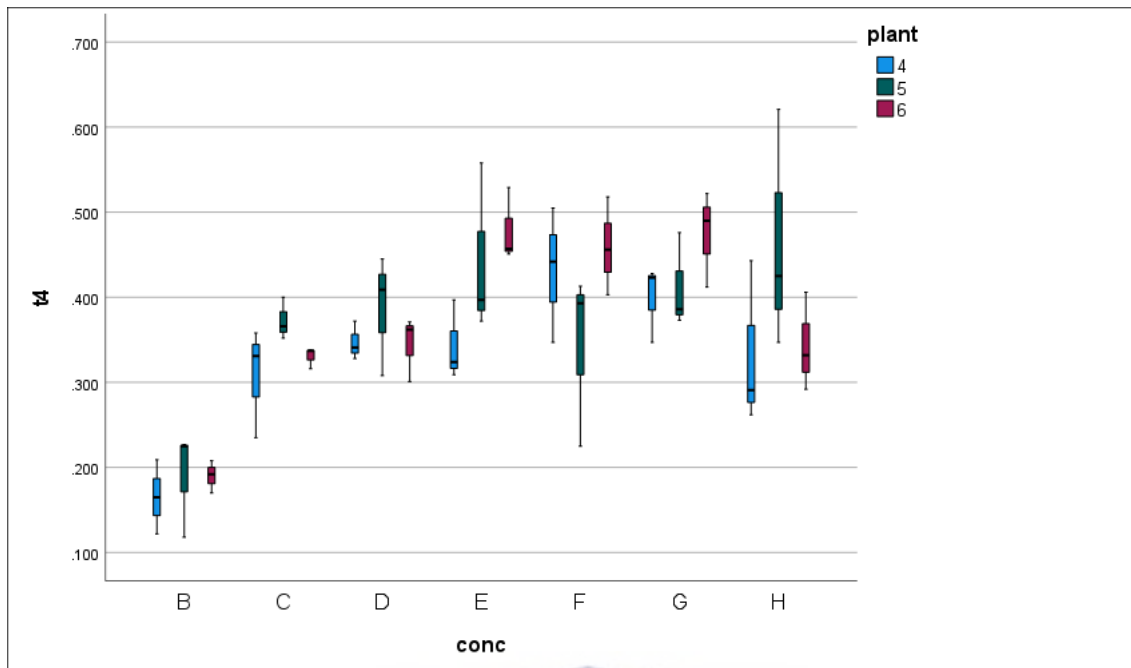


Figure 45. All plant extracts at T4 (48 hours) at various concentrations

Figure 46 reflects the qualitative reduction in *Candida albicans* growth where the lighter the colour clear indicates lower growth and the deeper colour indicating higher growth. The colour development from clear to yellow is in an opposite gradient to the plant extract where row B had 100% plant extract concentration diluted two folds with each subsequent row from B to H. The MIC could not be determined for the plant extract as time played a big factor in the potency of the plant extract. By looking at Figure 46, it can be seen that there was qualitatively no colour changed as previously mentioned for MIC in the AgNPs.

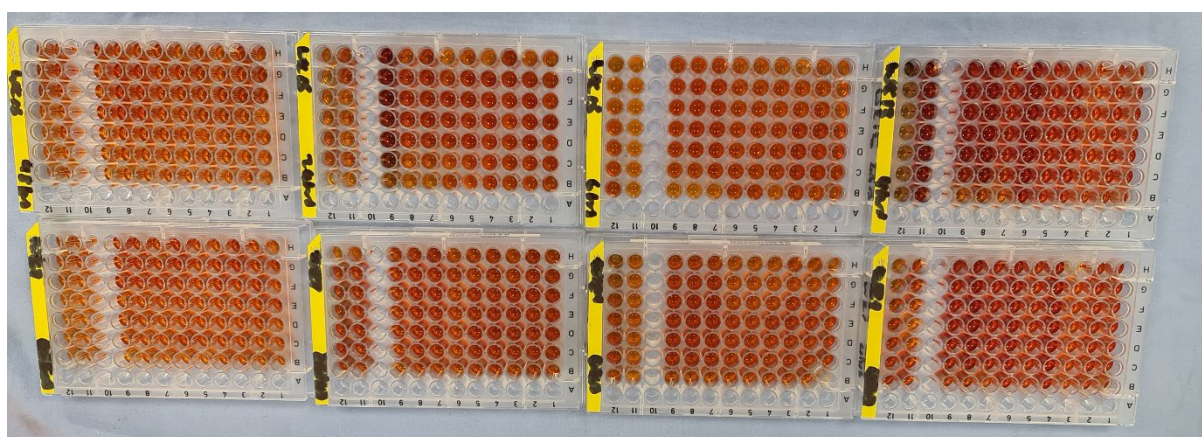


Figure 46. The growth pattern of *Candida albicans* when combined with the plant extract and XTT over 48 hours

It has been observed that AgNPs exhibited antifungal activity against *Candida albicans*. It has shown to cause fungal membrane depolarization and disruption with an increase in the amounts of intracellular and released glucose and trehalose, damage in the envelope structure, and inhibition of the normal budding process. Although the microbiological effects underlying the activity against *Candida albicans* observed in this study was not explored, it was stated that the AgNPs solution inhibited the growth through destruction of membrane integrity (Wady *et al.*, 2012). According to a study by Lara *et al* in 2015 results indicated a dose-dependent and potent inhibitory effect of AgNPs on biofilm formation. The AgNPs also showed to be effective when tested against pre-formed *Candida albicans* biofilms, the activity was however detected at higher concentrations than those required to inhibit biofilm formation (Lara *et al.*, 2015).

CYTOTOXICITY

Key:

- 1: WK 13 - Berzelia lanuginose (AgNP)
- 2: WK 18 - Helichrysum cymosum (AgNP)
- 3: EL 4 - Searsia crenata (AgNP)
- 4: WK 13 - Berzelia lanuginose (EXTRACT)
- 5: WK 18 - Helichrysum cymosum (EXTRACT)
- 6: EL 4 - Searsia crenata (EXTRACT)

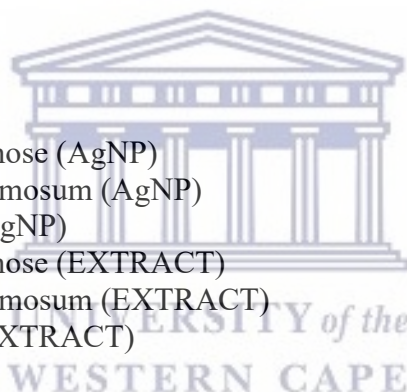


Table 10. Indicates the nanoparticles and plant extract, showing their respective cell survival rate

sample 1	Average 1	Cell survival 1	sample 2	Average 2	Cell survival 2	sample 3	average 3	cell survival 3	sample 4	average 4	cell survival 4	sample 5	average 5	cell survival 5	sample 6	average 6	cell survive 6
1%	0,355	92	1%	0,415	108,37	1%	0,404	105,51	1%	0,415	127,27	1%	0,395	119,98	1%	0,417	126,39
3%	0,374	97,78	3%	0,419	109,55	3%	0,354	93,78	3%	0,398	120,81	3%	0,455	138,02	3%	0,386	117,11
5%	0,338	88,36	5%	0,411	107,27	5%	0,347	90,65	5%	0,397	120,45	5%	0,463	140,52	5%	0,402	121,87
10%	0,283	74,14	10%	0,383	99,92	10%	0,152	39,4	10%	0,376	114,18	10%	0,337	102,28	10%	0,302	91,67
15%	0,163	42,47	15%	0,207	53,98	15%	0,108	28,17	15%	0,38	115,32	15%	0,37	111,9	15%	0,315	95,43
25%	0,153	40,32	25%	0,117	30,48	25%	0,0967	25,27	25%	0,474	143,9	25%	0,494	149,96	25%	0,382	116,03

Table 10 (above) indicates the 3 AgNPs, 3 relevant plant extracts and their cell survival percentage at 6 different concentrations namely 1%, 3%, 5%, 10%, 15%, 25%. For sample 1 (WK 13 AgNP) the cell survival was highest between 1-3%, for sample 2 (WK 18

AgNP) the highest survival rate was found between 1-3%, for sample 3 (EL 4 AgNP) the highest survival rate was found between 1-3% these high survival rates are excellent for biomaterials. The lowest survival rates were found at 25% for sample 1-3 with survival rates being under 50% and not ideal for a biomaterial at this concentration.

Table 11 (below) shows that there is a statistical difference between survival rate of the AgNP sample 1 and plant extract sample 4 at 0.05 level of significance.* Survival rate for AgNPs sample 1 is statistically lower than survival rate for plant extract sample 2.

Table 11. Difference between AgNPs sample 1 (WK 13 AgNPs) and plant extracts samples 4 (WK 13 Plant extract)

Paired t test						
Variable	Obs	Mean	Std.Err.	std.Dev.	[95% Conf. Interval]	
*Cellsu~1	6	72.51167	10.34555	25.34131	45.91759	99.10574
*Cellsu~4	6	123.655	4.474156	10.9594	112.1538	135.1562
diff	6	-51.14333	12.58229	30.82019	--83.48713	-
	18.79953					
Mean(diff) = mean(cellsurvival2 – cellsurvival5)					t= --4.0647	
Ho: mean(diff) = 0			degrees of freedom = 5			
Ha: mean(diff)<0		Ha: mean(diff) !=0		Ha:mean(diff)>0		
Pr(T < t) = 0.0048		Pr(T > t) = 0.0097		Pr(T > t) = 0.9952		

Table 12 (below) shows a statistical difference between survival rate AgNPs sample 2 and plant extract sample 5 at 0.05 level of significance. Survival rate for AgNPs sample 2 is statistically lower than survival rate for plant extract sample 5.*

Table 12. Difference between AgNPs sample 2 (WK 18 AgNPs) and plant extracts samples 5 (WK 18 Plant extract)

Paired t test						
Variable	Obs	Mean	Std. Err.	Std. Dev.	[95% Conf. Interval]	
Cells~2	6	84.92833	13.9069	34.06482	49.1795	120.6772
Cells~5	6	127.1017	7.572766	18.54941	107.6353	146.5681
diff	6	-42.17333	17.33394	42.45931	-86.73164	2.384975
Mean(diff) = mean(cellsurvival2 – cellsurvival5)				t= -2.4330		
Ho: mean(diff) = 0				degrees of freedom = 5		
Ha: mean(diff)<0		Ha: mean(diff) !=0		Ha:mean(diff)>0		
Pr(T < t) = 0.0296		Pr(T > t) = 0.0592		Pr(T > t) = 0.9704		

Table 13 (below) shows there is a statistical difference between survival rate AgNPs sample 3 and plant extract sample 6 at 0.05 level of significant. Survival rate for AgNPs sample 3 is statistically lower than survival rate for plant extract sample 6.*

Table 13. Difference between AgNPs sample 3 (EL 4 AgNPs) and plant extracts samples 6 (EL 4 Plant extract)

Paired t test						
Variable	Obs	Mean	Std. Err.	Std. Dev.	[95% Conf. Interval]	
Cells~3	6	63.79667	14.95422	36.63022	25.35561	102.2377
Cells~6	6	111.4167	5.867067	14.37132	96.33489	126.4984
diff	6	-47.62	11.31.725	27.72148	-76.71191	-18.52809
Mean(diff) = mean(cellsurvival3 – cellsurvival6)				t= -4.2007		
Ho: mean(diff) = 0				degrees of freedom = 5		
Ha: mean(diff)<0		Ha: mean(diff) !=0		Ha:mean(diff)>0		
Pr(T < t) = 0.0042		Pr(T > t) = 0.0084		Pr(T > t) = 0.9958		

Table 14 (below) shows a difference in survival rate across the 6 concentrations of samples there is statistical difference between survival rates of the 6 concentrations of the nanoparticle samples at 0.05 level of significant.*

Table 14. Difference in survival rate across concentrates of AgNPs samples

NPs sample	Summary of npsCell survival				
	Mean	Std.Dev.	Freq		
Fifteenpercent	41.54	12.930108	3		
Fivepercent	95.426667	10.320341	3		
Onepercent	101.96	8.743346	3		
Tenpercent	71.153333	30.370343	3		
Threepercent	100.37	8.1978229	3		
Twentyfive	32.023333	7.6427765	3		
Total	73.745556	31.692621	18		
Analysis of variance					
Source	SS	df	MS	F	Prob > F
Between groups	14278.9432	5	2855.78865	12.26	0.0002
Within groups	2796.2346	12	233.01955		
Total	17075.1778	17	100442223		

Table 15. Difference in survival rate between concentrates of AgNPs samples

Nps Cell Survival	Tukey				Tukey	
	Contrast	STD.Err.	t	P> t	[95% Conf. Interval]	
Sample11						
*fivepercent vs fifteenper	53.88667	12.4638	4.32	0.010	12.02174	95.72159
*onepercent vs fifteenper	60.42	12.4638	4.85	0.004	18.55507	102.2849
tenpercent vs fifteenper	29.61333	12.4638	2.38	0.238	-12.25159	71.47826
threepercent vs fifteenper	58.83	12.4638	4.72	0.005	16.96507	100.6949
twentyfiveper vs fifteenper	-9.516667	12.4638	-0.76	0.969	-51.38159	32.34826
onepercent vs fivepercent	6.533333	12.4638	0.52	0.994	-35.33159	48.39826
tenpercent vs fivepercent	-24.27333	12.4638	-1.95	0.422	-66.13826	17.59159
threepercent vs fivepercent	4.943333	12.4638	0.40	0.998	-36..92159	46.80826
*twentyfiveper vs fivepercent	-63.40333	12.4638	-5.09	0.003	-105.2683	-21.53841
tenpercent vs onepercent	-30.80667	12.4638	-2.47	0.207	-72.67159	11.05826
threepercent vs onepercent	-1.59	12.4638	-0.13	1.000	-43.45493	40.27493
*twentyfiveper vs onepercent	-69.93667	12.4638	-5.61	0.001	-111.8016	-28.07174
*threepercent vs tenpercent	29.21667	12.4638	2.34	0.249	-12.64826	71.08159
twentyfiveper vs tenpercent	-39.13	12.4638	-3.14	0.072	-80.99493	2.734926
twntyfiveper vs threepercent	-68.34667	12.4638	-5.48	0,002	-110.2116	26.48174

Table 15 (above) indicates the survival rate for 5% concentrates of AgNPs samples are statistically different from that 15% (p-value=0.010).*

The survival rate for 1% concentrates of AgNPs samples are statistically different from that 15% (p-value=0.004).*

The survival rate for 5% concentrates of AgNPs samples are statistically different from that 15% (p-value=0.005).*

The survival rate for 25% concentrates of AgNPs samples are statistically different from that 5% (p-value=0.003).*

The survival rate for 25% concentrates of AgNPs samples are statistically different from that 1% (p-value=0.001).*

The survival rate for 25% concentrates of AgNPs samples are statistically different from that 3% (p-value=0.002).*

The statistics for plant extracts showed that there was a P-value=0.032 hence there is a statistical difference in the cell survival rate of the different concentrations of the plant extract samples shown in Table 16 (below). There is a statistical difference between 25% concentration and 10% concentration cell survival rate for the plant extract.

Table 16. Difference in survival rate across concentrates of plant extract samples

pesample	Summary pf pecell surv				
	Mean	Std,Dev.	Freq.		
Fifteenpe	107.55	10.644609	3		
Fiveperce	127.61333	11.2000028	3		
Onepercen	124.53	4.0079421	3		
Tenpercen	102.71	11.261159	3		
Threeperc	125.31333	11.15872	3		
twentyfiv	136.63	18.095604	3		
Total	120.72444	15.659936	18		
Analysis of variance					
Source	SS	df	MS	F	Prob > F
Between groups	2502.20951	5	500.441902	3.60	0.0320
Within Groups	1666.76153	12	138.89674		
Total	4168.97104	17	245.233591		
Bartlett's test for equal variance: $\chi^2(5) = 3.0261$ Prob> $\chi^2 = 0.969$					

peCellSurv	Tukey				Tukey	
	Contrast	STD.Err.	t	P> t	[95% Conf. Interval]	
Sample12						
fivepercent vs fifteenper	20.06333	9,622778	2.08	0.355	-12.25882	52.38548
onepercent vs fifteenper	16.98	9,622778	1.76	0.520	-15.34215	49.30215
tenpercent vs fifteenper	-4.84	9,622778	-0.50	0.995	-37.16215	27.48215
threepercent vs fifteenper	17.76333	9,622778	1.85	0.475	-14.55882	50.08458
twentyfiveper vs fifteenper	29,08	9,622778	3.02	0.087	-3.24151	61.20215
onepercent vs fivepercent	-3.083333	9,622778	-0.32	0.999	-35.40548	29.23882
tenpercent vs fivepercent	-24.90333	9,622778	-2.59	0.174	-57.22548	7.418818
threepercent vs fivepercent	-2.3	9,622778	-0.24	1.000	-34.62215	30.02215
twentyfiveper vs fivepercent	9.016667	9,622778	0.94	0.929	-23.30548	41.33882
tenpercent vs onepercent	-21.82	9,622778	-2.27	0.278	-54.14215	10.50215
threepercent vs onepercent	.7833333	9,622778	0.08	1.000	-31.53882	33.10548
twentyfiveper vs onepercent	12.1	9,622778	1.26	0.801	-20.22215	44.42215
threepercent vs tenpercent	22.60333	9,622778	2.35	0.248	-9.718818	54.92548
*twentyfiveper vs tenpercent	33.92	9,622778	3.52	0.038	1.597849	66.24215
twntyfiveper vs threepercent	11.31667	9,622778	1.18	0.840	-21.00548	43.63882

Concentrates of nanoparticles and plant extract together there is no statistical difference in the survival rate of the different concentrations of the nano particles at p-value 0.05 (p=0.172) as seen in Table 17 (below).

Table 17. Concentrates of nanoparticles and plant extract together

sample	Summary of NPs Cell survival				
	Mean	Std. Dev.	Freq		
Fifteenper	74.545	37.673719	6		
Fivepercent	111.52	20.089163	6		
Onepercent	113.245	13.777712	6		
Tenpercent	86.931667	26.803275	6		
Threepercent	112.84167	16.227738	6		
Twentyfive..	84.326667	58.626885	6		
Total	97.235	34.270893	36		
Analysis of variance					
Source	SS	df	MS	F	Prob > F
Between groups	8949.4153	5	1789.88306	1.67	0.1724
Within groups	32157.8776	30	1071.92925		
Total	41107.2929	35	1071.49408		
Bartlett's test for equal variances: $\chi^2(5) = 14.2238$ Prob> $\chi^2 = 0.014$					

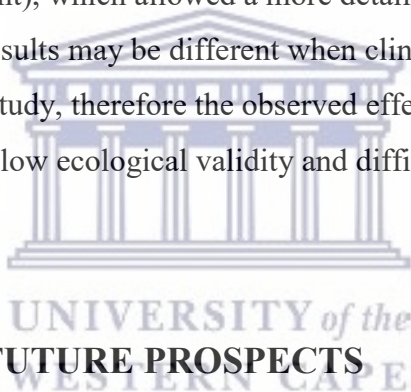
The cytotoxicity of AgNPs is determined by the difference in the size of the particle. AgNPs have shown to have a vital effect on cell viability, lactate dehydrogenase activity, and reactive oxygen species generation in a size-dependent manner in different cell lines (Akter *et al.*, 2018). Numerous studies have been carried out to determine the particle size effect of AgNPs on different cell lines and have come to the conclusion that the smaller the particle size the more cytotoxic the AgNP would be (Liu *et al.*, 2010, Wang *et al.*, 2014, Park *et al.*, 2010 and Greulich *et al.*, 2009). According to a study done by Paknejadi *et al.* in 2018, small nano-sized silver particles could potentially have cytotoxic effects on normal cells, especially at high concentrations and prolonged exposure times (Paknejadi *et al.*, 2018). You *et al.* in 2012 also stated that a high concentration of AgNPs can cause apoptosis in human cells (You *et al.*, 2012). From the results obtained it can be concluded that WK 13 nanoparticle size was the smallest and thus had the highest cell death when compared to WK 18 and EL 4.

Very little research has been conducted on the relationship between cytotoxicity of AgNPs and concentration.

LIMITATIONS

The following were considered limitations to this study:

- a. Only indigenous plants were used to synthesize silver nanoparticles.
- b. Sample sizes for antibacterial studies were small.
- c. The range of concentrations were limited in the studies for antibacterial testing.
- d. The used organism was a laboratory isolate (i.e., isolated from their usual biological environment), which allowed a more detailed or more convenient analysis. However, results may be different when clinical isolate is used.
- e. This was an *in vitro* study, therefore the observed effects of the green NPs on yeast cells may be of low ecological validity and difficult to generalise to actual clinical situations.



CONCLUSION AND FUTURE PROSPECTS

For the first time AgNPs was synthesized by *Berzelia lanuginose*, *Helichrysum cymosum*, and *Searsia crenata* plant extracts. The biosynthesized AgNPs synthesis protocol established in this research study followed basic green protocols to formulate the intended NPs. Results revealed that AgNPs were obtained from the abovementioned extracts with high purity.

Characterization of the AgNPs was validated using visual inspection, UV-Vis, FTIR, HRTEM (EDX and SAED) and DLS. The leaf extract from *Berzelia lanuginose* (WK 13), *Helichrysum cymosum* (WK 18) and *Searsia crenata* (EL 4) showed rapid conversion of silver nitrate into silver nanoparticles which was indicated by distinct colour changes from clear to yellow to dark brownish yellow within few minutes of the extract addition in AgNO₃ (1 mM) The UV-Vis results for *Berzelia lanuginose*, *Helichrysum cymosum*, and *Searsia crenata* revealed AgNPs with a peak at 430±1.5 nm,

440±1.5 nm and 428±1.5 nm respectively whilst HRTEM revealed that *Helichrysum cymosum* revealed various shapes and sizes.

The shapes predominantly seen were triangular, hexagonal, spherical, and pentagonal shapes. *Berzelia lanuginosa* and *Searsia crenata* revealed spherical shapes of different sizes. The AgNPs size for *Berzelia lanuginosa*, *Helichrysum cymosum*, and *Searsia crenata* were 16-20nm, 31-60nm and 57-72nm respectively. Stability testing revealed that *Berzelia lanuginosa* and *Helichrysum cymosum* were stable and *Searsia crenata* had a moderate shift and a decrease in the surface plasmon resonance. SAED revealed that *Berzelia lanuginosa*, *Helichrysum cymosum*, and *Searsia crenata* had diffraction spots of 111, 200, 220 and 311.

FTIR results for *Berzelia lanuginosa* showed C=C stretching, C=O stretching and O-H bonds. *Helichrysum cymosum* revealed C=O stretching and O-H stretching bonds. *Searsia crenata* showed C=C stretching, C=O stretching and O-H stretching bonds. *Candida* growth inhibition zones for *Berzelia lanuginosa*, *Helichrysum cymosum*, and *Searsia crenata* ranging between 18mm, 18.67mm and 18.33mm were recorded in response to AgNPs exposure. The XTT testing revealed that at 4 hours, *Helichrysum cymosum* showed consistently higher growth than *Berzelia lanuginosa* and *Searsia crenata* (OD at 562-630nm). *Berzelia lanuginosa* lowered the fungal growth the most across the observed time. MIC for all 3 AgNPs was determined below 6.25%. The reduction of 90% of the yeast population occurred between SR 2 and SR 3 for all the plants at 4 hours. The plant extracts seemed to have a lower effect in 4-24 hours when compared to their respective AgNPs with OD readings consistently above 0.5 for the plant extract.

The cytotoxicity of AgNPs is determined by the difference in the size of the particle. From the results obtained it can be concluded that WK 13 nanoparticle size was the smallest and thus had the highest cell death when compared to WK 18 and EL 4.

Very little research was conducted on the relationship between cytotoxicity of AgNPs and concentration.

The AgNPs exhibited promising antifungal activity that was size- and concentration-dependent. *Berzelia lanuginosa* showed the most favourable antifungal results and satisfactory cytotoxic results.

For future prospects, biosynthesized AgNPs have shown to have excellent antifungal properties and excellent biocompatibility thus there is potential for use in various dental and medical biomaterials. More research is needed to test whether these biosynthesized AgNP biomaterials are a cost-effective option especially for product development when compared to conventional AgNPs and conventional dental materials.

The plants tested were indigenous to South Africa and more research on the chemical structure and benefits of these plants are required. In other words, not only microbiology testing on *Candida albicans* but a whole host of other microorganisms such as *Streptococcus mutans* to prevent caries development which would then solve the early loss of teeth. More importantly the incorporation of AgNPs into acrylic denture base material to reduce the incidence of denture stomatitis.

The incorporation of NPs into dental biomaterials has shown favourable antimicrobial effects. However, most of these studies are performed *in vitro*. The true environment and nature of the oral cavity is a complex ecosystem, and science has not yet fully established how the modifications of various modified dental materials may behave orally. It is thus imperative to consider issues like bioavailability, as well as the fact that the antimicrobial activity can be different in *in vivo* and *in vitro* conditions.

Green synthesised AgNPs have not been subjected to clinical testing. Thus, scientists need to take full advantage of this developing technology to formulate specific antimicrobial NPs against pathogens of human concern.

APPENDICES

Appendix A:

Information of plants tested in this thesis

Berzelia lanuginosa



Distribution: The natural distribution of *Berzelia lanuginosa* is from the South West to the North West parts of the Western Cape, between Bredasdorp and Clanwilliam. They usually occur on slopes and sandy flats in permanently moist areas.

Biomedical uses: None

Medical uses: No known medicinal use

Traditional uses: Used for decorative purposes

Helichrysum cymosum



Distribution: The natural distribution of *Helichrysum cymosum* is from the Western Cape, including the Peninsula, eastwards along the coast and the coastal mountain ranges, then north-east both along the coast and inland to Albany district, Katberg and the Amatola Mountains, and as far as Lake St Lucia in Natal.

Biomedical uses: The plants have antibacterial, antioxidant, antifungal, antiviral, anti-HIV, anti-inflammatory, antimalarial, and cytotoxicity activities

Traditional uses: Boiled in water and drunk as a tea for coughs and colds. Leaves are also traditionally used in wound dressings and to prevent infections

Searsia crenata



Distribution: *Searsia crenata* occurs from the Cape Peninsula to Umzumbe in southern KwaZulu-Natal where it grows in dense colonies on the coastal and inland dunes.

Biomedical uses: No known medical uses.

Traditional uses: It is used as formal hedging, screening against wind or to hold the fort in the background of a bed

UNIVERSITY of the
WESTERN CAPE

Appendix B:

Antibacterial results:

XTT testing

Key:

WK 13 - Plant D

T0 = 0 hours

F1 - 256nm

WK 18 - Plant E

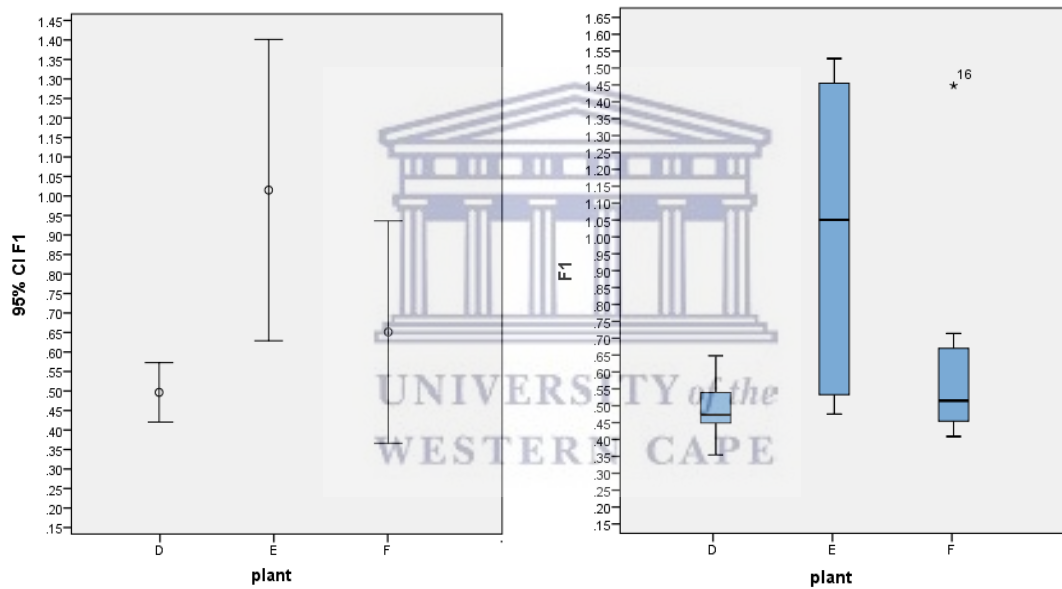
T2 = 2 hours

F2 - 630nm

EL 4 - Plant F

T3 = 3 hours

T2 F1



Shows XTT results for plant D, E and F at 2 hours at 256nm and the confidence index

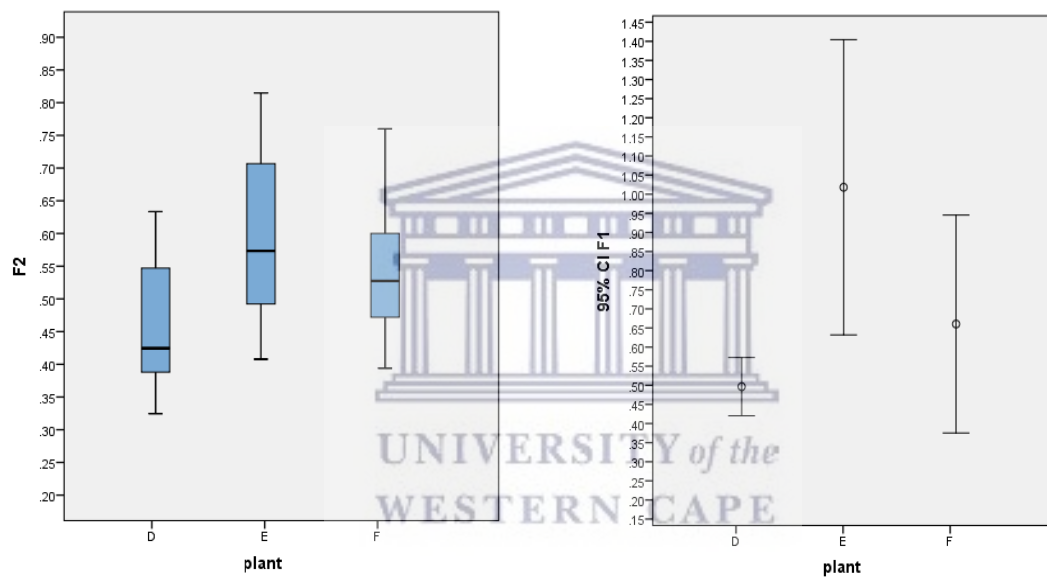
Appendix C:

XTT testing

Key:

WK 13 - Plant D	T0 = 0 hours	F1 - 256nm
WK 18 - Plant E	T2 = 2 hours	F2 - 630nm
EL 4 - Plant F	T3 = 3 hours	

T2 F2



Shows XTT results for plant D, E and F at 2 hours at 630nm and the confidence index

Appendix D:

XTT testing

Key:

WK 13 - Plant D

T0 = 0 hours

F1 - 256nm

WK 18 - Plant E

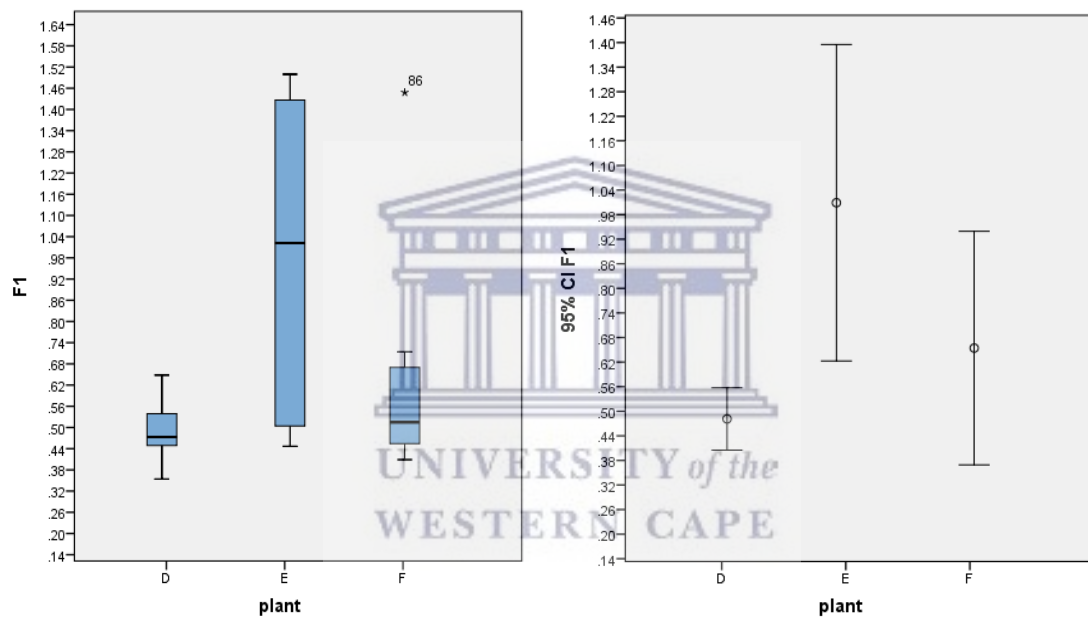
T2 = 2 hours

F2 - 630nm

EL 4 - Plant F

T3 = 3 hours

T3 F1



Shows XTT results for plant D, E and F at 3 hours at 256nm and the confidence index

Appendix E:

XTT testing:

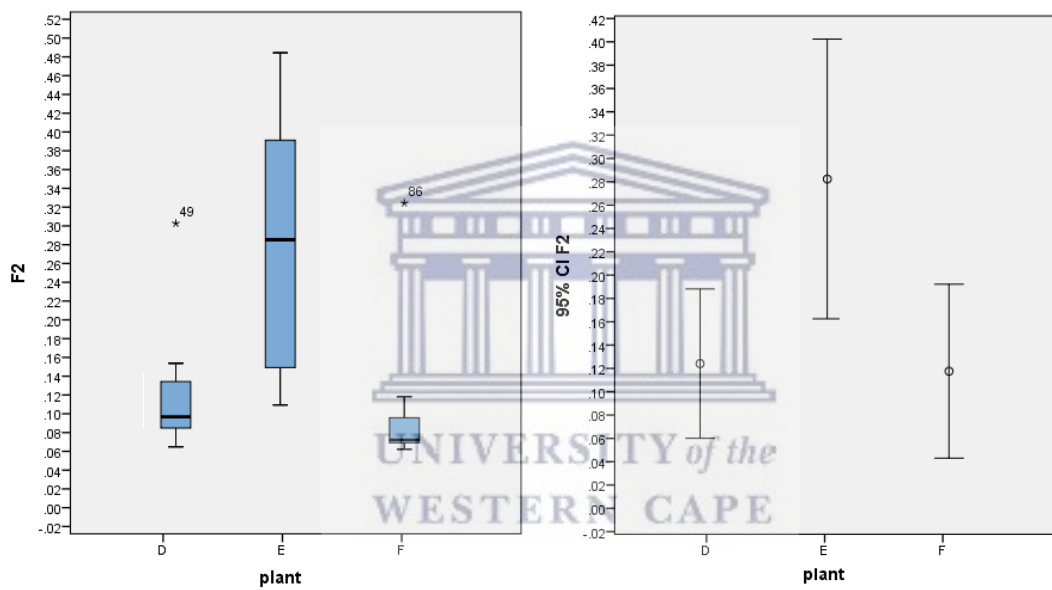
Key:

WK 13- Plant D
WK 18- Plant E
EL 4- Plant F

T0 = 0 hours
T2 = 2 hours
T3 = 3 hours

F1- 256nm
F2- 630nm

T3 F2



Shows XTT results for plant D, E and F at 3 hours at 630 nm and the confidence index

Appendix F:

Table 18. The difference between frequency (nm 256 – nm 630) at time T0 per plant.
Descriptives per plant.

T0							
plant	Mean	N	Std. Deviation	Kurtosis	Std. Error Kurtosis	Skewness	Std. Error Skewness
A	.021125	8	.0027484	2.656	1.481	-.173	.752
B	.018875	8	.0190671	6.954	1.481	2.582	.752
C	.019375	8	.0088146	3.488	1.481	-1.820	.752
D	.027625	8	.0034615	-.067	1.481	-.019	.752
E	.026500	8	.0151563	6.735	1.481	2.548	.752
F	.031125	8	.0094482	.352	1.481	.993	.752
G	.034625	8	.0220968	-1.097	1.481	.531	.752
H	.022625	8	.0218759	5.671	1.481	2.344	.752

Table 19. The difference between frequency (nm 256 – nm 630) at time T2 per plant.
Descriptives per plant.

T2							
plant	Mean	N	Std. Deviation	Kurtosis	Std. Error of Kurtosis	Skewness	Std. Error Skewness
D	.0344	8	.05588	.531	1.481	.514	.752
E	.4088	8	.35019	-1.883	1.481	-.268	.752
F	.0979	8	.30475	7.143	1.481	2.618	.752

Table 20. The difference between frequency (nm 256 – nm 630) at time T4 per plant.
Descriptives per plant.

t4							
plant	Mean	N	Std. Deviation	Kurtosis	Std. Error Kurtosis	Skewness	Std. Error Skewness
D	.364375	8	.0798426	2.252	1.481	.938	.752
E	.723500	8	.3266050	-2.053	1.481	-.072	.752
F	.535625	8	.2564538	4.902	1.481	2.139	.752

BIBLIOGRAPHY

Aazam, E. S. and Zaheer, Z. (2016) 'Growth of Ag-nanoparticles in an aqueous solution and their antimicrobial activities against Gram positive, Gram negative bacterial strains and Candida fungus', *Bioprocess and Biosystems Engineering*, 39(4), pp. 575–584. doi: 10.1007/s00449-016-1539-3.

Abiodun Solanke, I., Ajayi, D. and Arigbede, A. (2014) 'Nanotechnology and its application in dentistry', *Annals of Medical and Health Sciences Research*, 4(9), p. 171. doi: 10.4103/2141-9248.141951.

Acosta-Torres, L. S. *et al.* (2012) 'Cytocompatible antifungal acrylic resin containing silver nanoparticles for dentures', *International Journal of Nanomedicine*, 7, pp. 4777–4786. doi: 10.2147/IJN.S32391.

Afkhami, F. *et al.* (2015) 'Antibiofilm efficacy of silver nanoparticles as a vehicle for calcium hydroxide medicament against *Enterococcus faecalis*', *Journal of Dentistry*, 43(12), pp. 1573–1579. doi: 10.1016/j.jdent.2015.08.012.

Ahmad, S. *et al.* (2019) 'Green nanotechnology: a review on green synthesis of silver nanoparticles - an ecofriendly approach.', *International journal of nanomedicine*, 14, pp. 5087–5107. doi: 10.2147/IJN.S200254.

Ahmed, S. *et al.* (2016) 'A review on plants extract mediated synthesis of silver nanoparticles for antimicrobial applications: A green expertise', *Journal of Advanced Research*. Elsevier, 7(1), pp. 17–28. doi: 10.1016/j.jare.2015.02.007.

Aiswariya, K. S. and Jose, V. (2021) 'Photo-Mediated Facile Synthesis of Silver Nanoparticles Using Curcuma zanthorrhiza Rhizome Extract and Their In Vitro Antimicrobial and Anticancer Activity', *Journal of Inorganic and Organometallic Polymers and Materials*. Springer US, 31(7), pp. 3111–3124. doi: 10.1007/s10904-021-01951-0.

Akter, M. *et al.* (2018) 'A systematic review on silver nanoparticles-induced cytotoxicity: Physicochemical properties and perspectives', *Journal of Advanced Research*. Cairo University, 9, pp. 1–16. doi: 10.1016/j.jare.2017.10.008.

Alahmad, A. *et al.* (2021) 'Hypericum perforatum L.-mediated green synthesis of silver nanoparticles exhibiting antioxidant and anticancer activities', *Nanomaterials*, 11(2), pp. 1–26. doi: 10.3390/nano11020487.

Alaqad, K. and Saleh, T. A. (2016) 'Gold and Silver Nanoparticles: Synthesis Methods, Characterization Routes and Applications towards Drugs', *Journal of Environmental & Analytical Toxicology*, 6(4). doi: 10.4172/2161-0525.1000384.

Ali, E. M. and Abdallah, B. M. (2020) 'Effective inhibition of candidiasis using an eco-friendly leaf extract of calotropis-gigantean-mediated silver nanoparticles', *Nanomaterials*, 10(3), pp. 1–16. doi: 10.3390/nano10030422.

AlKahtani, R. N. (2018) 'The implications and applications of nanotechnology in dentistry: A review', *Saudi Dental Journal*. King Saud University, 30(2), pp. 107–116. doi: 10.1016/j.sdentj.2018.01.002.

Almaguer-Flores, A., Ximénez-Fyvie, L. A. and Rodil, S. E. (2010) 'Oral bacterial adhesion on amorphous carbon and titanium films: Effect of surface roughness and culture media', *Journal of Biomedical Materials Research - Part B Applied Biomaterials*, 92(1), pp. 196–204. doi: 10.1002/jbm.b.31506.

Almatroudi, A. (2020) 'Silver nanoparticles: synthesis, characterisation and biomedical applications', *Open Life Sciences*, 15(1), pp. 819–839. doi: 10.1515/biol-2020-0094.

Altarawneh, S. *et al.* (2013) 'Clinical and Histological Findings of Denture Stomatitis as Related to Intraoral Colonization Patterns of Candida albicans, Salivary Flow, and Dry Mouth', *Journal of Prosthodontics*, 22(1), pp. 13–22. doi: 10.1111/j.1532-849X.2012.00906.x.

Anand, S. and Prasad, R. (1991) 'Growth and Respiration Characteristics of Candida albicans', *Candida Albicans*, pp. 46–61. doi: 10.1007/978-3-642-75253-7_4.

Anandalakshmi, K., Venugobal, J. and Ramasamy, V. (2016) 'Characterization of silver nanoparticles by green synthesis method using Pedalium murex leaf extract and their antibacterial activity', *Applied Nanoscience (Switzerland)*. Springer Berlin Heidelberg, 6(3), pp. 399–408. doi: 10.1007/s13204-015-0449-z.

Anuj, S. A. and Ishnava, K. B. (2013) 'Plant mediated synthesis of silver nanoparticles

by using dried stem powder of *Tinospora Cordifolia*, its antibacterial activity and comparison with antibiotics', *International Journal of Pharma and Bio Sciences*, 4(4).

Athie-García, M. S. *et al.* (2018) 'Cell wall damage and oxidative stress in *Candida albicans* ATCC10231 and *Aspergillus niger* caused by palladium nanoparticles', *Toxicology in Vitro*. Elsevier, 48(August 2017), pp. 111–120. doi: 10.1016/j.tiv.2018.01.006.

Aygün, A. *et al.* (2020) 'Biological synthesis of silver nanoparticles using *Rheum ribes* and evaluation of their anticarcinogenic and antimicrobial potential: A novel approach in phytonanotechnology', *Journal of Pharmaceutical and Biomedical Analysis*, 179. doi: 10.1016/j.jpba.2019.113012.

Bagyalakshmi, J. and Haritha, H. (2017) 'Green Synthesis and Characterization of Silver Nanoparticles Using *Pterocarpus marsupium* and Assessment of its In vitro Antidiabetic Activity', *American Journal of Advanced Drug Delivery*, 5(3). doi: 10.21767/2321-547x.1000019.

Bakopoulou, A., Papadopoulou, T. and Garefis, P. (2009) 'Molecular toxicology of substances released from resin-based dental restorative materials', *International Journal of Molecular Sciences*, 10(9), pp. 3861–3899. doi: 10.3390/ijms10093861.

Balouiri, M., Sadiki, M. and Ibsouda, S. K. (2016) 'Methods for in vitro evaluating antimicrobial activity: A review', *Journal of Pharmaceutical Analysis*. Elsevier, 6(2), pp. 71–79. doi: 10.1016/j.jpha.2015.11.005.

Banerjee, P. *et al.* (2014) 'Leaf extract mediated green synthesis of silver nanoparticles from widely available Indian plants: Synthesis, characterization, antimicrobial property and toxicity analysis', *Bioresources and Bioprocessing*, 1(1), pp. 1–10. doi: 10.1186/s40643-014-0003-y.

Bapat, R. A. *et al.* (2018) 'An overview of application of silver nanoparticles for biomaterials in dentistry', *Materials Science and Engineering C*. Elsevier, 91(September 2017), pp. 881–898. doi: 10.1016/j.msec.2018.05.069.

Bhat, R. *et al.* (2011) 'Photo-irradiated biosynthesis of silver nanoparticles using edible mushroom *Pleurotus florida* and their antibacterial activity studies', *Bioinorganic*

Chemistry and Applications, 2011. doi: 10.1155/2011/650979.

Bhavikatti, S. K., Bhardwaj, S. and Prabhuji, M. L. V. (2014) 'Current applications of nanotechnology in dentistry: A review', *General Dentistry*, 62(4), pp. 72–77. Available at: www.agd.org (Accessed: 18 February 2019).

Bianchi, C. M. P. de C. *et al.* (2016) 'Factors related to oral candidiasis in elderly users and non-users of removable dental prostheses', *Revista do Instituto de Medicina Tropical de Sao Paulo*, 58(3), pp. 6–10. doi: 10.1590/S1678-9946201658017.

Burduşel, A.-C. *et al.* (2018) 'Biomedical Applications of Silver Nanoparticles: An Up-to-Date Overview', *Nanomaterials*. Multidisciplinary Digital Publishing Institute, 8(9), p. 681. doi: 10.3390/nano8090681.

Carlos, A. *et al.* (2017) 'Toxicity Effects in Pathogen Microorganisms Exposed to Silver Toxicity Effects in Pathogen Microorganisms Exposed to Silver Nanoparticles', (February). doi: 10.1166/nml.2017.2275.

De Castro, D. T., Valente, M. L. C., Da Silva, C. H. L., *et al.* (2016) 'Evaluation of antibiofilm and mechanical properties of new nanocomposites based on acrylic resins and silver vanadate nanoparticles', *Archives of Oral Biology*, 67, pp. 46–53. doi: 10.1016/j.archoralbio.2016.03.002.

De Castro, D. T., Valente, M. L. C., Agnelli, J. A. M., *et al.* (2016) 'In vitro study of the antibacterial properties and impact strength of dental acrylic resins modified with a nanomaterial', *Journal of Prosthetic Dentistry*. Mosby, 115(2), pp. 238–246. doi: 10.1016/j.prosdent.2015.09.003.

Cavalheiro, M. *et al.* (2018) 'Candida Biofilms: Threats, challenges, and promising strategies', *Frontiers in Medicine*, 5(FEB), pp. 1–15. doi: 10.3389/fmed.2018.00028.

Cavassin, E. D. *et al.* (2015) 'Comparison of methods to detect the in vitro activity of silver nanoparticles (AgNP) against multidrug resistant bacteria', *Journal of Nanobiotechnology*. BioMed Central, 13(1), p. 64. doi: 10.1186/s12951-015-0120-6.

Chanda, N. *et al.* (2011) 'An effective strategy for the synthesis of biocompatible gold nanoparticles using cinnamon phytochemicals for phantom CT imaging and photoacoustic detection of cancerous cells', *Pharmaceutical Research*, 28(2), pp. 279–

291. doi: 10.1007/s11095-010-0276-6.

Cheloni, G., Marti, E. and Slaveykova, V. I. (2016) 'Interactive effects of copper oxide nanoparticles and light to green alga *Chlamydomonas reinhardtii*', *Aquatic Toxicology*. Elsevier B.V., 170, pp. 120–128. doi: 10.1016/j.aquatox.2015.11.018.

Chen, X. M., Li, Y. Y. and Guo, S. X. (2013) 'Candida albicans biofilms', *Chinese Pharmaceutical Journal*, 48(19), pp. 1629–1633. doi: 10.1016/j.micinf.2016.01.002.Candida.

Chladek, G. *et al.* (2011) 'Antifungal activity of denture soft lining material modified by silver nanoparticles-a pilot study', *International Journal of Molecular Sciences*, 12(7), pp. 4735–4744. doi: 10.3390/ijms12074735.

Chladek, G. *et al.* (2013) 'Sorption, solubility, bond strength and hardness of denture soft lining incorporated with silver nanoparticles', *International Journal of Molecular Sciences*, 14(1), pp. 563–574. doi: 10.3390/ijms14010563.

Cioffi, N. and Rai, M. (2012) *Nano-antimicrobials: Progress and prospects*, *Nano-Antimicrobials: Progress and Prospects*. doi: 10.1007/978-3-642-24428-5.

CLSI (2017) 'Performance Standards for Antifungal Susceptibility Testing of Yeasts', *M60*, pp. 1–12. Available at: https://clsi.org/media/1895/m60ed1_sample.pdf.

Corrêa, J. M. *et al.* (2015) 'Silver nanoparticles in dental biomaterials', *International Journal of Biomaterials*, 2015. doi: 10.1155/2015/485275.

Coutinho, I. F., Aras, M. A. and D'souza, K. M. (2018) 'Nanomaterials and their application in prosthodontics: a review', *Journal of Research in Dentistry*, 6(6), p. 124. doi: 10.19177/jrd.v6e62018124-131.

Dadar, M. *et al.* (2018) 'Candida albicans - Biology, molecular characterization, pathogenicity, and advances in diagnosis and control – An update', *Microbial Pathogenesis*. Elsevier Ltd, 117(April), pp. 128–138. doi: 10.1016/j.micpath.2018.02.028.

Danelon, M. *et al.* (2015) 'Effect of toothpaste with nano-sized trimetaphosphate on dental caries: In situ study', *Journal of Dentistry*, 43(7), pp. 806–813. doi:

10.1016/j.jdent.2015.04.010.

Das, D., Ghosh, R. and Mandal, P. (2019) 'Biogenic synthesis of silver nanoparticles using S1 genotype of *Morus alba* leaf extract: characterization, antimicrobial and antioxidant potential assessment', *SN Applied Sciences*. Springer International Publishing, 1(5), pp. 1–16. doi: 10.1007/s42452-019-0527-z.

Detara, M., Triaminingsih, S. and Irawan, B. (2018) 'Effects of nano calcium carbonate and siwak toothpaste on demineralized enamel surface roughness', *Journal of Physics: Conference Series*, 1073(3), pp. 0–7. doi: 10.1088/1742-6596/1073/3/032011.

Dipankar, C. and Murugan, S. (2012) 'The green synthesis, characterization and evaluation of the biological activities of silver nanoparticles synthesized from *Iresine herbstii* leaf aqueous extracts', *Colloids and Surfaces B: Biointerfaces*. Elsevier B.V., 98, pp. 112–119. doi: 10.1016/j.colsurfb.2012.04.006.

Djordjevic, M. *et al.* (2017) 'Denture stomatitis: Etiopathogenesis and therapeutic approach', *Acta stomatologica Naissi*, 33(75), pp. 1730–1740. doi: 10.5937/asn1775730d.

Dube, P. *et al.* (2020) 'Antibacterial activity of biogenic silver and gold nanoparticles synthesized from *Salvia africana-lutea* and *Sutherlandia frutescens*', *Nanotechnology*, 31(50). doi: 10.1088/1361-6528/abb6a8.

Durán, N., Nakazato, G. and Seabra, A. B. (2016) 'Antimicrobial activity of biogenic silver nanoparticles, and silver chloride nanoparticles: an overview and comments', *Applied Microbiology and Biotechnology*, 100(15), pp. 6555–6570. doi: 10.1007/s00253-016-7657-7.

Ealias, A. M. and Saravanakumar, M. P. (2017) 'A review on the classification, characterisation, synthesis of nanoparticles and their application', *IOP Conference Series: Materials Science and Engineering*, 263(3). doi: 10.1088/1757-899X/263/3/032019.

Ebadifar, A., Nomani, M. and Fatemi, S. A. (2017) 'Effect of nano-hydroxyapatite toothpaste on microhardness of artificial carious lesions created on extracted teeth', *Journal of Dental Research, Dental Clinics, Dental Prospects*, 11(1), pp. 14–17. doi:

10.15171/joddd.2017.003.

Elbagory, A. M. *et al.* (2016) 'Large scale screening of southern African plant extracts for the green synthesis of gold nanoparticles using microtitre-plate method', *Molecules*, 21(11). doi: 10.3390/molecules21111498.

Eren, A. and Baran, M. F. (2019) 'Green synthesis, characterization and antimicrobial activity of silver nanoparticles (AgNPs) from maize (*Zea Mays L.*)', *Applied Ecology and Environmental Research*, 17(2), pp. 4097–4105. doi: 10.15666/aeer/1702_40974105.

Fourie, J. *et al.* (2016) 'Oral candidosis: an update on diagnosis, aetiopathogenesis and management', *South African Dental Journal*, 71(7), pp. 314–318.

Gao, Y. *et al.* (2016) 'Synthesis of gold Nanoshells through Improved Seed-Mediated Growth Approach: Brust-like, in Situ Seed Formation', *Langmuir*, 32(9), pp. 2251–2258. doi: 10.1021/acs.langmuir.5b04344.

Geethalakshmi, R. and Sarada, D. V. L. (2012) 'Gold and silver nanoparticles from *Trianthema decandra*: Synthesis, characterization, and antimicrobial properties', *International Journal of Nanomedicine*, 7, pp. 5375–5384. doi: 10.2147/IJN.S36516.

Ghahremanloo, A. and Movahedzadeh, M. (2015) 'The Effect of Silver Nano Particles on *Candida Albicans* and *Streptococcus Mutans* in Denture Acrylic Resins', *Journal of Dental Materials and Techniques*, 5(1), pp. 23–30. Available at: http://jdmtd.mums.ac.ir/article_6248_5.html.

Gligorijević, N. *et al.* (2017) 'Antimikrobna svojstva akrilatnih smola za stomatološke proteze impregniranih nanočesticama srebra', *Acta Stomatologica Naissi*, 32(75), pp. 1696–1702. doi: 10.5937/asn1775696G.

Greulich, C. *et al.* (2009) 'Studies on the biocompatibility and the interaction of silver nanoparticles with human mesenchymal stem cells (hMSCs)', *Langenbeck's Archives of Surgery*, 394(3), pp. 495–502. doi: 10.1007/s00423-009-0472-1.

Grobler, S R *et al.* (2014) 'Cytotoxic Effect of Chitosan-H, Resveratrol, β -Carotene and Propolis and their Chitosan Hydro-gels On Balb/C Mouse 3T3 Fibroblast Cells', *Int J Dentistry Oral Sci*, 1(2), pp. 10–14. doi: 10.19070/2377-8075-140003.

- Gudikandula, K. and Charya Maringanti, S. (2016) ‘Synthesis of silver nanoparticles by chemical and biological methods and their antimicrobial properties’, *Journal of Experimental Nanoscience*. Taylor & Francis, 11(9), pp. 714–721. doi: 10.1080/17458080.2016.1139196.
- Gulati, M. *et al.* (2018) ‘In Vitro Culturing and Screening of *Candida albicans* Biofilms’, *Current Protocols in Microbiology*, 50(1), pp. 1–62. doi: 10.1002/cpmc.60.
- Gupta, S. *et al.* (2013) ‘Role of Nanotechnology and Nanoparticles in Dentistry: A Review’, *Int. J. Res. Dev*, 1(3), pp. 95–102.
- Hanan, N. A. *et al.* (2018) ‘Cytotoxicity of plant-mediated synthesis of metallic nanoparticles: A systematic review’, *International Journal of Molecular Sciences*, 19(6), p. 1725. doi: 10.3390/ijms19061725.
- Hanna, M. C. (2019) ‘Clinical Manifestations of Candidiasis: Beyond *Candida albicans*’, *Virology & Immunology Journal*, 3(3). doi: 10.23880/vij-16000219.
- Hasan, S. (2014) ‘A Review on Nanoparticles : Their Synthesis and Types’, *Research Journal of Recent Sciences Res. J. Recent. Sci. Uttar Pradesh (Lucknow Campus)*, 4, pp. 1–3.
- Hashemi, S. F., Tasharrofi, N. and Saber, M. M. (2020) ‘Green synthesis of silver nanoparticles using *Teucrium polium* leaf extract and assessment of their antitumor effects against MNK45 human gastric cancer cell line’, *Journal of Molecular Structure*, 1208. doi: 10.1016/j.molstruc.2020.127889.
- He, X. (2016) ‘Ti release from dental implants in human jawbone and the toxicity and cellular uptake of Ti particles in human cells’.
- Hein, A. M. and Baxter, S. (2019) ‘Artificial intelligence for interstellar travel’, *JBIS - Journal of the British Interplanetary Society*, 72(4), pp. 125–143.
- Hu, L. *et al.* (2019) ‘Characterization of oral candidiasis and the *Candida* species profile in patients with oral mucosal diseases’, *Microbial Pathogenesis*. Elsevier Ltd, 134(February), p. 103575. doi: 10.1016/j.micpath.2019.103575.
- Hwang, I. S. *et al.* (2012) ‘Silver nanoparticles induce apoptotic cell death in *Candida*

albicans through the increase of hydroxyl radicals', *FEBS Journal*, 279(7), pp. 1327–1338. doi: 10.1111/j.1742-4658.2012.08527.x.

Ii, G. V. W. *et al.* (2012) 'Green Synthesis of Robust , Biocompatible Silver Nanoparticles Using Garlic Extract', 2012. doi: 10.1155/2012/730746.

Iqbal, Z. and Zafar, M. S. (2016) 'Role of antifungal medicaments added to tissue conditioners: A systematic review', *Journal of Prosthodontic Research*. Japan Prosthodontic Society, 60(4), pp. 231–239. doi: 10.1016/j.jpjor.2016.03.006.

Jabra Rizk, M. A. (2014) 'Oral Candidiasis: An Opportunistic Infection of AIDS', *Journal of AIDS & Clinical Research*, 05(09), pp. 23–27. doi: 10.4172/2155-6113.1000i101.

Jadhav, R. *et al.* (2016) 'Applications of silver nanoparticles in prosthodontics: An overview', *European Journal of Prosthodontics*. Medknow Publications and Media Pvt. Ltd., 4(3), p. 45. doi: 10.4103/ejp.ejp_24_16.

Jung, M., Sehr, K. and Klimek, J. (2007) 'Surface Texture of Four Nanofilled and One Hybrid Composite After Finishing', *Operative Dentistry*, 32(1), pp. 45–52. doi: 10.2341/06-9.

Kamikawa, Y. Y. *et al.* (2014) 'In vitro antifungal activity against oral Candida species using a denture base coated with silver nanoparticles', *Journal of Nanomaterials*, 2014, pp. 1–7. doi: 10.1155/2014/780410.

Kane, S. F. (2017) 'The effects of oral health on systemic health', *General Dentistry*, 65(6), pp. 30–34.

Kane, S. N., Mishra, A. and Dutta, A. K. (2016) 'Preface: International Conference on Recent Trends in Physics (ICRTP 2016)', *Journal of Physics: Conference Series*, pp. 1–5. doi: 10.1088/1742-6596/755/1/011001.

Kartini, K. *et al.* (2020) 'Process optimization for green synthesis of silver nanoparticles using indonesian medicinal plant extracts', *Processes*, 8(8). doi: 10.3390/PR8080998.

Kashem, S. W. *et al.* (2015) 'Candida albicans morphology and dendritic cell subsets determine T helper cell differentiation', *Immunity*, 42(2), pp. 356–366. doi:

10.1016/j.immuni.2015.01.008.

Kaur, P. and Luthra, R. (2016) 'Silver nanoparticles in dentistry: An emerging trend', *SRM Journal of Research in Dental Sciences*, 7(3), p. 162. doi: 10.4103/0976-433x.188808.

Khalil, M. M. H. *et al.* (2014) 'Green synthesis of silver nanoparticles using olive leaf extract and its antibacterial activity', *Arabian Journal of Chemistry*. King Saud University, 7(6), pp. 1131–1139. doi: 10.1016/j.arabjc.2013.04.007.

Khan, I. *et al.* (2015) 'in Pharmaceutical and Nano Sciences ANALYTICAL TECHNIQUES (CHROMATOGRAPHY , SPECTROSCOPY ', 4(1), pp. 19–27.

Khan, I. I., Saeed, K. and Khan, I. I. (2017) 'Nanoparticles: Properties, applications and toxicities', *Arabian Journal of Chemistry*. The Authors, pp. 908–931. doi: 10.1016/j.arabjc.2017.05.011.

Khan, Mujeeb *et al.* (2013) 'Green synthesis of silver nanoparticles mediated by *Pulicaria glutinosa* extract', *International Journal of Nanomedicine*, 8, pp. 1507–1516. doi: 10.2147/IJN.S43309.

Khatoun, N. *et al.* (2019) 'Mode of action and anti-*Candida* activity of Artemisia annua mediated-synthesized silver nanoparticles', *Journal de Mycologie Medicale*. Elsevier Masson SAS, 29(3), pp. 201–209. doi: 10.1016/j.mycmed.2019.07.005.

Khatoun, U. T. *et al.* (2017) 'Antibacterial and antifungal activity of silver nanospheres synthesized by tri-sodium citrate assisted chemical approach', *Vacuum*, 146, pp. 259–265. doi: 10.1016/j.vacuum.2017.10.003.

Kim, K. J. *et al.* (2009) 'Antifungal activity and mode of action of silver nano-particles on *Candida albicans*', *BioMetals*, 22(2), pp. 235–242. doi: 10.1007/s10534-008-9159-2.

Kiran Kumar, H. A. *et al.* (2014) 'Antimicrobial and antioxidant activities of *Mimusops elengi* seed extract mediated isotropic silver nanoparticles', *Spectrochimica Acta - Part A: Molecular and Biomolecular Spectroscopy*. Elsevier B.V., 130, pp. 13–18. doi: 10.1016/j.saa.2014.03.024.

Kong, E. and Jabra-Rizk, M. A. (2015) 'The Great Escape: Pathogen Versus Host',

PLoS Pathogens, 11(3), pp. 1–5. doi: 10.1371/journal.ppat.1004661.

KÖROĞLU, A. *et al.* (2016) ‘Silver nanoparticle incorporation effect on mechanical and thermal properties of denture base acrylic resins’, *Journal of Applied Oral Science*. Faculdade De Odontologia De Bauru - USP, 24(6), pp. 590–596. doi: 10.1590/1678-775720160185.

Kreve, S. *et al.* (2019) ‘Influence of AgVO₃ incorporation on antimicrobial properties, hardness, roughness and adhesion of a soft denture liner’, *Scientific Reports*, 9(1), pp. 1–9. doi: 10.1038/s41598-019-48228-8.

Kreve, S. and Dos Reis, A. C. (2019) ‘Denture Liners: A Systematic Review Relative to Adhesion and Mechanical Properties’, *Scientific World Journal*, 2019. doi: 10.1155/2019/6913080.

Kumar, S. *et al.* (2017) ‘Plant latex capped colloidal silver nanoparticles: A potent anti-biofilm and fungicidal formulation’, *Journal of Molecular Liquids*. Elsevier B.V., 230, pp. 705–713. doi: 10.1016/j.molliq.2017.01.004.

Kumar, S. S. *et al.* (2013) ‘Synthesis, characterization and optical properties of zinc oxide nanoparticles’, *International Nano Letters*, 3(1), p. 30. doi: 10.1186/2228-5326-3-30.

Lalla, R. V. and Dongari-Bagtzoglou, A. (2014) ‘Antifungal medications or disinfectants for denture stomatitis: Commentary’, *Evidence-Based Dentistry*. Nature Publishing Group, 15(2), pp. 61–62. doi: 10.1038/sj.ebd.6401032.

Lara, H. H. *et al.* (2015) ‘Effect of silver nanoparticles on *Candida albicans* biofilms: An ultrastructural study’, *Journal of Nanobiotechnology*. BioMed Central, 13(1), pp. 1–12. doi: 10.1186/s12951-015-0147-8.

Lee, D. K. *et al.* (2015) ‘Nanodiamond-Gutta Percha Composite Biomaterials for Root Canal Therapy’, *ACS Nano*, 9(11), pp. 11490–11501. doi: 10.1021/acsnano.5b05718.

Leite, R. F. *et al.* (2018) ‘Antimicrobial activity of crude extracts from actinomycetes against mastitis pathogens’, *Journal of Dairy Science*. American Dairy Science Association, 101(11), pp. 10116–10125. doi: 10.3168/jds.2018-14454.

- Li, F. *et al.* (2013) ‘Comparison of quaternary ammonium-containing with nano-silver-containing adhesive in antibacterial properties and cytotoxicity’, *Dental Materials*. The Academy of Dental Materials, 29(4), pp. 450–461. doi: 10.1016/j.dental.2013.01.012.
- Li, Z. *et al.* (2016) ‘Effect of a denture base acrylic resin containing silver nanoparticles on *Candida albicans* adhesion and biofilm formation’, *Gerodontology*. Wiley/Blackwell (10.1111), 33(2), pp. 209–216. doi: 10.1111/ger.12142.
- Liu, W. *et al.* (2010) ‘Impact of silver nanoparticles on human cells: Effect of particle size’, *Nanotoxicology*, 4(3), pp. 319–330. doi: 10.3109/17435390.2010.483745.
- Lukman, A. I. *et al.* (2011) ‘Facile synthesis, stabilization, and anti-bacterial performance of discrete Ag nanoparticles using *Medicago sativa* seed exudates’, *Journal of Colloid and Interface Science*. Elsevier Inc., 353(2), pp. 433–444. doi: 10.1016/j.jcis.2010.09.088.
- Maharramov, A. M. *et al.* (2019) ‘The engineered nanoparticles in food chain: potential toxicity and effects’, *SN Applied Sciences*. Springer International Publishing, 1(11), pp. 1–25. doi: 10.1007/s42452-019-1412-5.
- Marquez, L. and Quave, C. L. (2020) ‘Prevalence and therapeutic challenges of fungal drug resistance: role for plants in drug discovery’, *Antibiotics*, 9(4), pp. 1–9. doi: 10.3390/antibiotics9040150.
- Matsuura, T. *et al.* (1997) ‘Prolonged antimicrobial conditioners containing’, *Science*, 25(5).
- De Matteis, V. *et al.* (2019) ‘Silver nanoparticles addition in poly(methyl methacrylate) dental matrix: Topographic and antimycotic studies’, *International Journal of Molecular Sciences*. MDPI AG, 20(19). doi: 10.3390/ijms20194691.
- Melo, M. A. S. *et al.* (2013) ‘Novel dental adhesives containing nanoparticles of silver and amorphous calcium phosphate’, *Dental Materials*. The Academy of Dental Materials, 29(2), pp. 199–210. doi: 10.1016/j.dental.2012.10.005.
- Miculescu, F. *et al.* (2014) ‘Handbook of Bioceramics and Biocomposites’, *Handbook of Bioceramics and Biocomposites*, pp. 1–30. doi: 10.1007/978-3-319-09230-0.

- Midha, K. *et al.* (2017) 'Potential Application of Silver Nanoparticles in Medicine', *Nanoscience & Nanotechnology-Asia*, 6(2), pp. 82–91. doi: 10.2174/2210681205666150818230319.
- Milorad Cakić *et al.* (2018) 'Green Synthesis, Characterization and Antimicrobial Activity of Silver Nanoparticles Produced from *Fumaria officinalis* L. Plant Extract', *Colloid Journal*, 80(6), pp. 803–813. doi: 10.1134/S1061933X18070013.
- Monteiro, D. R. *et al.* (2012) 'Silver nanoparticles: Influence of stabilizing agent and diameter on antifungal activity against *Candida albicans* and *Candida glabrata* biofilms', *Letters in Applied Microbiology*, 54(5), pp. 383–391. doi: 10.1111/j.1472-765X.2012.03219.x.
- Monteiro, D. R. *et al.* (2014) 'Silver colloidal nanoparticle stability: Influence on *Candida* biofilms formed on denture acrylic', *Medical Mycology*, 52(6), pp. 627–635. doi: 10.1093/mmy/myu021.
- Monteiro, D. R. *et al.* (2015) 'Susceptibility of *Candida albicans* and *Candida glabrata* biofilms to silver nanoparticles in intermediate and mature development phases', *Journal of Prosthodontic Research*. Japan Prosthodontic Society, 59(1), pp. 42–48. doi: 10.1016/j.jpjor.2014.07.004.
- Moteriya, P., Padalia, H. and Chanda, S. (2017) 'Characterization, synergistic antibacterial and free radical scavenging efficacy of silver nanoparticles synthesized using *Cassia roxburghii* leaf extract', *Journal of Genetic Engineering and Biotechnology*, 15(2), pp. 505–513. doi: 10.1016/j.jgeb.2017.06.010.
- Mourdikoudis, S., Pallares, R. M. and Thanh, N. T. K. (2018) 'Characterization techniques for nanoparticles: Comparison and complementarity upon studying nanoparticle properties', *Nanoscale*. Royal Society of Chemistry, 10(27), pp. 12871–12934. doi: 10.1039/c8nr02278j.
- Mousavi, S. A. *et al.* (2019) 'Evaluation of antibacterial and antifungal properties of a tissue conditioner used in complete dentures after incorporation of ZnO–Ag nanoparticles', *Journal of Dental Research, Dental Clinics, Dental Prospects*, 13(1), pp. 11–18. doi: 10.15171/joddd.2019.002.

- Murugan, K. *et al.* (2014) 'Biosynthesis of silver nanoparticles using Acacia leucophloea extract and their antibacterial activity', *International Journal of Nanomedicine*, 9(1), pp. 2431–2438. doi: 10.2147/IJN.S61779.
- Musa, S. F. *et al.* (2018) 'Pleurotus sajor-caju can be used to synthesize silver nanoparticles with antifungal activity against *Candida albicans*', *Journal of the Science of Food and Agriculture*, 98(3), pp. 1197–1207. doi: 10.1002/jsfa.8573.
- Muthamil, S. *et al.* (2018) 'Green synthesized silver nanoparticles demonstrating enhanced in vitro and in vivo antibiofilm activity against *Candida spp.*', *Journal of Basic Microbiology*. Wiley-VCH Verlag, 58(4), pp. 343–357. doi: 10.1002/jobm.201700529.
- Nagar, N. and Devra, V. (2019) 'A kinetic study on the degradation and biodegradability of silver nanoparticles catalyzed Methyl Orange and textile effluents', *Heliyon*. Elsevier Ltd, 5(3), p. e01356. doi: 10.1016/j.heliyon.2019.e01356.
- Naidoo, S. *et al.* (2001) 'Perceptions of oral health: the South African Demographic and Health Survey of 1998.', *SADJ: journal of the South African Dental Association = tydskrif van die Suid-Afrikaanse Tandheelkundige Vereniging*, 56(11), pp. 505–10. Available at: <http://www.ncbi.nlm.nih.gov/pubmed/11885425>.
- Nam, K.-Y. Y. (2011) 'In vitro antimicrobial effect of the tissue conditioner containing silver nanoparticles', *Journal of Advanced Prosthodontics*. Korean Academy of Prosthodontics, 3(1), pp. 20–24. doi: 10.4047/jap.2011.3.1.20.
- Napierska, D. *et al.* (2010) 'The nanosilica hazard : another variable entity', pp. 1–32.
- Neel, E. A. A. *et al.* (2015) 'Nanotechnology in dentistry: Prevention, diagnosis, and therapy', *International Journal of Nanomedicine*, 10, pp. 6371–6394. doi: 10.2147/IJN.S86033.
- Neelakandan, M. S. and Thomas, S. (2018) 'Applications of Silver Nanoparticles for Medicinal Purpose', *JSM Nanotechnol Nanomed*, 6(1), p. 1063. Available at: <https://www.jscimedcentral.com/Nanotechnology/nanotechnology-6-1063.pdf>.
- Neville, B. A., d'Enfert, C. and Bougnoux, M. E. (2015) '*Candida albicans* commensalism in the gastrointestinal tract', *FEMS yeast research*, 15(7), pp. 1–13. doi:

10.1093/femsyr/fov081.

Nikawa, H. *et al.* (1997) 'Antifungal effect of zeolite-incorporated tissue conditioner against *Candida albicans* growth and/or acid production', *Journal of Oral Rehabilitation*, 24(5), pp. 350–357. doi: 10.1111/j.1365-2842.1997.tb00339.x.

Nitschke, I. *et al.* (2021) 'Considerations for the Prosthetic Dental Treatment of Geriatric Patients in Germany', *Journal of Clinical Medicine*, 10(2), p. 304. doi: 10.3390/jcm10020304.

Noronha, V. T. *et al.* (2017) 'Silver nanoparticles in dentistry', *Dental Materials*. The Academy of Dental Materials, 33(10), pp. 1110–1126. doi: 10.1016/j.dental.2017.07.002.

Ocsoy, I. *et al.* (2017) 'A green approach for formation of silver nanoparticles on magnetic graphene oxide and highly effective antimicrobial activity and reusability', *Journal of Molecular Liquids*. Elsevier B.V., 227, pp. 147–152. doi: 10.1016/j.molliq.2016.12.015.

Oei, J. D. *et al.* (2012) 'Antimicrobial acrylic materials with in situ generated silver nanoparticles', *Journal of Biomedical Materials Research Part B: Applied Biomaterials*, 100B(2), pp. 409–415. doi: 10.1002/jbm.b.31963.

Olusegun, A. *et al.* (2012) 'We are IntechOpen , the world ' s leading publisher of Open Access books Built by scientists , for scientists TOP 1 %', *Intech*, i(tourism), p. 38. doi: 10.1016/j.colsurfa.2011.12.014.

Oves, M. *et al.* (2018) 'Antimicrobial and anticancer activities of silver nanoparticles synthesized from the root hair extract of *Phoenix dactylifera*', *Materials Science and Engineering: C*. Elsevier, 89(April), pp. 429–443. doi: 10.1016/j.msec.2018.03.035.

Padalia, H. and Chanda, S. (2017) 'Characterization, antifungal and cytotoxic evaluation of green synthesized zinc oxide nanoparticles using *Ziziphus nummularia* leaf extract', *Artificial Cells, Nanomedicine, and Biotechnology*. Taylor and Francis Ltd., 45(8), pp. 1751–1761. doi: 10.1080/21691401.2017.1282868.

Paknejadi, M. *et al.* (2018) 'No Title', *Iranian red crescent medical journal*, 20(10).

- Pareek, V. *et al.* (2017) 'Synthesis and Applications of Noble Metal Nanoparticles: A Review', *Advanced Science, Engineering and Medicine*, 9(7), pp. 527–544. doi: 10.1166/ asem.2017.2027.
- Park, E. J. *et al.* (2010) 'Silver nanoparticles induce cytotoxicity by a Trojan-horse type mechanism', *Toxicology in Vitro*. Elsevier Ltd, 24(3), pp. 872–878. doi: 10.1016/j. tiv.2009.12.001.
- Parlinska-Wojtan, M. *et al.* (2018) 'Green synthesis and antibacterial effects of aqueous colloidal solutions of silver nanoparticles using clove eugenol', *Applied Organometallic Chemistry*, 32(4), pp. 1–9. doi: 10.1002/aoc.4276.
- Philip, D. *et al.* (2011) 'Murraya Koenigii leaf-assisted rapid green synthesis of silver and gold nanoparticles', *Spectrochimica Acta - Part A: Molecular and Biomolecular Spectroscopy*. Elsevier B.V., 78(2), pp. 899–904. doi: 10.1016/j. saa.2010.12.060.
- Poopathi, S. *et al.* (2015) 'Synthesis of silver nanoparticles from *Azadirachta indica*—a most effective method for mosquito control', *Environmental Science and Pollution Research*, 22(4), pp. 2956–2963. doi: 10.1007/s11356-014-3560-x.
- Protima Rauwel, Siim Küünal, Stanislav Ferdov, and E. R. (2014) 'a Review on Green Synthesis of Silver', *Advances in Materials Science and Engineering*, 2015(March), pp. 1–9.
- Qasim, M. *et al.* (2015) 'Silver nanoparticles embedded mesoporous SiO₂ nanosphere: An effective anticandidal agent against *Candida albicans* 077', *Nanotechnology*. IOP Publishing, 26(28). doi: 10.1088/0957-4484/26/28/285102.
- Radhakrishnan, V. S. *et al.* (2018) 'In vitro studies on oxidative stress-independent, Ag nanoparticles-induced cell toxicity of *Candida albicans*, an opportunistic pathogen', *International journal of nanomedicine*, 13, pp. 91–96. doi: 10.2147/IJN.S125010.
- Rahisuddin *et al.* (2015) 'Biosynthesis of silver nanoparticles and its antibacterial and antifungal activities towards Gram-positive, Gram-negative bacterial strains and different species of *Candida* fungus', *Bioprocess and Biosystems Engineering*, 38(9), pp. 1773–1781. doi: 10.1007/s00449-015-1418-3.
- Rao, A. *et al.* (2013) 'Nanodentistry: New buzz in dentistry', *European Journal of*

General Dentistry, 2(2), p. 109. doi: 10.4103/2278-9626.112305.

Sabuncu, A. C. *et al.* (2012) 'Colloids and Surfaces B : Biointerfaces Probing nanoparticle interactions in cell culture media', *Colloids and Surfaces B: Biointerfaces*. Elsevier B.V., 95, pp. 96–102. doi: 10.1016/j.colsurfb.2012.02.022.

Sadeghi, B., Rostami, A. and Momeni, S. S. (2015) 'Facile green synthesis of silver nanoparticles using seed aqueous extract of *Pistacia atlantica* and its antibacterial activity', *Spectrochimica Acta - Part A: Molecular and Biomolecular Spectroscopy*. Elsevier B.V., 134, pp. 326–332. doi: 10.1016/j.saa.2014.05.078.

Salati, S., Doudi, M. and Madani, M. (2018) 'The biological synthesis of silver nanoparticles by mango plant extract and its anti-candida effects', *Journal of Applied Biotechnology Reports*, 5(4), pp. 157–161. doi: 10.29252/JABR.05.04.04.

Dos Santos, C. A. *et al.* (2014) 'Silver nanoparticles: Therapeutical uses, toxicity, and safety issues', *Journal of Pharmaceutical Sciences*. Elsevier Masson SAS, 103(7), pp. 1931–1944. doi: 10.1002/jps.24001.

Santos, G. C. d. O. *et al.* (2018) 'Candida infections and therapeutic strategies: Mechanisms of action for traditional and alternative agents', *Frontiers in Microbiology*, 9(JUL), pp. 1–23. doi: 10.3389/fmicb.2018.01351.

Saratale, R. G. *et al.* (2018) 'New insights on the green synthesis of metallic nanoparticles using plant and waste biomaterials: current knowledge, their agricultural and environmental applications', *Environmental Science and Pollution Research*. Environmental Science and Pollution Research, 25(11), pp. 10164–10183. doi: 10.1007/s11356-017-9912-6.

Schmalz, G. *et al.* (2017) 'Nanoparticles in dentistry', *Dental Materials*. The Academy of Dental Materials, 33(11), pp. 1298–1314. doi: 10.1016/j.dental.2017.08.193.

Schmalz, G. *et al.* (2018) 'Scientific update on nanoparticles in dentistry', *International Dental Journal*, 68(5), pp. 299–305. doi: 10.1111/idj.12394.

Shah, M. *et al.* (2015) 'Green Synthesis of Metallic Nanoparticles via Biological Entities', *Materials*, 8(11), pp. 7278–7308. doi: 10.3390/ma8115377.

- Shankar, S. S. *et al.* (2004) 'Rapid synthesis of Au, Ag, and bimetallic Au core-Ag shell nanoparticles using Neem (*Azadirachta indica*) leaf broth', *Journal of Colloid and Interface Science*, 275(2), pp. 496–502. doi: 10.1016/j.jcis.2004.03.003.
- Sharma, D., Kanchi, S. and Bisetty, K. (2019) 'Biogenic synthesis of nanoparticles: A review', *Arabian Journal of Chemistry*. King Saud University, 12(8), pp. 3576–3600. doi: 10.1016/j.arabjc.2015.11.002.
- Shetty, N. J., Swati, P. and David, K. (2013) 'Nanorobots : Future in dentistry', *The Saudi Dental Journal*. King Saud University, 25(2), pp. 49–52. doi: 10.1016/j.sdentj.2012.12.002.
- Shvero, D. K. *et al.* (2015) 'Characterisation of the antibacterial effect of polyethyleneimine nanoparticles in relation to particle distribution in resin composite', *Journal of Dentistry*, 43(2), pp. 287–294. doi: 10.1016/j.jdent.2014.05.003.
- Singh, H. *et al.* (2018) 'Role of green silver nanoparticles synthesized from *Symphytum officinale* leaf extract in protection against UVB - induced photoaging', *Journal of Nanostructure in Chemistry*. Springer Berlin Heidelberg, 8(3), pp. 359–368. doi: 10.1007/s40097-018-0281-6.
- Singh, P. *et al.* (2015) 'Biosynthesis, characterization, and antimicrobial applications of silver nanoparticles', *International Journal of Nanomedicine*, 10, pp. 2567–2577. doi: 10.2147/IJN.S72313.
- Singh, P., Kim, Yeon Ju, *et al.* (2016) 'Biogenic silver and gold nanoparticles synthesized using red ginseng root extract, and their applications', *Artificial Cells, Nanomedicine and Biotechnology*, 44(3), pp. 811–816. doi: 10.3109/21691401.2015.1008514.
- Singh, P., Kim, Yu Jin, *et al.* (2016) 'Biological Synthesis of Nanoparticles from Plants and Microorganisms', *Trends in Biotechnology*. Elsevier Ltd, 34(7), pp. 588–599. doi: 10.1016/j.tibtech.2016.02.006.
- Song, J. Y. and Kim, B. S. (2009) 'Rapid biological synthesis of silver nanoparticles using plant leaf extracts', *Bioprocess and Biosystems Engineering*, 32(1), pp. 79–84. doi: 10.1007/s00449-008-0224-6.

De Stefani, A. *et al.* (2020) ‘Application of Nanotechnology in Orthodontic Materials: A State-of-the-Art Review’, *Dentistry Journal*, 8(4), p. 126. doi: 10.3390/dj8040126.

Sun, J. *et al.* (2011) ‘Cytotoxicity, permeability, and inflammation of metal oxide nanoparticles in human cardiac microvascular endothelial cells: Cytotoxicity, permeability, and inflammation of metal oxide nanoparticles’, *Cell Biology and Toxicology*, 27(5), pp. 333–342. doi: 10.1007/s10565-011-9191-9.

Terzano, C. *et al.* (2010) ‘Air pollution ultrafine particles: Toxicity beyond the lung’, *European Review for Medical and Pharmacological Sciences*, 14(10), pp. 809–821.

Totu, E. E. *et al.* (2021) ‘Corrigendum to “Poly(methyl methacrylate) with TiO₂ nanoparticles inclusion for stereolithographic complete denture manufacturing the future in dental care for elderly edentulous patients?” [Journal of Dentistry 59 (2017) 68–77] (Journal of Dentistry (2017), *Journal of Dentistry*. Elsevier Ltd, 112(July), p. 103739. doi: 10.1016/j.jdent.2021.103739.

Tsakos, G. *et al.* (2013) ‘Social relationships and oral health among adults aged 60 years or older’, *Psychosomatic Medicine*, 75(2), pp. 178–186. doi: 10.1097/PSY.0b013e31827d221b.

Tsui, C., Kong, E. F. and Jabra-Rizk, M. A. (2016) ‘Pathogenesis of *Candida albicans* biofilm’, *Pathogens and disease*, 74(4), p. ftw018. doi: 10.1093/femspd/ftw018.

Utneja, S. *et al.* (2015) ‘Current perspectives of bio-ceramic technology in endodontics: calcium enriched mixture cement - review of its composition, properties and applications’, *Restorative Dentistry & Endodontics*, 40(1), p. 1. doi: 10.5395/rde.2015.40.1.1.

Vahabi, S. and Mardanifar, F. (2014) ‘Archive of SID Review Article □ Applications of Nanotechnology in Dentistry : A Review Introduction : Archive of SID Review of Literatures ’, 32(4), pp. 228–239.

Verma-Gaur, J. and Traven, A. (2016) ‘Post-transcriptional gene regulation in the biology and virulence of *Candida albicans*’, *Cellular Microbiology*, 18(6), pp. 800–806. doi: 10.1111/cmi.12593.

Verma, S. K. *et al.* (2017) ‘Mechanistic insight into the rapid one-step facile

- biofabrication of antibacterial silver nanoparticles from bacterial release and their biogenicity and concentration-dependent in vitro cytotoxicity to colon cells', *RSC Advances*. Royal Society of Chemistry, 7(64), pp. 40034–40045. doi: 10.1039/c7ra05943d.
- Vila, T. *et al.* (2020) 'Oral Candidiasis: A Disease of Opportunity', *Journal of Fungi*. MDPI AG, 6(1), p. 15. doi: 10.3390/jof6010015.
- Wady, A. F. *et al.* (2012) 'Evaluation of *Candida albicans* adhesion and biofilm formation on a denture base acrylic resin containing silver nanoparticles', *Journal of Applied Microbiology*, 112(6), pp. 1163–1172. doi: 10.1111/j.1365-2672.2012.05293.x.
- Wang, L. *et al.* (2016) 'Photothermo-chemotherapy of cancer employing drug leakage-free gold nanoshells', *Biomaterials*. Elsevier Ltd, 78, pp. 40–49. doi: 10.1016/j.biomaterials.2015.11.024.
- Wang, L., Hu, C. and Shao, L. (2017) 'The-antimicrobial-activity-of-nanoparticles--present-situati', *International journal of nanomedicine*, 12, pp. 1227–1249. Available at: <https://www.ncbi.nlm.nih.gov/pmc/articles/PMC5317269/pdf/ijn-12-1227.pdf>.
- Wang, X. *et al.* (2014) 'Use of coated silver nanoparticles to understand the relationship of particle dissolution and bioavailability to cell and lung toxicological potential', *Small*, 10(2), pp. 385–398. doi: 10.1002/smll.201301597.
- Wei, L. *et al.* (2015) 'Silver nanoparticles: Synthesis, properties, and therapeutic applications', *Drug Discovery Today*. Elsevier Ltd, 20(5), pp. 595–601. doi: 10.1016/j.drudis.2014.11.014.
- Wilson, D., Naglik, J. R. and Hube, B. (2016) 'The Missing Link between *Candida albicans* Hyphal Morphogenesis and Host Cell Damage', *PLoS Pathogens*, 12(10), pp. 1–5. doi: 10.1371/journal.ppat.1005867.
- Wu, K. *et al.* (2015) 'Antimicrobial activity and cytocompatibility of silver nanoparticles coated catheters via a biomimetic surface functionalization strategy', *International Journal of Nanomedicine*, 10, pp. 7241–7252. doi: 10.2147/IJN.S92307.
- van Wyk, C. W. *et al.* (1994) 'Observations on the effect of areca nut extracts on oral fibroblast proliferation', *Journal of Oral Pathology & Medicine*, 23(4), pp. 145–148.

doi: 10.1111/j.1600-0714.1994.tb01103.x.

Xie, X. *et al.* (2016) 'Protein-repellent and antibacterial functions of a calcium phosphate rechargeable nanocomposite', *Journal of Dentistry*, 52, pp. 15–22. doi: 10.1016/j.jdent.2016.06.003.

Xing, M. M. Q. *et al.* (2014) 'Nanosilver particles in medical applications: Synthesis, performance, and toxicity', *International Journal of Nanomedicine*, 9(1), pp. 2399–2407. doi: 10.2147/IJN.S55015.

Yoda, M. (2012) *Encyclopedia of Nanotechnology*, *Encyclopedia of Nanotechnology*. doi: 10.1007/978-90-481-9751-4.

You, C. *et al.* (2012) 'The progress of silver nanoparticles in the antibacterial mechanism, clinical application and cytotoxicity', *Molecular Biology Reports*, 39(9), pp. 9193–9201. doi: 10.1007/s11033-012-1792-8.

Zafar, S. and Zafar, A. (2019) 'Biosynthesis and Characterization of Silver Nanoparticles Using Phoenix dactylifera Fruits Extract and their In Vitro Antimicrobial and Cytotoxic Effects', *The Open Biotechnology Journal*, 13(1), pp. 37–46. doi: 10.2174/1874070701913010037.

Zahir, A. A. *et al.* (2015) 'Green synthesis of silver and titanium dioxide nanoparticles using Euphorbia prostrata extract shows shift from apoptosis to G0/G1 arrest followed by necrotic cell death in Leishmania donovani', *Antimicrobial Agents and Chemotherapy*, 59(8), pp. 4782–4799. doi: 10.1128/AAC.00098-15.

Zhang, X. F. *et al.* (2016) 'Silver nanoparticles: Synthesis, characterization, properties, applications, and therapeutic approaches', *International Journal of Molecular Sciences*, 17(9). doi: 10.3390/ijms17091534.